UNIVERSIDADE FEDERAL DE MINAS GERAIS

Curso de Pós-Graduação em Engenharia Metalúrgica e de Minas

Dissertação de Mestrado

“Precipitação de escorodita a partir de soluções industriais contendo arsênio”

Autora: Michelle Lara Caetano

Orientadora: Profª. Virgínia S. T. Ciminelli

Co-Orientadora: Profª. Sônia D. Ferreira Rocha

Abril de 2006

UNIVERSIDADE FEDERAL DE MINAS GERAIS

Curso de Pós-Graduação em Engenharia Metalúrgica e de Minas

Michelle Lara Caetano

Precipitação de escorodita a partir de soluções industriais contendo arsênio

Scorodite precipitation from industrial solutions containning arsenic

Dissertação de Mestrado apresentada ao Curso de Pós-Graduação em Engenharia Metalúrgica e de Minas da Universidade Federal de Minas Gerais

Área de Concentração: Tecnologia Mineral

Orientadora: Profª. Virgínia S. T. Ciminelli

Co-Orientadora: Profª. Sônia D. Ferreira Rocha

Belo Horizonte

Escola de Engenharia da UFMG

2006

AGRADECIMENTOS

É chegado o término de mais uma etapa, e com ele a sensação de alívio e realização, aliados a incerteza e saudade. Se cheguei até aqui, sei que não foi sozinha. Assim, agradeço aqueles que contribuiram direta e indiretamente para mais uma realização:

À Professora Virgínia Ciminelli, pela oportunidade, o suporte fundamental e por todos os ensinamentos profissionais e pessoais adquiridos ao longo desses dois anos.

À Professora Sônia, pela compreensão exata de quais eram meus objetivos ao sair da graduação, e assim ter me indicado o caminho da hidrometalurgia. Obrigada pelo apoio, carinho, amizade e acima de tudo por acreditar em mim.

Sandro, Madalena e Judith do Laboratório de Análises Químicas pela compreenção, amizade, prestatividade e boa vontade. Patrícia (MEV), Andréia (Difração de Raios-X) e Sica (RAMAN), pelo suporte técnico.

Aos amigos do Laboratório de Hidrometalurgia, obrigada por tudo: Ilda, João, Bruno, Maycon, Raquel, Júlio, Christina, Katharina e Rodrigo (mais que um amigo). Não posso deixar de destacar as valiosas colaborações da Cláudia (obrigada por todas as idéias compartilhadas, pelo apoio e incentivo) e do Fernando (não só pelas idéias, pelo carinho e amizade, mas também pela ajuda direta na montagem do sistema contínuo entre muitas outras coisas que fez por mim: Muito Obrigada!). Aqui encontrei pessoas que, mesmo que o tempo e a distância insistam, sempre estarão presentes no meu coração e na minha vida.

Aquele que mais colaborou para a realização desse trabalho, sem o qual certamente eu não não teria conseguido resultados tão positivos: Mateus Calonge, muito mais que Muito Obrigada !!!!!! Pelo carinho, dedicação, empenho e amizade.

À uma das pessoas mais especiais que apareceu no meu caminho, amiga e irmã: Obrigada Gra, simplesmente por estar ao meu lado, fazendo parte dos melhores e piores acontecimentos da minha vida. Um obrigado, nada menor, a Cynthia (participação especial na elaboração da Figura 4.2), Carol, e Denise: nossa amizade é o sentimento mais pleno que pode existir, hoje e sempre.

À minha mãe e minhas irmãs, Gagau e Andreza, base do meu sucesso; e aos meus sobrinhos, que apesar da bagunça e do constante *stress*, conseguem encher minha vida de alegria. Amo vocês, sempre!

TABLE OF CONTENTS

LIST OF FIGURES

LIST OF TABLES

LIST OF SYMBOLS

AsFH = arsenical ferrihydrite

B^o = nucleation rate

C = solute concentration

C_{eq} and c* = equilibrium concentration

c_b = the bulk concentration

C_c = critical supersaturation

c_i = concentration at the crystal-solution interface and fed concentration solution

c_0 = solute concentration discharge

D_{50} = average diameter

G = growth rate

G_1 = growth rate of crystals of size L_1

G_2 = growth rate of crystals of size L_2

K_{eq} = equilibrium constant

L = crystal size

L_1 and L_2 = crystal size in the fed and in the discharge, respectively

MPL = maximum permitted level

MSMPR = Mixed Suspension Mixed Product Removal

MSMPRR = Mixed Suspension Mixed Product Removal with Recycle

$\bar{n}_i$ = average population density

n^o = population density of the embryo-size crystals

n_1 and n_2 = population density

Q_0 = rate of suspension discharge

Q_i = volumetric flow rate in the fed

S = saturation ratio

S_c = critical supersaturation ratio

SSA = specific surface area

SPI = solid production index

t = period of time

TCLP = Toxicity Characterization Leach Procedure

USEPA = U.S. Environmental Protection Agency

V = reactor volume

WHO = World Health Organization

z = valency of the ions

$\gamma_A$and γ_B= activities coefficient of the species A and B

δ = stagnant film thickness

θ = contact angle formed between the crystalline solid and the foreign solid phase

τ = mean residence time

RESUMO

Escorodita ($FeAsO_4*2H_2O$) tem sido considerada a forma preferida para a disposição de resíduos contendo arsênio. Comparada com a ferridrita arsenical, a escorodita oferece vantagens que combinam elevado teor de arsênio e solubilidade em água menor que 1mg/L em pH 5. O presente trabalho investigou a remoção de arsênio de uma solução diluída (1g/L As) produzida na torre de lavagem de gases do processo de ustulação de um minério refratário de ouro. Pela primeira vez foi mostrado que soluções industriais com baixas concentrações de arsênio (1,1 – 0,1g/L) podem ser tratadas em um estágio de precipitação de escorodita sob condições de pressão ambiente, com uma remoção na faixa de 80,5 a 94,6% . A precipitação foi realizada a 95ºC. Visando controlar a supersaturação e evitar a nucleação heterogênea que leva a produção do arsenato férrico amorfo, o pH foi ajustado de acordo com a concentração inicial de arsênio. A remoção aumentou com o aumento da concentração de sementes de escorodita até 20g/L. Foi demonstrado que uma área superficial maior que 270 m^2/g As em solução foi necessária para promover uma remoção de arsênio de aproximadamente 85%. O desempenho de sementes de gesso foi comparado com o da escorodita e os resultados mostraram que o gesso é uma boa semente apenas para soluções concentradas (10g/L). No entanto, mesmo para esse nível de concentração a remoção foi superior com o uso de sementes de escorodita (91%). Uma metodologia para remoção de arsênio através da precipitação da escorodita em sistema contínuo foi estabelecida. Foi demonstrado que, devido à baixa taxa de crescimento dos cristais (cerca de 10^{-12}m/s), o reciclo de sementes é sempre necessário (para um tempo de residência de 1 hora). Os testes TCLP - Toxicity Characterization Leach Procedure (EPA, 1992) (equivalente a ABNT NBR 10005/2004) mostraram que o envelhecimento tem um importante papel na solubilidade da escorodita, que diminuiu de 13,6 mg/L para 1mg/L após 8 horas de precipitação em batelada. De acordo com os testes TCLP, a solubilidade dos sólidos é influenciada pela morfologia das partículas. Para uma mesma área superficial específica, partículas com formato arredondado apresentam uma solubilidade superior àquela encontrada em partículas com formato de placas. Em todo o trabalho, escorodita foi a única fase identificada por análises de espectroscopia micro-Raman e difração de raios-X dos sólidos precipitados.

ABSTRACT

Scorodite ($FeAsO_4*2H_2O$) has been considered as a preferable form for arsenic disposal. Compared to the AsFH, the crystalline scorodite offers the advantages of combining a relatively high arsenic content and solubility in water of less than 1mg As/L at pH 5. The present work investigated the removal of arsenic from a diluted solution (1 g/L As) generated in the washing gas tower during the roasting process. It was demonstrated that industrial solutions with low arsenic concentrations (1.1 – 0.1 g/L) could be treated in one stage of scorodite precipitation under atmospheric pressure conditions, with a removal in a range of 80.5 to 94.6%. Precipitation was carried out at 95^{o}C. In order to control supersaturation and to avoid homogeneous nucleation that yields amorphous ferric arsenate, pH was adjusted according to the initial arsenic concentration. The removal increased with the increase of the scorodite seed concentration until 20g/L. It was shown that a surface area higher than 270 m^2/g As in solution was necessary to promote an arsenic removal of approximately 85%. The performance of gypsum seeds was compared with that of scorodite and the results showed that the gypsum was a good seed only with concentrated solutions (10g/L). However, even under this level of concentration, arsenic removal was smaller (61%) than that obtained with scorodite seeds (91%). A procedure to achieve high yields of arsenic removal in continuous system was established. The recycle of seeds was required. The Toxicity Characterization Leach Procedure tests suggested that ageing plays an important role on scorodite dissolution. Scorodite was the only phase identified by micro-Raman and X-Ray diffraction analyses of the precipitates.

1 INTRODUCTION

Arsenic is one of the contaminants of concern in wastes from metallurgical and mining industries. Due to arsenic's high toxicity, the environmental regulations are becoming increasingly stringent regarding the use and disposal of As compounds. In Brazil, the maximum permitted level (MPL) in waters used for the human consumption is of 0.01mg As/L, following recommendations of the World Health Organization (Portaria Nº 1469/2000; WHO 1993). The regulation on pollutant discharges in waters of the state of Minas Gerais establishes a limit of arsenic concentration of 0.2mg As/L (*Deliberação Normativa* COPAM 10/86). Thus, the arsenic removal from industrial effluents becomes often necessary in order to comply with the environmental legislation. However, it is also important that arsenic residues are disposed in a safe form, in order to avoid its further release to the environment.

The environmental concern has led to the development of disposal technologies that are environmentally safe and costly attractive. In the mineral industry, the most commonly methods used to treat effluents containing arsenic are the precipitation of arsenical ferrihydrite - AsFH at ambient temperature and the hydrothermal precipitation of iron arsenates (Harris, 2003). The AsFH process route generates large volumes of waste with low arsenic concentration (3-6%) (Caldeira *et al*., 2005). Thus, large areas for the final disposal are needed, which in turn results in additional costs of operation.

Crystalline ferric arsenate, such as scorodite ($FeAsO_4*2H_2O$), has been considered as a preferable form for arsenic disposal because of its relatively high arsenic content and low solubility in water (typically smaller than 1mg/L arsenic at pH 5, when subjected to 24 hour toxicity characteriscs leaching procedure – TCLP) (Filippou and Demopoulos, 1997). The relatively lower Fe:As molar ratio (1:1), the smaller waste volume and the good capacity of sedimentation offer additional advantages for the disposal of scorodite (Debekaussen *et al.*, 2001) in comparison with the conventional ferrihydrite process. The scorodite is produced in hydrothermal processes at temperatures of 150ºC or higher, such as in acid pressure oxidation of auriferous sulfides for the extraction of refractory gold ores. However, this process has high

costs associated with the requirement of an autoclave and is economically attractive only if it can be combined with the processing of a valuable concentrate, such as gold. Due to the aforementioned advantages related of the precipitation of arsenic as scorodite, there have been attempts to develop a process under more benign conditions. Demopoulos and co-workers (Demopoulos *et al*., 1995; Filippou and Demopoulos, 1997; Debekaussen *et al.*, 2001; Demopoulos, 2005; Singhania *et al.*, 2005) demonstrated the possibility to precipitate scorodite at ambient pressure conditions, and temperatures below the water boiling point (95ºC). This process of scorodite production is cheaper than the hydrothermal process and can be applied regardless to the metal recovery (Singhania *et al.*, 2006). Feasibility studies of scorodite precipitation at ambient pressure indicated that the process is competitive with the ferryhydrite process in terms of capital cost. Regarding the operation, the largest costs are associated with the use of $Fe_2(SO_4)_3$ (60%) and H_2O_2 (20%) (Filippou and Demopoulos, 1997). The ambient-pressure precipitation technique involves the supersaturation control and the addition of seeds, in order to favor crystal growth instead of homogeneous nucleation.

A significant operational difficulty in the scorodite production at ambient pressure is the supersaturation control (by means of pH control) at the working temperature (95ºC). The pH is expected to decrease during scorodite precipitation owing to the productions of sulfuric acid ($2H_3AsO_4 + Fe_2(SO_4)_3 + 4H_2O \rightarrow 2FeAsO_4{*}2H_2O + 3H_2SO_4$) (Debekaussen *et al.*, 2001). Therefore, the first studies assumed that a strict pH control, and consequently base addition during the process, was necessary to assure the required supersaturation level. In batch tests, arsenic concentration decreases with time. Thus, it is difficult to assure that the reaction is occurring within of the working region, defined as the area within the critical supersaturation line and the equilibrium line. In a continuous system, the arsenic concentration remains constant during the reaction, thus allowing a better supersaturation control, which in turn favors scorodite production. However, until now the publications focusing scorodite precipitation describe results obtained under batch conditions. Despite the advantages, industrial application is probably hindered so far by factors such as the cost of the reagents required for arsenic and iron oxidation and the difficulty to control pH at high temperatures. It is not established yet if the scorodite precipitation at

ambient pressure is competitive with the arsenic ferrihydrite process (adopted by the industry) for the treatment of effluents with arsenic concentrations in a level of 1 g/L.

The present work investigates the removal of arsenic from a solution produced in a washing tower of the exit gas from the roasting of a refractory gold ore. Arsenic is currently removed as arsenical ferryhydrite (3-6% As) and disposed as a toxic waste in tailing dams. The expansion of the roasting plant motivated the search for process alternatives, such as scorodite precipitation. Thus, this work seeks the establishment of operational conditions for scorodite precipitation from solutions 10 times more diluted than those described in the literature. Firstly, the effect of the initial arsenic concentration is evaluated in tests carried out in batch systems. The effect of the seeds concentration is also evaluated in order to determine the better conditions for precipitation. The surface area of the seeds affects the available area for crystals growth, which in turn affects arsenic removal. In a further step, scorodite precipitation in a continuous system is investigated and reported by the first time. In addition to allow a better control of process variables, the continuous system represents best the process conditions applied by the industry. Additionally, the solubility of the precipitates is evaluated through standard leaching tests - TCLP (EPA, 1992) (equivalent to ABNT NBR 10005/2004; (ABNT, 2004)). It is necessary to determine the conditions in which a solid with low solubility is produced, and then to avoid arsenic further release to the environment. The broader aim is to evaluate the possibility of obtaining an industrial waste more stable and with larger arsenic concentration than the one currently produced by the ferryhydrite process. This, in turn, will reduce the volume of wastes and the associated costs with the final disposal.

2 LITERATURE REVIEW

2.1 Arsenic chemistry speciation

The determination of the concentration of different solid and aqueous species in water is defined as speciation analysis. All the species together will dictate the total element concentration in the sample, and the individual physico-chemical forms may include particulate matter in water and dissolved species, such as inorganic or organic species. As the various species exhibit different toxicity levels, the analysis of arsenic speciation in the environment is of considerable importance (Kumaresan and Riyazuddin, 2001).

Inorganic arsenic is mostly found in aqueous systems as arsenite As(III) and arsenate As(V) species. The dominant arsenic species will be determined mainly by pH and redox potential. Figures 2.1 and 2.2 show the species distributions as a function of the pH and Eh. The thermodynamically stable species in surface (aerated) waters is arsenate. The pentavalent species may exist as the four derivatives of arsenic acid: H_3AsO_4, $H_2AsO_4^-$, $HAsO_4^{2-}$ and AsO_4^{3-}. The neutral molecule predominates only at extremely low pH (<2), being further replaced by $H_2AsO_4^-$ and $HAsO_4^{2-}$ at pH 2-11. Therefore, these are the most likely species to occur in surface water and relatively high Eh. Arsenite may occur in aqueous solutions as the derivatives of the arsenous acid: H_3AsO_3, $H_2AsO_3^-$, $HAsO_3^{-2}$ and AsO_3^{-3}. The uncharged arsenite species (H_3AsO_3) will predominate under reducing conditions and relatively low Eh, up to pH 9.2, being then replaced by $H_2AsO_3^-$. The $HAsO_3^{2-}$ form appears only when pH exceeds 12. At low pH and in the presence of sulphide, $HAsS_2$ can be formed; under extreme reducing conditions arsine, arsine derivatives and arsenic metal may also occur (Smedley and Kinniburgh, 2002; Dutré and Vandecasteele, 1998; Cheng *et al.*, 1994).

According to Kumaresan and Riyazuddin (2001) arsenite is the one of the highest interest among the arsenic compounds present in the environment. It is 10 times more toxic than arsenate and 70 times more toxic than the dimethylarsinate ($(CH_3)_2AsOH$ and $(CH_3)_2OAsOH$) and monomethylarsonate ($CH_3AsO_2H_2$, and $CH_3AsO_3H_2$) species. In addition to its toxicity, arsenite is the most mobile species in the environment, as a

result of its weaker, reversible adsorption on soil constituents, such as iron and aluminum oxyhydroxides (Ladeira and Ciminelli, 2004).

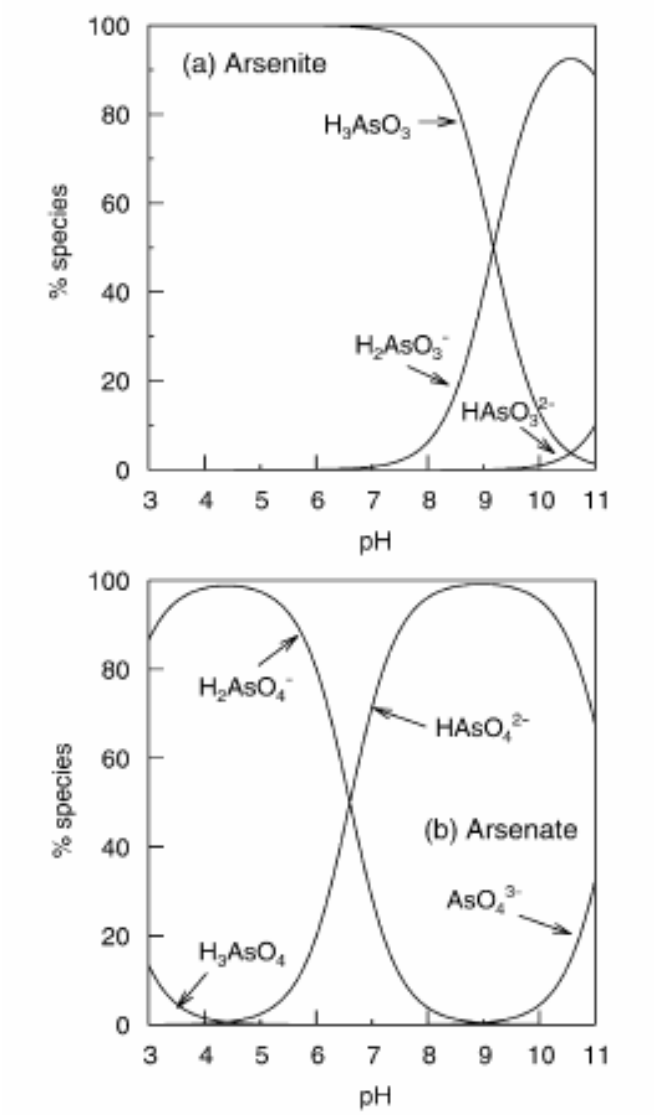

Figure 2.1 – (a) Arsenite and (b) arsenate speciation as a function of the pH (ionic strength of about 0.01M) (Smedley and Kinniburgh, 2002).

As(III) reacts with sulphur and sulphydryl groups such as cystine, organic dithiols, proteins and enzymes, but it does not react with amine groups or organics with reduced nitrogen constituents. On the other hand, As(V) reacts with reduced nitrogen groups such as amines, but not with sulphydryl groups. Both the trivalent and pentavalent forms can form organoarsenical compounds with carbon. The complexation of As (III and V) in natural environments by dissolved organic matter

prevents sorption and co-precipitation, thus increasing the arsenic mobility in soil and in aquatic systems (Kumaresan and Riyazuddin, 2001).

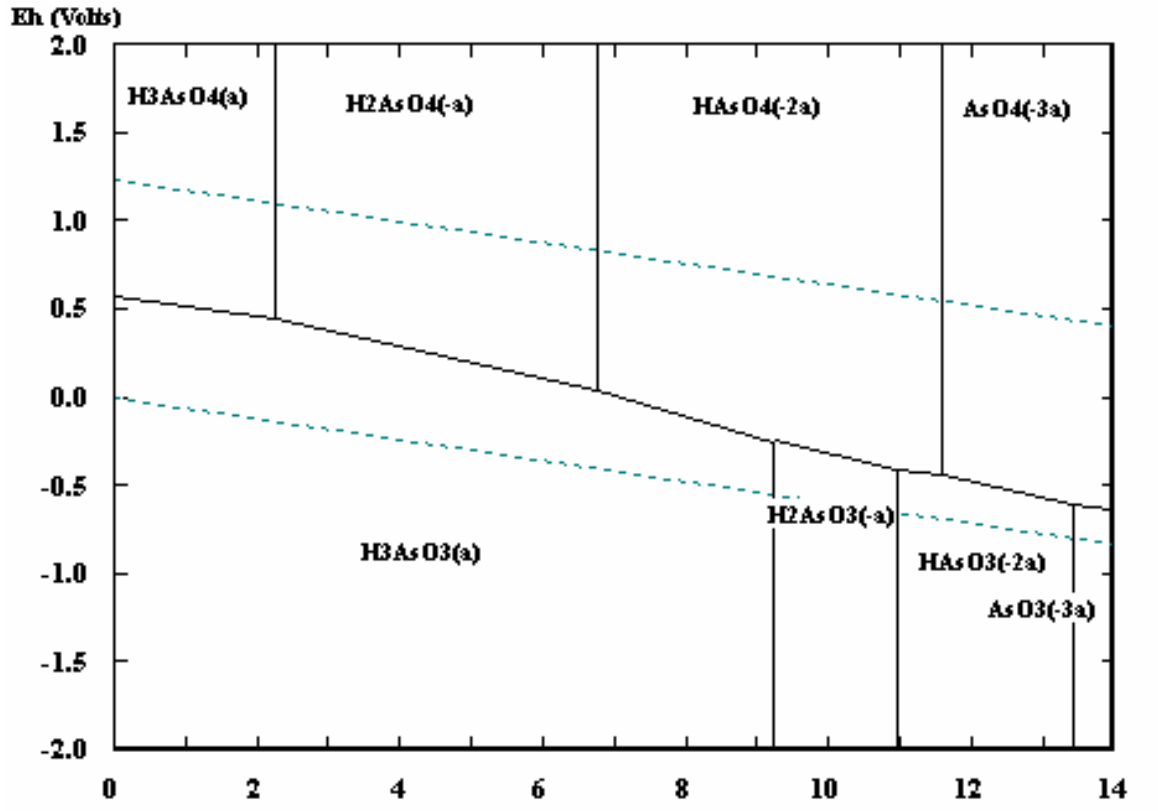

Figure 2.2 – Eh-pH diagram for As–H_2O system at 25ºC and 0.1 mol/ kg H_20, considering only the derivatives of the acid arsenic and arsenious acids (HSC Chemistry, 1999).

Various studies focusing the treatment of effluents and water for human consumption by various methods demonstrated that arsenate is more effectively removed than arsenite, thus oxidation is usually required to achieve effective arsenic removal (Cheng *et al.*, 1994; Ladeira and Ciminelli, 2004; Deschamps *et al.*, 2005). This is associated with the fact that As(III) compounds are less reactive than those of As(V). As mentioned before, in the pH range of 2-9 the arsenite occurs as neutral molecule, which results in a less favorable interaction between this and the solution species or solid sorbents if compared to arsenic (V). The effective oxidation of arsenic (III) with oxygen is observed only when conditions such as high temperature and pressure, alkaline environment or copper catalyst are used. Consequently, chemical oxidants are normally required (Emett *et al*., 2001). According to Debekaussen *et al.* (2001)

hydrogen peroxide is the environmentally preferred agent, because it has a high oxidation potential, is easily handled and the reactions products, water and oxygen, are harmless.

2.2 The disposal of arsenical wastes: technologies and environmental considerations

The arsenic is one of the most toxic pollutants found in the industrial effluents of the metals extraction, mainly copper, zinc, lead, gold and silver (Mambote *et al.*, 2001). It can be released in the beneficiation of ores containing arsenic, during hydrometallurgical or pyrometallurgical processes (Demopoulos, 2005). The production far exceeds demand and, because of the more restrictive discharge limits for arsenic emission, increasingly larger amounts of arsenic should be recovered and disposed. The stricter environmental laws on the use of arsenic has also reduced its consumption for wood preservatives, fungicides, glass, ceramics, non-ferrous alloys and other lesser uses. These factors contribute to increase the problems of oversupply and the need for safe methods of disposal (Swash and Monhemius, 1995).

Safe disposal of arsenic wastes presents various problems. The use of incineration is limited because of the volatilization of arsenic compounds while its recovery has little economic interest because of arsenic's limited applications. Arsenic cannot be destroyed; it can only be transformed into insoluble compounds in combination with other elements, such as iron. There are many techniques for arsenic removal such as ion exchange, adsorption by activated alumina or activated carbon, ultrafiltration, reverse osmosis, and co-precipitation or adsorption by metals (predominantly ferric chloride) followed by coagulation (Leist *et al.*, 2000). According to these authors, the most secure option for the treatment of arsenic wastes is the encapsulation of the contaminated material, generally through solidification/stabilization techniques, also known as fixation, and disposal of the treated wastes in monitored landfills. This technology is used to transform hazardous wastes into less hazardous solids, and consists of mixing the arsenic with various combinations of cement, lime, iron, silicates and other compounds. For the U.S. Environmental Protection Agency – USEPA this technique is ‘‘the best demonstrated available technology" for land disposal of most toxic elements. However, it is not currently considered for any arsenic waste or

wastewater due to cost constraints. A work published by Harris (2003) shows a survey on industrial methods that are currently applied for the removal and disposal of arsenic from process solutions in the mining industry. Table II.1 presents a summary of the industrial operating practices.

Table II.2.I – Summary of industrial operating practice (as of years 2000/2001) (Harris, 2003).

Operation	Comments
Arsenical Ferrihydrite	
Agua Rica, Argentina	Amorphous process planned
Barrick Goldstrike	Used for groundwaters
Billiton Fairview	Sufficient Fe from BIOX® to fix arsenic during neutralization
Codelco – Chuquicamata	Investigating BioCOP® process with Billiton, wherein arsenic will be fixed during neutralization of BioCOP® liquors
Deloro, Ontario	Poorly controlled. Plant shut down, but remains an environmental liability
Falconbridge, Kristiansand	In operation for several years – sludge stored in secure area
Giant Yellowknife	Effluent treatment – highly effective for many years, still being operated. Most arsenic, however, was stored as As_2O_3, and needs re-treatment
Goldcorp, Red Lake	Ferric treatment of mill tailings, but currently no arsenic oxidation; sludges believed to be mostly in reduced form
Hudson's Bay	Smelter dust fixed in neutralization along with pressure leach residue
Inco CRED	Well proven – consistently very low As in discharge. High Fe/As molar ratio
Morro Velho	In-situ oxidation of ferrous sulphate. Process was not well controlled, resulting in groundwater contamination. Ecological treatment being investigated
Noranda Horne	Well proven – includes base metals to make up for Fe shortfall
Outokumpu, Kokkoka	Included in jarosite peocess
Pasminco	Included in paragoethite process
Placer Dome Getchell	Sludge ponded
São Bento	BIOX® residue uses Fe from pressure leach, and two are mixed prior to ponding
Union Minière	Sludge disposed of in secure areas. Few details
Western Mining Corporation	Very high Fe/As ratio, but from alkaline medium. Passes all regulatory
High Temperature Minerals	
Arcata, Peru	Autoclave under consideration
Codelco - Chuquicamata	Autoclave was under consideration, with other options, as primary means of fixing arsenic

General Gold, Mauritânia	Autoclave chosen. Project seeking financing
Giant Mine	Autoclave was one option considered. No definitive selection has yet been made
Goldcorp, Red Lake	Autoclave being constructed for concentrate. Same logic as for Campbell next door
Hudson's Bay	Arsenic fixed during pressure leach of zinc concentrate
Miramar Con Mine	Recently switched to the mineral from arsenic trioxide

Table II.1 – Summary of industrial operating practice (as of years 2000/2001) (Harris, 2003), cont..

Placer Dome Campbell	Type II mineral – has been in sucessful operation for over a decade. Autoclave replaced roaster for arsenic environmental reasons
São Bento, Brazil	Most of arsenic fixed in autoclave as Type II mineral. Sufficient iron from this to BIOX® material as arsenical ferryhydrite. Residues are combined
TVX Hellas, Greece	Autoclave was planned, in conjunction with BIOX®
Lime Neutralization – Calcium Arsenate/Arsenite	
Anglo Platinum, South Africa	Lime, but under consideration
Codelco - Chuquicamata	Current process. Very little iron, and residue sent to secure area. Conditions are, however, arid. Alternatives being seriously investigated
Codelco – El Teniente	Calcium arsenate is calcined to impart crystallinity. Material passes TCLP most of the time. However, government has mandated changes of process
Codelco – Potrerillos	Current process
MDK, Bulgaria	No longer acceptable. Ferrihydrite process planned
Noranda Altonorte	Current process. Very little iron, and residue sent to secure area. Conditions are, however, arid
Copper Arsenate	
Cominco, Trail	Process in operation for several years. Product sold in US
Inco, Thompson	Process developed, but not implemented
Mount Isa	Process in operation for several years, combined with solvent extraction. Product sold directly to wood preservative companies in Australia
Outokumpu, Pori	Product sold as wood preservative
San Luis Potosi, Mexico	Developed process, but no market
Arsenic Sulphide	
Rio Tinto Kennecott	Process Successfully operated for several years. Believed to be studying alternatives processes
Arsenic Trioxide	
ASARCO	No longer practiced
Barrick El Indio	Product sold. Stockpile being re-treated
Boliden	No longer practiced
Giant Mine	Evaluation of methods for stockpiled product
Miramar Con Mine	Stockpile reprocessed, initially for sale as pure As_2O_3, but now as stable arsenic mineral

Placer Dome Campbell	Replaced by autoclave operation to form stable mineral
La Oroya	Product mostly sold. Off-spec material stockpiled, needs to be re-treated
San Luis Potosi, Mexico	Product sold into the US

The author's comments on the data shown in Table II are summarized in the following paragraphs (Harris, 2003). The most widely applied method for arsenic removal from mining effluents is the co-precipitation with ferric iron as amorphous ferric arsenates. These precipitates have shown to be adequately stable if the Fe:As molar ratio is higher than 4 (Harris and Krause, 1993); addition of extra ferric iron to the system is often required. It is reported that Inco's CRED plant in Sudbury has been operating for close to thirty years, with no sign of ferrihydrite breakdown, or of arsenic release. The incorporation of small amounts of both cations and anions into the ferrihydrite matrix was shown to delay the recrystallization process of the more stable goethite or hematite, and hence the consequent release of adsorbed ions (Dutrizac and Jambor, 1998). The US EPA considers the arsenical ferrihydrite process as the BDAT (Best Available Demonstrated Technology), and operations applying it correctly have not reported any contamination of local groundwaters. The second most popular approach is the formation of ferric arsenates in autoclaves, at high temperatures. This process has been applied for many years by the gold industry, with success. Similarly, no problem has been identified if the process is carried out in a proper form.

The operations of Noranda and Codelco in Chile are still based on simple lime neutralization. However, the residue formed is not environmentally stable and can react with atmospheric carbon dioxide, releasing soluble arsenic. The Chilean government has indicated that such practices disposal will probably not be tolerated by much longer time, thus research has been carried out to find out alternatives to treat the arsenic wastes. The most obvious conclusion to be drawn is that operations have adopted generally site-specific practices, and the cheapest approach.

According to Harris (2003) the vehicles considered the most appropriate for the elimination of arsenic from mining effluents are scorodite ($FeAsO_4*2H_2O$), together with minerals synthesized in high temperatures and the high iron ferrihydrites. There are other three commercial methods for the control of the arsenic in metallurgic circuits. The most predominant in the past was the roasting of ore or concentrate to form arsenic trioxide. In this process arsenic sulphide is volatilized and subsequently oxidized in the gas phase. With a careful control of the process conditions, a product of purity greater than 95% As_2O_3 can be obtained, and this product can be commercialized with wood preservative industry. Another two of the employed

methods are carried out in aqueous solution, these being sulphide precipitation and the manufacture of copper arsenate. With regard to copper arsenate, it has been demonstrated that arsenic is not released to the environment. However, there is an understandably strong environmental lobby against its use. Copper arsenate has been an effective wood preservative, however this market is small. The sulphide precipitation method is effective, and can remove arsenic to very low levels. However, there are some problems associated with its use, such as the release of toxic gases by formation of hydrogen sulphide. The possibility of encapsulating arsenic sulphide within a glassy block of elementary sulphur is also being investigated. Such materials pass in the TCLP test (Toxicity Characterization Leach Procedure; EPA, 1992), but it was still not demonstrated that the slow devitrification, and the consequent release of arsenic, does not take place.

2.3 Solubilities and stabilities of ferric arsenate compounds

The formations of arsenical ferrihydrites and calcium arsenates are attractive options as these require lower investment and simple technology if compared to the arsenical cements and hydrothermal precipitation routes. However, it is important to consider the long-term stabilities of the different arsenical products (Swash and Monhemius, 1995). Practical alternatives for arsenic disposal together with some considerations about the long-term stability of the arsenical products are shown in Table II.2. Many factors can influence the stability of the solid wastes. Among them, crystallinity, the Fe:As molar ratio and the possible phenomenon of transformation into other solid phases, such as calcium carbonate and goethite can be highlighted. These factors will be discussed in the following sections.

2.3.1 Crystallinity

In order to predict the long-term stability of arsenic wastes, it is necessary to identify the arsenic phase, and to know how this phase responds to diverse environmental conditions. The crystallinity will dictate the rate at which solids will attain the equilibrium with a contacting solution.

Table II. 2.II – Considerations on long term stability for the various arsenic disposal options (Swash and Monhemius, 1995).

Arsenical compound	Long term disposal considerations
Arsenical ferryhydrite (Fe:As > 3:1) Ambient temperature precipitation	• Dehydration leading to a more unstable compound. • Possibility of long-term structural reordering to more stable compounds, e.g. goethite.
Calcium-arsenates + Calcium-arsenites	• High intrinsic solubilities. • Ca-arsenates converted to $CaCO_3$ by CO_2 with release of arsenic. • High lime levels in the precipitated solids results in high pH (11-12), but lime is slowly converted to $CaCO_3$ – leading to reduced pH and increased solubility of the Ca-arsenate compounds.
Crystalline ferric arsenates (Scorodite or Type-2)	• Low solubility over long period of time. • Little physical or chemical change with time. • Long-term stability?
Arsenical slags (up to 10% arsenic)	• Long-term stability unknown – quenched slags show low solubility. • Possibility of recrystallisation – devitrification. • Requires highly specific conditions for incorporation into slag.
Arsenical cements	• Rely mainly on encapsulation for the stabilization of arsenic. • Arsenic may be chemically bond as calcium arsenate phases that are soluble. • If calcium compounds in the cement become fully carbonated, matrix pH will drop, increasing arsenic solubility.

The increase of both the size of particle and crystallinity, primarily via high temperature precipitation or hydrothermal processing are advantages claimed for scorodite precipitation. This would have the effect of decreasing the arsenic release rate by reducing the exposed area of scorodite. According to Welham *et al.* (2000), the more negative free energy determined for the crystalline scorodite indicates that this is the most stable phase and could be expected to be the end product of an amorphous phase transformation at longer time.

2.3.2 Fe:As molar ratio

Different Fe:As ratios in the effluent liquors leads to solid products with different stabilities. The effectiveness of arsenic precipitation and settling rate increases with increasing Fe:As molar ratio (Papassiopi *et al.,* 1996). Swash and Monhemius (1994) demonstrated that the amorphous solids should exceed the Fe:As ratio of 3:1 for the product to be stable in terms of arsenic release and suitable for disposal. If the precipitation takes place with a Fe:As molar ratio greater than 1.0, the ratio will gradually return to 1.0 with the ageing process of the precipitate (Papassiopi *et al.,* 1996). These authors demonstrated that precipitates obtained at higher Fe:As molar ratios were even more stable (leached at 25ºC at pH = 5.0), resulting in a solubility of 0.05mg/L As.

Krause and Ettel (1989) showed that the Fe:As 2:1 precipitate had much lower As solubility than the 1:1 precipitate. For the amorphous 1:1 precipitate, the As concentration was initially 160mg/L at pH = 5.0 and increased to 299mg/L after 678 days (pH = 4.9), thus confirming its instability. The 2:1 precipitates presented an arsenic concentration varying between <0.20mg/L and 0.74mg/L after 893-905 days. The 2:1 basic ferric arsenates continue to show good stability after 2.5 years of ageing and have not broken down to produce the more soluble amorphous $FeAsO_4.xH_20$. According to these authors, arsenic solubility in a scorodite sample varied between 3.6 and 0.4mg/L at pH next to 5.0. This solubility value is about two orders of magnitude lower than those from the amorphous precipitates.

2.3.3 Carbonation with atmospheric CO_2

Calcium arsenate compounds, may react with atmospheric CO_2, thus being transformed into calcium carbonate, and leading to the release of chemically bound arsenic. The calcium arsenate precipitation carried out with lime ($Ca(OH)_2$) results in a high pH level of 11-12 in the metallurgical wastes. However, the excess lime is converted to calcium carbonate ($CaCO_3$), leading to reduced pH and increased calcium arsenate solubility (Swash and Monhemius, 1995).

2.3.4 Transformation into goethite

According to Krause and Ettel (1989), crystal-aging causes the amorphous ferric oxyhydroxide to be transformed into goethite (α-FeOOH) as a result of the loss of unstructured water. With time it is possible the transformation to α-Fe_20_3 (hematite). The many transformations occurring during this process can be expressed by the following equation:

$$\alpha\text{-FeOOH(aq)} \Rightarrow \alpha\text{-FeOOH} \Rightarrow \alpha\text{-}Fe_20_3\text{(aq)} \Rightarrow \alpha\text{-}Fe_20_3 \qquad (2.1)$$

It is possible that the stability of basic ferric arsenates is influenced by phase changes of a similar nature. However, the kinetics of decomposition to FeOOH is not known. The presence of scorodite after the aqueous oxidation of arsenopyrite suggests that the conversion rate is geologically slow (Welham *et al.*, 2000).

2.4 Fundamentals of precipitation

2.4.1 Precipitation processes (Söhnel and Garside, 1992)

Precipitation, or reactive crystallization, can be treated as a separation process, where a solid phase is created from a supersaturated liquid phase. The precipitation is a fast process, as a consequence of the high supersaturation level at which it happens. This high supersaturation ensures that primary nucleation rates are usually very high and because of this, nucleation has an important role in the precipitation processes. A large number of crystals is formed, which limits the average size to which the crystals

can grow. A number of secondary processes such as ageing, ripening, coagulation and agglomeration may occur if the precipitated crystals are sufficiently small, and these processes can cause significant changes in the final particle size distribution and in the product chemical stability. The precipitation processes usually take place at constant temperature. Frequently, the necessary supersaturation results from a chemical reaction, being important to consider the mixing mechanism because many such reactions are fast.

The properties of the precipitated particles have a great importance on its applications, in particular, the crystal size distribution and the corresponding solid specific surface area. Together with the particle habit or morphology, the particle size distribution has a major impact on the particle-processing characteristics. Many precipitated products can form a range of polymorphs, amorphous phases. In most of the applications, only one specific phase is acceptable and so the precipitation conditions need to be controlled in order to ensure the formation of the desired product. Also, the crystallinity degree of the product may be important.

Precipitation involves many steps and kinetics processes, which are illustrated in Figure 2.3. The time over which precipitation occurs can vary greatly, but the relative importance of the different rate processes always change during the course of a given reaction.

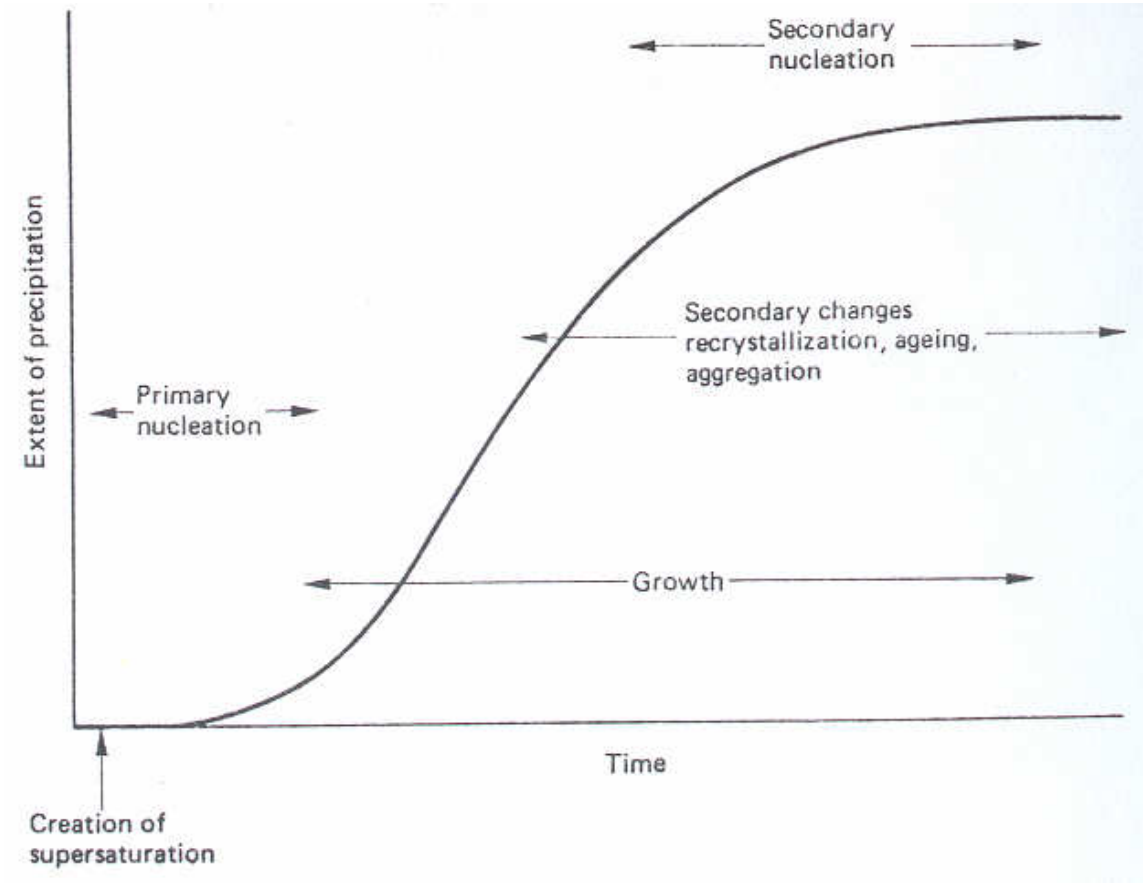

Figure 2.3 – Kinetic processes involved in precipitation (Söhnel and Garside, 1992).

Supersaturation is a very important parameter in any precipitation process; the level of supersaturation governs the rates of the different processes, such as nucleation ad crystal growth. In precipitation processes the level of supersaturation is often very high, resulting in high nucleation rates. Changes between different hydrates, polymorphs or other solvates are controlled by the kinetics of transformation. If the solid phase forms a number of crystalline modifications, a mixture of forms may be produced and, over a period of time, the thermodynamically less stable form will be transformed into the more stable one.

2.4.2 The driving force for crystallization

To induce crystallization or precipitation from a solution, the thermodynamic state of the system has to be shifted away from the conditions of phase equilibrium, so a driving force is needed. In these processes, the driving force is called supersaturation, and there are many ways to induce it in a solution. If solubility increases with temperature, cooling may be used to supersaturate the solution. On the other hand, for systems where the solubility decreases with temperature, heating can be used. Evaporation is typically used when the solubility is not a strong function of temperature. Elevated pressures may be mechanism to precipitate a particular crystal phase, which is not stable at atmospheric pressure. Another form to induce supersaturation is to add another component (anti-solvent) in the solution, reducing in this way the solubility of the solute. In precipitation processes the insoluble species are produced by chemical reaction (Söhnel and Garside, 1992).

The crystallization rate is often determined by the supersaturation degree, and the crystallization process takes place only in supersaturated phases (Mersmann *et al*., 2001). The supersaturation (S) can be expressed as a difference in concentration ($\Delta C = C - C_{eq}$) or as a relative supersaturation

$$S = \frac{C}{C_{eq}} \tag{2.2}$$

where C is the solute concentration and C_{eq} the equilibrium solubility of the solute at the temperature and pressure of the system. However, considering ionic species, the dissociation into anions and cations can occur, as presented in the equation 2.3.

$$A_x B_y \longleftrightarrow xA^{z+} + yB^{z-} \tag{2.3}$$

where z is the valency of the ions. In this case, the equilibrium constant may be expressed by the following equation:

$$K_{eq} = \left(a_{eqA}\right)^x \left(a_{eqB}\right)^y \tag{2.4}$$

where a_{eq} is the equilibrium activity; the supersaturation may be expressed by

$$S = \left(\frac{(C_A)^x (C_B)^y}{K_{eq}} \right)^{\frac{1}{(x+y)}} \quad (2.5)$$

For x = y = 1 and $\gamma_A = \gamma_B = 1$, where γ_A and γ_B are the activity coefficients of the species A and B, the equation 2.5 will be reduced to

$$S = \frac{C}{C_{eq}} = \frac{\sqrt{C_A C_B}}{\sqrt{Keq}} \quad (2.6)$$

Crystallization is usually the result of the three processes; (i) nucleation, (ii) growth and (iii) secondary changes, for example, agglomeration, ageing and recrystallization. Depending on the reaction conditions, these processes can proceed either in series or in parallel, during whole or only a part of the crystallization.

2.4.3 Nucleation

The formation of a solid phase by nucleation from a liquid is only possible if this liquid is supersaturated. The nucleation can occur by two different mechanisms called primary and secondary nucleation. Primary nucleation is the creation of a new phase from a clear liquid. This type of nucleation can be classified into homogeneous and heterogeneous. In the homogeneous nucleation, a solid substrate is absent and the formation of a new phase results from local fluctuations in concentration caused by the formation of numerous clusters. The occurrence of homogeneous nucleation is rare in practice; heterogeneous nucleation is in general the dominant mechanism. In heterogeneous nucleation, a foreign substrate (seeds), usually comprised of very small particles is present in solution on which nucleation will start (Söhnel and Garside, 1992).

Secondary nucleation, on the other hand, only happens because of the prior presence of the material being crystallized. In opposite to the relative high supersaturation required for primary nucleation, secondary nucleation already occurs from low to moderate values of supersaturation. There are different types of secondary nucleation

called as: (i) initial breeding, when dry seed crystals are introduced into the solution; (ii) dendritic breeding, where the corners and edges of the crystals suffer a higher supersaturation than the middle of the faces; (iii) contact nucleation that results from collision between the crystals and the impeller blades, the crystals and vessels walls or between crystals; and (iv) fluid shear breeding, that happens due to the turbulent fluid shear forces exerted on a crystal surface (IPT, 2004).

The mechanisms, which govern primary and secondary nucleation, are different, thus resulting in very different rate expressions. Therefore, the relative importance of each nucleation process varies with each specific precipitation reaction.

2.4.4 Crystal growth

After nucleation has taken place, the next step is to reduce the free energy of the small nuclei by growing it to larger sizes (Lawrence *et al*., 1986). The growth rate of the crystal faces determines the crystal shape, and also the surface structure and the purity of the crystal (IPT, 1997). Crystal growth can be controlled by diffusion through the crystal surface, reaction at the interface, and incorporation of the growth units into the crystal lattice. Generally, in an unstirred system the growth rate is diffusion-controlled. On the other hand, in the agitated system it is considered that the surface reaction becomes the rate-limiting step (Lawrence *et al*., 1986). The concentration profile perpendicular to the crystal surface during the growth process is shown in Figure 2.4.

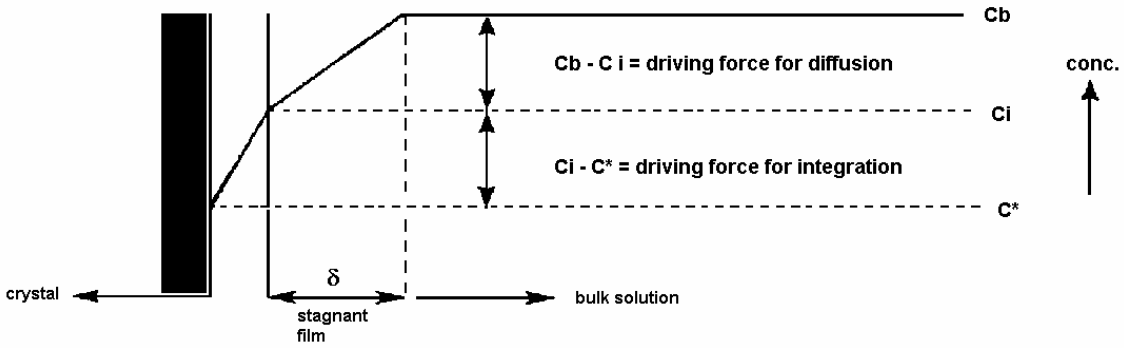

Figure 2.4 – Concentration profile perpendicular to the crystal surface during growth (IPT, 1997).

The bulk concentration is represented by c_b, c_i is the concentration at the crystal-solution interface and c* is the equilibrium concentration - the concentration where will happen the incorporation into the crystal surface, and consequently the crystal growth.

For very soluble compounds, the surface integration is not rate limiting, and the growth rate is determined by diffusion through the stagnant film with thickness δ at the interface. The driving force for the diffusion is then defined as c_b-c*, since c_i = c*. On the order hand, for compounds with very low solubility the incorporation of the growth units into the crystal lattice is rate limiting, and the driving force for this process is given by c_b-c*, since $c_i = c_b$. However, for the great part of the compounds both the diffusion through the crystal surface and the incorporation of the growth units into the crystal surface has to be taken into account. For very concentrated solutions, the transport of crystallization heat through the bulk phases becomes a third rate-limiting step (IPT, 1997).

2.4.5 The Mixed Suspension Mixed Product Removal (MSMPR) precipitator

The model known as Mixed Suspension Mixed Product Removal - *MSMPR* is based on the following assumptions (i) absence of particles in the feed, (ii) absence of attrition between particles, (iii) a steady state operation, and (iv) the system is perfectly mixed - the composition of the suspension leaving the reactor is identical to that at any point within the reactor (Söhnel and Garside, 1992). A schematic representation of a *MSMPR* precipitation reactor is shown in Figure 2.5:

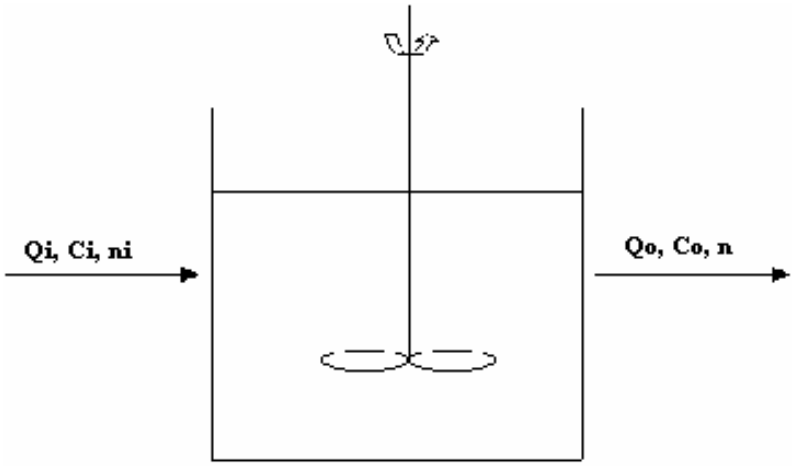

Figure 2.5 – Schematic representation of an *MSMPR* reactor of effective volume *V* (L) being fed by a solution of concentration c_i (mol/L) at rate Q_i (L/s) and suspension discharge at rate Q_0 (L/s) with solute concentration c_0 (mol/L).

To describe the crystal size distribution in a crystallizer operating in a continuous regimen it is necessary to apply the laws of mass conservation, energy and number of crystals and further to quantify the kinetics of nucleation and growth of crystals (Söhnel and Garside, 1992). To consider steady state condition implies that the feed rate, composition, temperature and the crystallizer volume remain constant. If the system operates at steady state, the number of crystals in a specific size range must be kept constant without accumulation. Considering an arbitrary size range L_1 to L_2 in the volume *V*, with population density n_1 and n_2 respectively, and that the growth rate of crystals of size L_1 is G_1 and that of size L_2 is G_2; for a period of time *t*, the number of crystals entering and leaving the reactor in this size range is given by equations 2.7 and 2.8, respectively (Randolph and Larson, 1998).

$$Vn_1G_1\Delta t \tag{2.7}$$

$$Vn_2G_2\Delta t \tag{2.8}$$

If the feed stream contains seed crystals in this range, then the distribution size in a volume *V* of the feed is

$$Q_i \bar{n}_i \Delta L \Delta t \tag{2.9}$$

where Q_i the volumetric flow rate, $\bar{n}_i$ is the average population density in the range L_1 to L_2 in the feed, and $\Delta L = L_2 - L_1$. For the bulk flow of crystals, the size distribution is given by

$$Q \bar{n} L \Delta t \tag{2.10}$$

By combining the equations (2.7), (2.8), (2.9) and (2.10), the population balance in a steady state is given by

$$Q_i \bar{n}_i \Delta L \Delta t + V G_1 n_1 \Delta t = Q \bar{n} L \Delta t + V G_2 n_2 \Delta t \tag{2.11}$$

After a mathematical rearrangement and considering a system without seeds in the feed solution (n_i=0), the population balance obtained for a *MSMPR* crystallizer becomes described by equation (2.12):

$$\frac{V}{Q} d(Gn)/dL + n = 0 \tag{2.12}$$

Assuming that *G* is not a *L* function and defining τ, the mean residence time, as *V/Q,* the equation becomes:

$$G\tau(dn/dL) + n = 0 \tag{2.13}$$

The equation (2.13) is integrated.

$$\int_{n^0}^{n} \frac{dn}{n} = -\int_{0}^{L} \frac{dL}{G\tau} \tag{2.14}$$

By defining n^o as the population density of the embryo-size crystals and assuming that these crystals will be decrease close to zero, the solution of this integration gives

$$n = n^0 \exp(-L/G\tau) \tag{2.15}$$

The parameter n^o is related to the nucleation kinetics according to equation (2.15) (Randolph and Larson, 1998).

$$B^0 = n^0 G \tag{2.16}$$

So, equation (2.15) can be rewritten as

$$n = \frac{B^0}{G} \exp(\frac{-L}{G\tau}) \tag{2.17}$$

This equation is widely used to analyze the behavior of *MSMPR* crystallizers. The equation indicates that when the mean residence time is increased, the average crystal size is also increased. However, this relationship is not simple. Although an increase in τ increases the time of crystal growth, it simultaneously causes the decrease of supersaturation, and hence of the growth rate. The average crystal size, which is proportional to the product $G\tau$, therefore increases less than does the value of τ. The supersaturation in the precipitator can not be established arbitrarily and an appropriate value to the particular feed concentrations, residence time, and kinetics of nucleation and growth is achieved (Söhnel and Garside, 1992).

In order to evaluate more adequately the results of experiments performed in a *MSMPR* crystallizer, equation 2.17 is rearranged as:

$$\ln n = \ln\left(\frac{B^0}{G}\right) - \frac{L}{G\tau} \tag{2.18}$$

A plot of ln(*n)* versus crystal size (*L)* gives the nucleation rate (B^o) by the intercept of the straight line on the Y-axis. The slope ($-1/G\tau$) of provides the growth rate (*G*) (Söhnel and Garside, 1992).

Some deviations in the MSMPR original assumptions may occur, due to mechanical (residence times that lead to attrition and breakage) or kinetic effects (slurry not ideally mixed, product classification removal, fines dissolution, particle agglomeration, size dependent growth and growth dispersion) (Mersmann *et al*., 2001). These deviations may affect the crystal size distribution as presented in Figure 2.6. In these cases the *MSMPR* crystallizer model can not be applied.

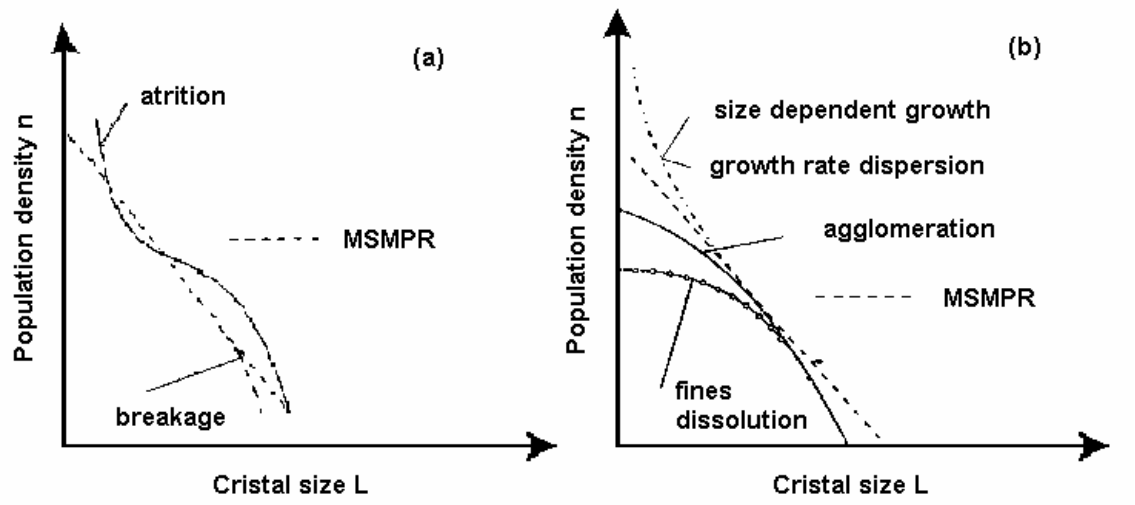

Figure 2.6 – Deviation from the straight line (a) due to mechanical effects (b) due to kinetic effects (Mersmann *et al*., 2001).

3 ARSENIC REMOVAL FROM DILUTE INDUSTRIAL EFFLUENTS BY SCORODITE PRECIPITATION

3.1 Introduction

As indicated in the literature review, the crystalline ferric arsenate, crystalline scorodite ($FeAsO_4*2H_2O$), has been considered as a preferable form for arsenic disposal because of its relatively high arsenic content and low solubility in water (typically smaller than 1mg/L arsenic at pH 5, when subjected to 24 hour toxicity characteristics leaching procedure – TCLP) (Filippou and Demopoulos, 1997). The relatively low Fe/As molar ratio (1:1 against approximately 4:1 in AsFH), the smaller waste volume due to its higher density, and the good capacity of sedimentation offer additional advantages for this disposal process in comparison to the conventional ferrihydrite process (Debekaussen *et al.*, 2001).

According to Krause and Ettel (1989) the solubility of this phase is about two orders of magnitude smaller than that of the amorphous ferric arsenate ($FeAsO_4.xH_2O$), expected to be found in arsenical ferryhydrites – AsFH, which is the most common form of arsenic disposal from mining effluents. The concentration of arsenic, 3-6% in arsenical ferrydrites, may be increased to about 25-30% in scorodite.

The literature provides a number of references describing the hydrothermal production of scorodite. Dutrizac and Jambor (1988) produced crystalline scorodite by precipitation from a solution containing 0.3mol/L $Fe(NO_3)_3$ and 25g/L As(V), pH near to 0.7 and 24 hours. According to the authors, it is necessary to maintain the temperature higher than 125ºC to assure a good crystallinity of the solid, the preferred temperature being 160ºC. Swash and Monhemius (1994) studied the hydrothermal precipitation of scorodite from aqueous solutions containing iron (III), arsenate and sulfate at temperatures of 150 to 225ºC. These authors showed that more than 90% of the arsenic can be precipitated from solutions under conditions of pH <1, a molar ratio Fe:As >1, and temperatures above 150ºC. The solids formed are crystalline and can be a defined compound or a mixture of scorodite and two other arsenate compounds that have been designated as Type-1 ($Fe_2(HAsO_4)_3.zH_2O$) and Type-2 ($Fe_4(AsO_4)_3(OH)_x(SO_4)_y$). The results obtained by Swash and Monhemius (1995)

showed that above 175ºC, basic iron sulfate and Type-2 arsenate are formed, from a mixture of iron(III) sulfate and As(V) solutions, with a high sulfate to iron molar ratios. On the other hand, at lower temperatures (150-175ºC) scorodite predominates. Papangelakis and Demopoulos (1990) showed that scorodite is one of the main products of the aqueous pressure oxidation of arsenopyrite in sulphuric acid solution (0.5mol/L), after 2 hours and temperatures of 130 to 180ºC. The high costs of a hydrothermal operation make this process economically attractive only if it can be combined with the processing of a valuable concentrate, such as gold.

Due to the aforementioned advantages related of the precipitation of arsenic as scorodite, there have been attempts in order to develop a process to be carried under conditions that are more benign. Demopoulos and co-workers (Demopoulos *et al*., 1995; Filippou and Demopoulos, 1997; Debekaussen *et al.*, 2001; Demopoulos, 2005; Singhania *et al.*, 2005) demonstrated the possibility to precipitate scorodite at conditions of ambient pressure, and temperatures below the water boiling point. The process involves a strict control of supersaturation and addition of seeds. The crystal growth is favored in opposition to homogeneous nucleation, and as a result, the precipitation of an amorphous phase is prevented. The underlying principle of the process is schematically shown in Figure 3.1.

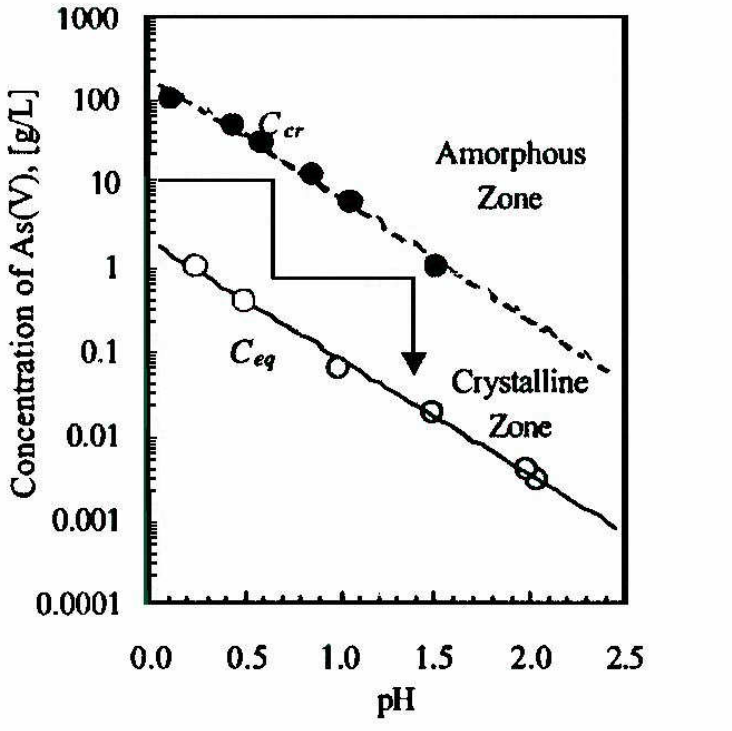

Figure 3.1 – Supersaturation control area for atmospheric precipitation of scorodite, where C_{eq} is the equilibrium concentration and C_{cr} is the critical supersaturation (95ºC, Fe:As = 1.0, and sulfate media) (Demopoulos, 2005).

According to Figure 3.1, the equilibrium line (C_{eq}) and the critical supersaturation line (C_{cr}) defines a working region for scorodite precipitation, as a function of pH and arsenic concentration [As]. The pH is the most important variable in this process. A fast increase in pH will result in high supersaturation, which is unwanted. The conditions at the critical supersaturation line (C_{cr}) must not be exceeded, and this limit is defined by the induction pH, and corresponds to the pH in which the homogeneous nucleation will occur (Fillipou and Demopoulos, 1997). According to Singhania *et al.* (2006) the solution pH is raised up to the induction pH and once the precipitation of an amorphous phase had been noted, H_2SO_4 is added in the system to clear the solution. Thus, a pH lightly below the induction pH is assured. Therefore, a more practical way to adjust supersaturation is needed.

Another important aspect of the atmospheric scorodite production is the requirement of scorodite seeds. Filippou and Demopoulos (1997) showed that in sulfate media, seed concentrations of 50g/L or higher are needed to accelerate the crystallization

kinetics, and that more than 90% of arsenic was removed from solution in three hours as crystalline scorodite. The scorodite seeds were produced from nitrate solution in an autoclave at 150ºC. Wang *et al*. (2000) also studied scorodite precipitation in sulfate media. It was shown that the arsenic removal increases with the increase of seeds concentration. In the absence of seeds, the crystallization was found to be slow and inefficient. These authors showed that about 90% of the initial 10g/L of arsenic present in the solution was precipitated in the first hour, using 160g/L of seeds. The experiments were carried out at 95ºC, Fe/As molar ratio of 1:1 and pH 0.9, in two hours of reaction. Caldeira e*t al*. (2005) showed that 200g/L of scorodite seeds were needed to assure 80% arsenic removal from an industrial solution with 1g/L of As. The initial seeds were produced at 95ºC for 12 hours. It is not well understood the relationship between amount of seeds and surface area; thus it would be relevant to establish a selection criteria based on the primary variable affecting crystal growth – the specific surface area (SSA) - rather than on the empirical selection of the amount of seeds.

In some cases, the scorodite crystallization requires the addition of a neutralizing agent, and lime (CaO) or limestones ($CaCO_3$) are the preferred ones owing to their relatively low cost (Demopoulos, 2005). The industrial solution presents sulfate that reacts with calcium thus forming gypsum, so it became interesting to test gypsum efficiency as seed material for scorodite precipitation. Wang *et al*. (2000) and Singhania *et al.* (2005) showed that hematite or gypsum, formed from the neutralization reaction with lime or limestone, can be used as seeds in the precipitation of scorodite. Demopoulos (2005) claim that either gypsum added from an external source or generated in *situ* by neutralization reactions are excellent seeding materials. The adopted experimental conditions by Demopoulos (2005) were initial arsenic concentration of 10g/L, iron arsenic molar ratio of 1:1, 95ºC and 2 hours of reaction. An important aspect about the use of gypsum seeds is that, according to Singhania *et al.* (2005), the gypsum decreases the TCLP solubility of the precipitates. The results obtained by these authors showed that the mixed gypsum/scorodite presents an arsenic leachability of 1 to 2 mg/L against 3mg/L of the pure scorodite.

Debekaussen *et al.* (2001) showed that 90% of arsenic could be removed as scorodite from synthetic solutions containing initial arsenic concentrations of 33g/L,

50g/L and 100g/L. Wang *et al*. (2000) showed that arsenic concentration could be reduced from a solution of 10g/L, with an overall arsenic removal of 99.4%, in two stages, without pH control. Demopoulos (2005) worked at the same condition as Wang *et al*. (2000) and obtained an overall arsenic removal higher than 98%. Therefore, yields superior to 90% have been reported for arsenic removal from solutions of 10g As/L or higher. Caldeira e*t al.* (2005) showed that 80% of arsenic could be removed in one stage from an industrial solution containing 1.5g/L As. Wang *et al*. (2000) and Demopoulos (2005) reached an arsenic removal of only 11.4% and 7%, respectively, working with an initial arsenic concentration of approximately 0.5g/L in a second stage of precipitation. Therefore, it is not clear how the efficiency of arsenic removal varies with the initial arsenic concentration and what would be the concentration threshold for which the process would be competitive with ferrihydrite precipitation process.

Despite its potential advantages, the precipitation of scorodite at ambient pressure has not been implemented in industrial scale. Difficulties such as the cost of the reagents required for the oxidation of iron and arsenic in the treatment of large volumes of solutions and the difficulty in controlling pH (i.e. supersaturation) at high temperatures are probably some of the factors that explain the lack of industrial applications. As most of the reported studies were carried out with reagent-grade sources of arsenic and iron, it is not really clear how would be the performance of the process in comparison with the ferrihydrite precipitation for the treatment of more complex (multicomponent and diluted) solutions.

The present work investigates the removal of arsenic from a dilute solution produced in a washing tower of the exit gas in the roasting of a refractory gold ore. Arsenic is currently removed as arsenical ferryhydrite (3-6% As) and disposed as a toxic waste in tailings dams. The expansion of the roasting plant motivated the search for process alternatives, such as scorodite precipitation. The scorodite precipitation is expected to combine an adequate stability of the residues according to the environmental legislation and a decrease of the disposal areas. The effect of the initial arsenic concentration is evaluated in detail in order to establish the yields in systems more diluted than those reported in the literature. The effect of the seeds concentration on arsenic removal is also evaluated, with emphasis on the specific surface area rather

than on the mass of seeds. The effect of sulfate concentration and the performance of the gypsum seeds also are investigated. Finally, the solubility of the precipitated are evaluated according to the Toxicity Leaching Procedure -TCLP (EPA, 1992).

3.2 Experimental Procedure

An industrial solution containing 1.1 g/L As (As_{total} = 1.1g/L; As(III) = 0.96g/L; Fe_{total} = 0.15g/L, Fe(II) = 0.13g/L; pH = 2.3; SO_4^{2-} = 2.85g/L; Cu = 7.6mg/L; Ni = 0.51mg/L; Mn = 25.1mg/L) and Fe/As molar ratio equal to 0.2, provided by *AngloGold Ashanti*, *Nova Lima (MG),* was used as the feed solution. Firstly, it is necessary an oxidation step of iron and arsenic present in the solution. According to Debekaussen *et al.* (2001) this oxidation must be carried out at high temperature and controlled addition of hydrogen peroxide (H_2O_2). However, Caldeira *et al.* (2005) showed that the oxidation is not significantly affected by the temperature, and with a controlled addition of H_2O_2 a complete iron and arsenic oxidation is observed in 20 minutes. In this work the oxidation was carried out in a stirred reactor and ambient temperature according to the conditions established by Caldeira *et al.* (2005). Ferrous sulfate or ferric chloride salts were added to the system in order to adjust the Fe/As molar ratio to 1, which is required for the formation of scorodite. After the Fe/As ratio was adjusted, hydrogen peroxide was added (1.75mol/L, 20% stoichiometric excess) in a amount to assure the total oxidation of Fe(II) and As(III). The pH was kept at 1.2 (mensured at 25ºC), with the addition of concentrated H_2SO_4, in order to avoid the precipitation of the amorphous arsenate phases.

Seeds were used in the precipitation tests in order to increase the reaction rate. According to Singhania *et al.* (2005), the best seed material is the fine hydrothermal scorodite. In the present work, the preparation of the seeds was carried out in a 2L PARR autoclave using concentrated $Fe_2(SO_4)_3.xH_2O$ and $Na_2HAsO_4.7H_2O$ (Fe/As molar ratio of 1:1) solutions prepared with reagent grade chemicals. The initial arsenic concentration was 33g/L or 25g/L, and the pH of 1.3 or 1.5, respectively, adjusted with the addition of sulfuric acid. The temperature was kept at 150ºC, and the reaction time was of 2 hours.

Following the oxidation of Fe(II) and As(III) and seeds production, the experiments of batch precipitation were carried out in a stirred reactor (1L). The temperature was maintained at 95ºC while the Fe/As molar ratio was within a range of 0.9 to 1.2. After a reaction time of two hours, the solids were vacuum filtered and the solution was diluted using 50µL of concentrated nitric acid to prevent the formation of amorphous solid material. A comparative study of scorodite and gypsum seeds (calcium sulfate P.A -$CaSO_4$*$2H_2O$) was also carried out. The effects of the initial arsenic concentration and sulfate concentration on arsenic removal have been evaluated as well. A schematic flowsheet of the process is shown in Figure 3.2.

Preliminary tests were carried out in triplicate to evaluate the experimental error. Different initial arsenic concentration (0.1 and 1g/L) and scorodite seed concentrations (10 and 40g/L) were evaluated. The standard deviation remained in a range of 1.3 – 7.3% with respect to arsenic removal. However, a small variation in pH was found to affect the arsenic removal, due to fluctuations in supersaturation. Thus, the standard deviation of the results includes a variation of 10% in the adopted pH value.

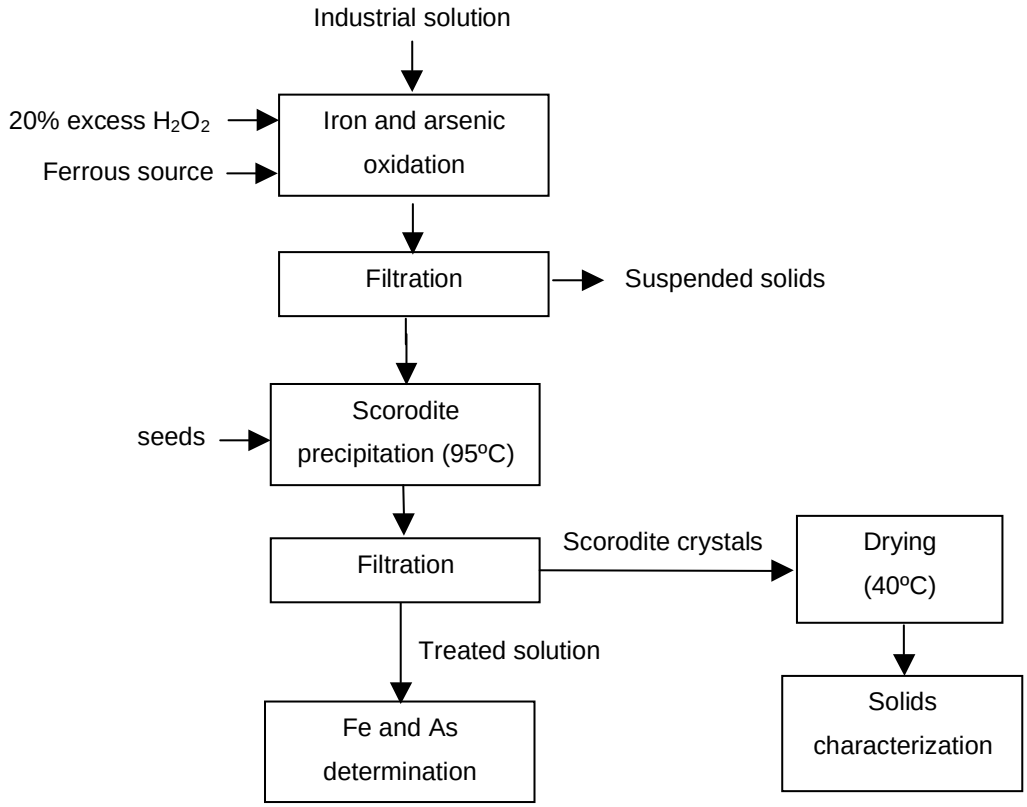

Figure 3.2 – Block diagram of the experimental procedure in tests carried out in batch system.

The As_{total} and Fe_{total} concentration were determined by atomic absorption spectrometry (Perkin Elmer AAnalyst 300), with the air/acetylene flame (wavelength of 328.1nm and 248.3nm for As_{total} and Fe_{total}, respectively). The SO_4^{2-} concentrations were determined by turbidimetry (Micronal model B382) according to the procedure described in the Standard Methods for the Examination of Water and Wastewater (1998). The scorodite seeds produced in autoclave, and the products obtained in the precipitation tests were dried at 40ºC for 24 hours, and characterized by X-ray diffraction (Philips model PW1710), scanning electron microscopy (MEV) (JEOL model JSM-6360L VI coupled to an energy dispersive spectrometer - EDS), and Micro-Raman spectroscopy (Jobin Yvon/Horiba model LabRam HR 800). In the micro-Raman analyses a He-Ne laser with 632.8nm wavelength and power output of 20mW was used as the excitation source with a liquid nitrogen cooled CCD. In order to

obtain the MEV images, the samples were covered with a carbon layer to assure the electron conduction and heat dissipation. The particle size distribution and the specific surface areas were determined by laser scattering (Cilas 1064) and nitrogen adsorption (Quantachrome, model Nova 1200). Leaching tests were carried out in order to examine the solubility of the precipitates, according to the Toxicity Characterization Leach Procedure -TCLP tests, recommended by the US Environmental Protection Agency (EPA, 1992). This procedure was recently adopted as the ABNT NBR-10005/2004. Nevertheless, the maximum accepted limit for arsenic concentration in the extract (1.0mg/L) by the Brazilian standards (ABNT, 2004) is five times smaller than that allowed by the American standards. The determination of arsenic and iron concentrations in the extract was carried out by an ELAN ® 9000 ICP-MS instrument (Perkins Elmer SCIEX, Concord, Ontario, Canada).

3.3 Results and discussion

3.3.1 Effect of pH and Initial arsenic concentration

At fixed arsenic and iron concentrations, pH becomes the most important process variable, once it determines the supersaturation level in the system. An increase in supersaturation provides an increase in the driving force for precipitation, and consequently an increase of arsenic removal from solution. A general definition of relative supersaturation is provided by the equation:

$$S = \frac{C}{C_{eq}} \tag{3.1}$$

where C is the solute concentration and C_{eq} the equilibrium solubility of the solute at the temperature and pressure of the system.

In the present work the dissociation of the ionic species into anions and cations was considered (pH<2.0), and supersaturation was defined by the initial concentrations of iron, arsenic, and by the initial pH.

$$FeAsO_4 * 2H_2O_{(s)} + 3H^+ \rightarrow Fe_{(aq)}{}^{+3} + H_3AsO_{4(aq)} + 2H_2O \quad (3.2)$$

At a constant temperature and pH, S was calculated by

$$S = \frac{\sqrt{C_{As}C_{Fe}}}{\sqrt{\left(C_{eqAs}\right)^2}} \quad (3.3)$$

where C_{As} and C_{Fe} are the arsenic and iron concentrations and the C_{eqAs} is the equilibrium concentration of arsenic in the adopted pH, according to the literature (Demopoulos, 2005).

The pH is expected to decrease during scorodite precipitation owing to the production of sulfuric acid (Eq. 3.2). The variation becomes less evident at low arsenic concentration. Demopoulos (2005), Singhania *et al.* (2005) and Singhania *et al.* (2006) showed that once the precipitation has been initiated, the control of pH becomes unnecessary. According to these authors, the pH control even slows down the reaction rate by the formation of amorphous phases in areas with high local supersaturation. The formation-redissolution of these amorphous phases is believed to decrease the process rate (Singhania *et al.,* 2006). Thus, it is important to define an initial pH that guarantees that the reaction will occur within the working region defined in Figure 3.1. The literature describes values for the induction pH at 95ºC (Figure 3.1). In order to adjust the pH, a complex procedure involving the dissolution of the initial precipitates is described in the literature (Singhania *et al.*, 2006).

In the present work, pH was measured at ambient temperature. The so-called adopted pH is the one, close to the induction pH, that did not cause the precipitation of solids with the elevation of the temperature. A “practical” critical supersaturation line (C_{cr}), defined by an induction pH measured at ambient temperature, was established (Figure 3.3). The supersaturation was calculated according to Eq. (3.3). Table III.1 summarizes the removal obtained for the different initial arsenic concentrations and the initial (Si) and critical (Scr) supersaturation. The critical supersaturation was estimated considering the critical arsenic concentration in the induction pH value, according to the solubility curve (Demopoulos, 2005). Arsenic removal can not be

related to the Si values as each experiment was carried out under different pH condition. The largest Si value corresponds to the adopted pH closest to the induction pH. Supersaturations in a range of 1.3 - 7.3 were found under equilibrium conditions (t> 1h). The critical supersaturation value was not exceeded in any condition.

Table III.I – Removal obtained at different initial arsenic concentration (seeds concentration = 40g/L, T = 95ºC).

$[As]_i$ (g/L)	Induction pH[1] (95ºC)	Adopted pH (25ºC)	Removal (%)	Si	Scr
0.1	2.3	1.6	94.6/89.0	8.1	75
0.5	1.8	1.1	80.5	4.1	85
1.1	1.5	1.1	93.8/92.4	9.9	100
2.4	1.3	1.2	86.3	46.5	100
10.0	0.9	0.6	90.2	19.8	60

[1] Demopoulos (2005).

The effect of the initial arsenic concentration was investigated within a range from 0.1 to 10 g/L. Less concentrated solutions were prepared by dilution of the original industrial solution (1.1g/L As). Sodium arsenate ($Na_2HAsO_4.7H_2O$) was added to increase arsenic concentration at levels higher than that in the original solution. The pH was adjusted according to the initial arsenic concentration.

The results showed that it is possible to precipitate scorodite from industrial solutions with arsenic concentration of approximately 1g/L. Figure 3.4 shows the decrease of arsenic concentration for the different initial concentrations. The arsenic removal from solutions with concentrations of 0.5 and 0.1g/L was of 80.5 and 94.6%, respectively. Residual arsenic concentrations of 90mg/L and 10mg/L (Figure 3.4) are higher than the limits established by legislation for arsenic discharge (0.2mg/L). Thus, a subsequent polishing stage is necessary. However, the amount of iron required to precipitate arsenic in a polishing stage of co-precipitation with Fe(III)/As(V), at pH 4, would be very low if compared with the amount of iron in the current AsFH

precipitation. Furthermore, the fine amorphous ferryhydrite may be recycled as seeds to the scorodite reactor. Thus, an industrial waste more stable and with larger arsenic concentration can be formed, in comparison with the traditional ferrihydrite process. Furthermore, both the waste volume and the associated costs with the final residue disposal can be reduced.

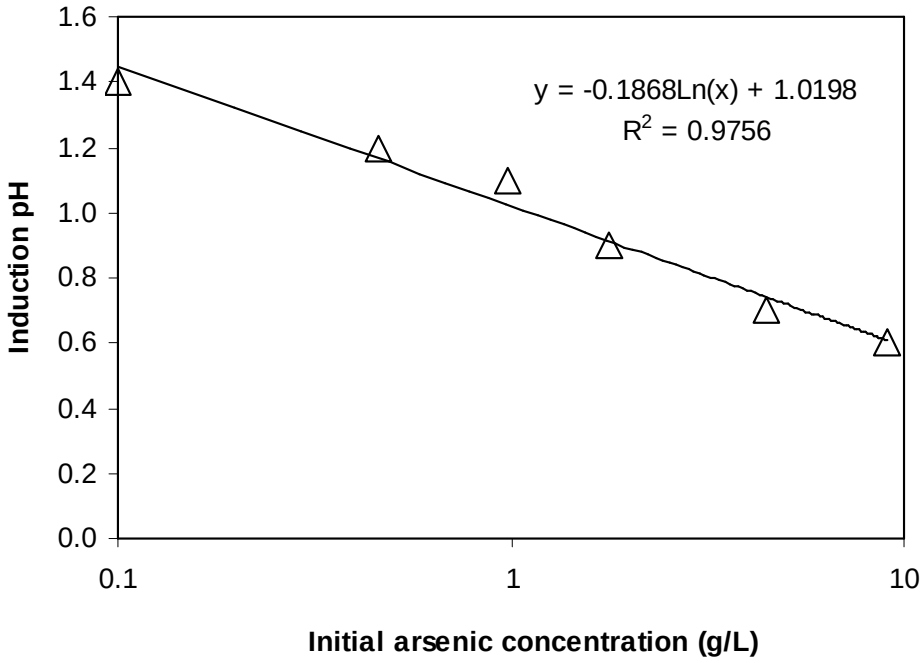

Figure 3.3 – Critical supersaturation line (C_{cr}), defined by an induction pH measured at ambient temperature.

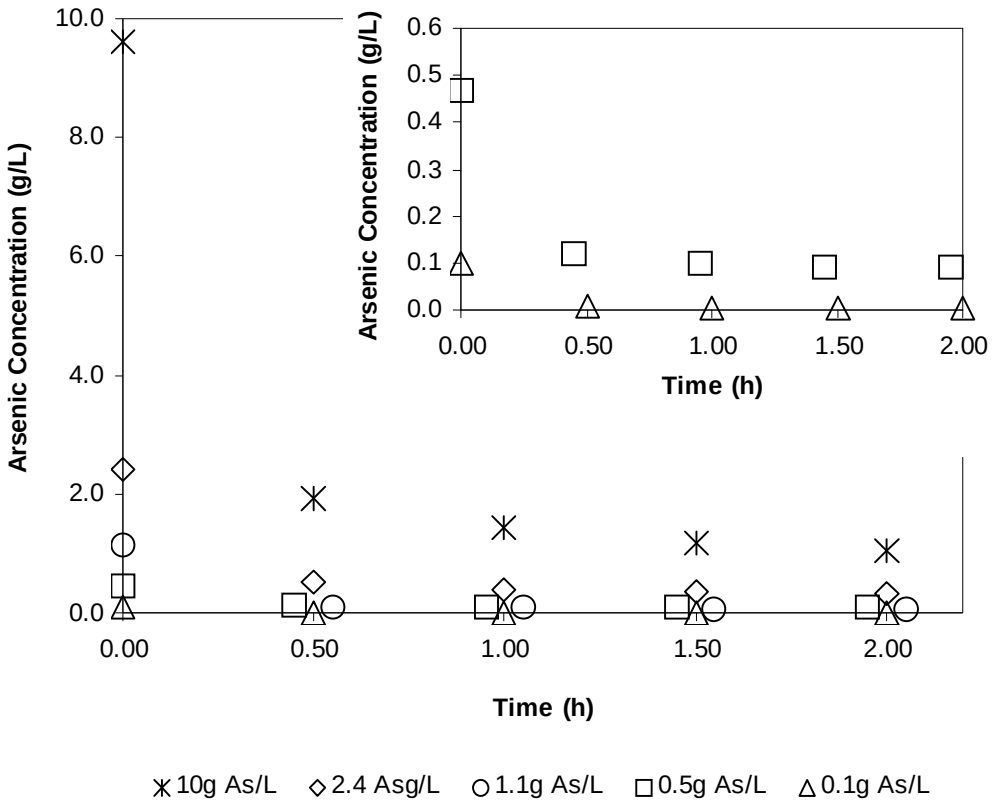

Figure 3.4 – Scorodite precipitation at different initial arsenic concentrations (T = 95ºC, scorodite seeds concentration = 40g/L).

3.3.2 Effect of seed concentration

Figure 3.5 shows the decrease of arsenic concentration in the industrial solution for different seed concentrations. In these experiments the initial supersaturation, calculated according to Eq. (3.3), varied in a range of 7-10, well below the Scr value (100) for an adopted pH of 0.9. Under equilibrium conditions, supersaturation remained close to a value of 2. The results showed that arsenic removal is possible, even for the lowest seed concentration (5g/L), that yielded 73% of As removal. The recovery increases up to 80% for 10g/L of seeds, reaching the maximum level at a concentration of 40g/L. Differences in the removal efficiency observed with 20 g/L (86.2%), 40g/L (87.6%) and 80g/L of seeds (85.6%) are within the experimental error, that is approximately 7%. Thus, it can be concluded that arsenic removal is approximately constant in a range of 20 to 80g/L of seeds. The concentration of solids affects the available area for crystal growth and as a result, the arsenic removal.

These results agree with the findings of Wang *et al.* (2000) and Singhania *et al.* (2005), however the effect was more pronounced with the concentrated solutions used in those studies. At an initial arsenic concentration of 10g/L, Wang *et al.* (2000) showed that the removal decreased from 85 to 60% when the seed concentration decreased from 80 to 20g/L and further to 45% when only 10g/L of seeds were used. Singhania *et al.* (2005) also observed the dependence of seed concentration in the removal of arsenic, and showed that the same efficiency was obtained when 160g/L of atmospheric seeds and 20g/L of hydrothermal seeds were used. According to these authors, this difference can be attributed to differences in surface area and crystallinity, but quantitative parameters were not provided.

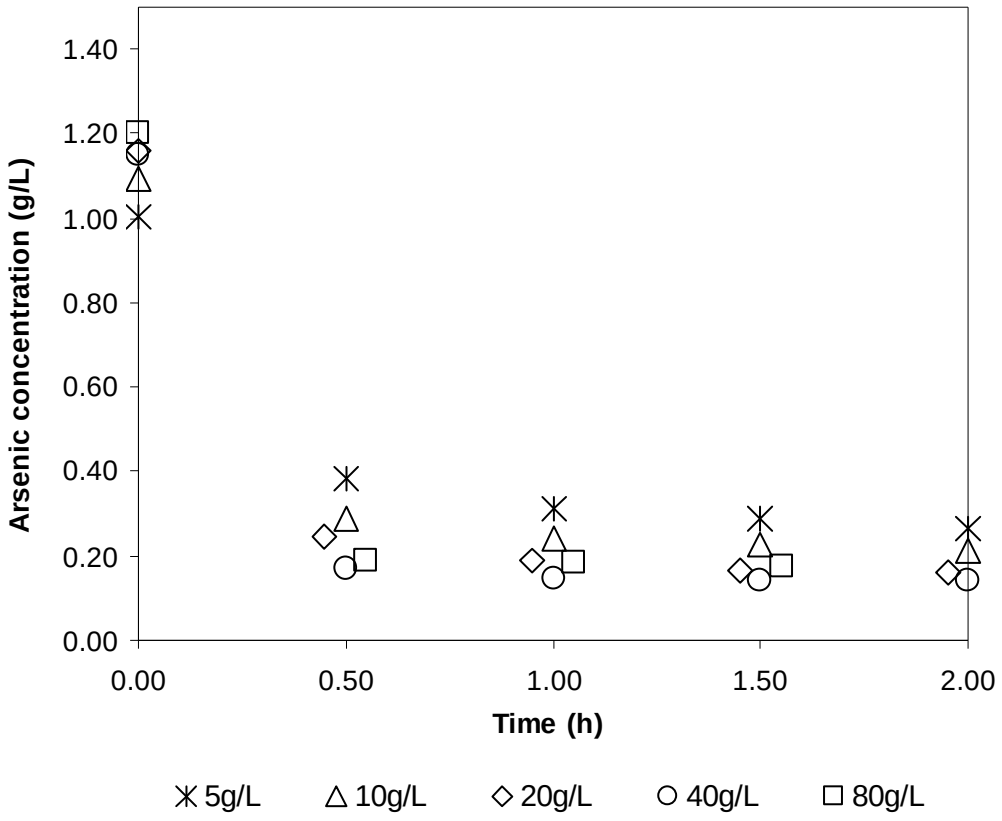

Figure 3.5 – Arsenic precipitation at different seed concentration (T = 95ºC, pH = 0.9, $[As]_i$ = 1.1g/L).

Figure 3.6 shows the arsenic removal as a function of the total seed's surface area (specific surface area x seeds concentration). As it can be observed, a surface area higher than 270m^2 is necessary to promote an arsenic removal of about 85% from a solution with 1g As/L. This area corresponds to a seed concentration of 20g/L. Previous studies did not report values of specific surface areas of the seeds used in scorodite precipitation, thus making it difficult a comparison of the different seed concentrations. We mensured the specific surface area of the scorodite used by Caldeira *et al.* (2005); the initial scorodite seeds were obtained at 95ºC in 12 hours. The low value found (0.9m^2/g) explain the relatively large concentration of seeds (200g/L) required in that study, and its restrict capacity of to act as precipitation nuclei. The results obtained in this work agree with the findings of Caldeira *et al.* (2005), which used a surface area lower than 175m^2 and obtained an arsenic removal of 80% (Figure 3.6).

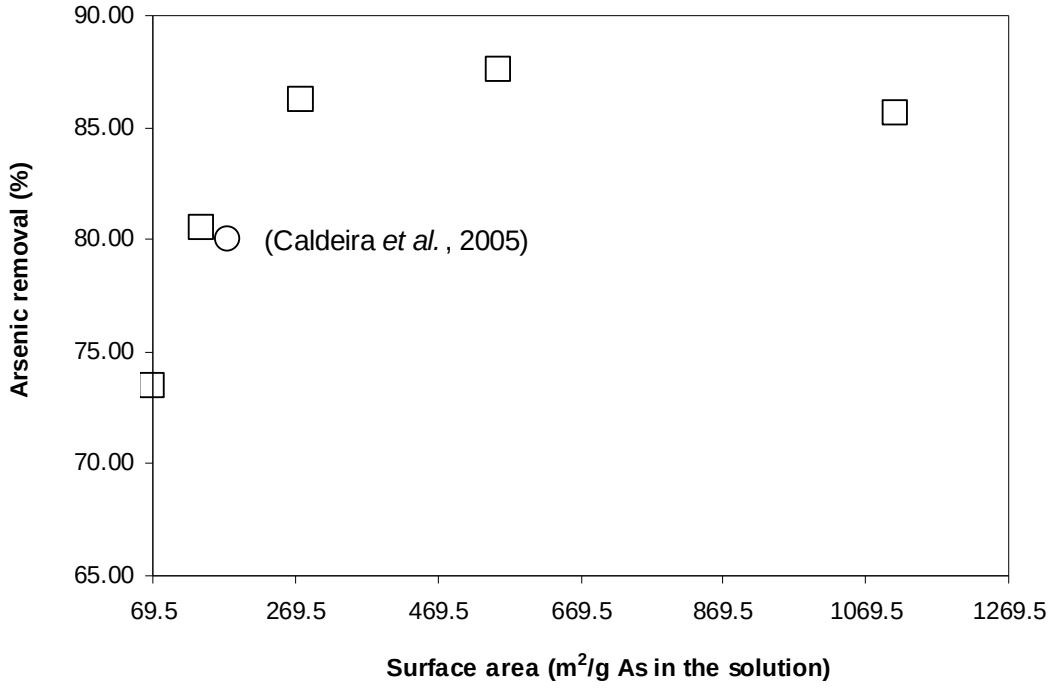

Figure 3.6 – Arsenic removal with the surface area available for the crystals growth (□). Data calculated from Caldeira *et al.* (2005) (○).

3.3.3 Comparison of gypsum and scorodite seeds

Gypsum ($CaSO_4*2H_2O$) is a common and often a major by-product in the precipitation of arsenic from sulfate solutions. The performance of gypsum seeds was compared with that of scorodite in experiments carried out with three levels of initial arsenic concentration (1.1, 2.4 and 10g/L), and pH 0.9, 1.2 and 0.6, respectively, and seeds concentration of 40g/L (Figure 3.7). The experimental conditions were selected according to the solubility curve shown in Figure 3.1 and the initial supersaturation was found as approximately 10, 45 and 20, respectively. The equilibrium condition was reached in a supersaturation range of 25 -1.3. The tests with an initial arsenic concentration of 10g/L were carried out for four hours.

The results showed that the performance of the gypsum seeds strongly depends on the initial arsenic concentration and is always inferior to the performance of scorodite seeds. In experiments carried out by Demopoulos (2005), 20 and 50g/L of gypsum seeds were added to a solution with 10g/L of arsenic; the removal efficiencies were of 50 and 75% respectively. Our results showed that the performance of the gypsum seeds very much strongly depends on the initial arsenic concentration. Let one consider a 10g/L solution (Figure 3.7). In the presence of scorodite, arsenic concentration drops abruptly in the first hour and remains constant after approximately 2 hours of reaction time. In the presence of gypsum, arsenic concentration decreases slowly, and the equilibrium is not reached even at 4 hours (Figure 3.7 inset). The final yields obtained with the scorodite and gypsum seeds were of 91% and 61%, respectively. At an initial arsenic concentration of 2.4g/L, only 13% of the metalloid is removed with gypsum; no removal is observed at 1.1 g/L. Figure 3.7 shows that under similar experimental conditions, arsenic removals of 86.3% and 87.6, respectively, are obtained with the scorodite seeds.

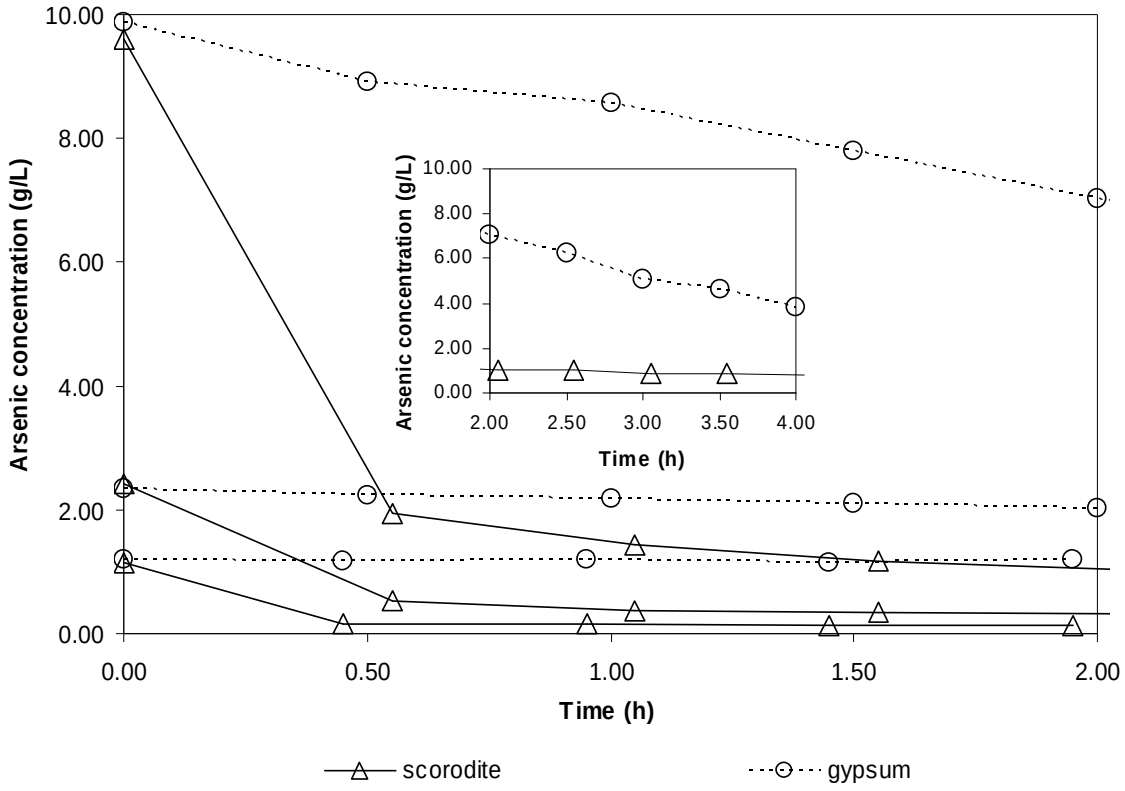

Figure 3.7 – Arsenic precipitation from the industrial solution using gypsum and scorodite seeds (T = 95ºC, seeds concentration = 40g/L).

As discussed previously, the rate of heterogeneous nucleation strongly depends on the specific surface area of the nucleus added in the system. The gypsum seeds presented a specific surface area of 3.8m^2/g, that is 3.6 times smaller than the specific surface area of the scorodite produced in autoclave (13.9m^2/g). According to the previews results, a surface area higher than 270m^2 is necessary to promote an arsenic removal of 85%. Thus, considering only the effect of surface area, about 70g/L of gypsum would be required to achieve the same arsenic removal obtained with 20g/L of hydrothermal scorodite seeds. According to Singhania *et al.* (2005), in order to achieve the same arsenic removal obtained with scorodite seeds, 80g/L of gypsum were needed in contrast with only 20g/L of scorodite hydrothermally prepared. The relatively low surface area of the gypsum seeds results in a restricted capacity to act as a precipitation nuclei and low arsenic removal.

The affinity between the foreign solid phase (seeds) and the solid to be precipitated is a function of the contact angle (θ) formed between the two species (Mersmann *et al*., 2001). Heterogeneous nucleation depends on this contact angle (θ). The contact angle indicates whether the presence of the substrate will substantially lower the nucleation barrier. If the angle θ = 180º, there is no chemical affinity between the crystalline solid and the foreign solid phase. If the angle θ is between 0 and 180º a partial chemical affinity exists, and if θ = 0º, a complete chemical affinity exists and the nucleation energy is zero (Mersmann *et al*., 2001). A schematic nucleation on a foreign particle and the different contact angles are illustrated in Figure 3.8.

With scorodite seeds, the chemical affinity is complete (θ = 0º). This justifies its better efficiency as precipitation nucleus and also the fast reaction rate. When gypsum seeds are used, the contact angle formed between the gypsum surface and the scorodite crystals is between 0 and 180º. As a consequence, the reaction rate is slower and the arsenic removal decreases in comparison with that obtained with scorodite seeds.

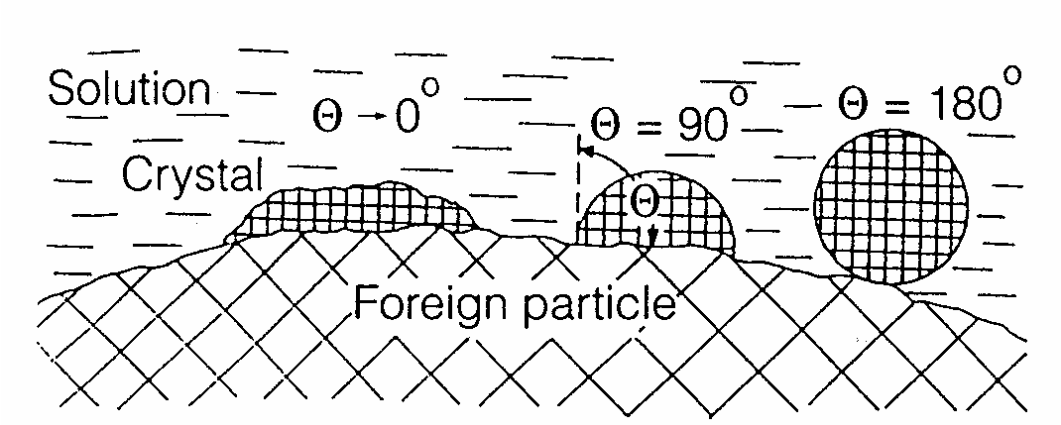

Figure 3.8 – Nucleation on the foreign particle for different contact angles (Mersmann *et al*., 2001).

3.3.4 Effect of sulfate concentration

According to Demopoulous *et al.* (1995) sulfate has an inhibitory effect on the rate of scorodite crystallization. The rate of scorodite production from a pure sulfate solution at 95ºC is lower than that from a pure chloride solution. Sulfate is, however, the most

frequent medium in mining and metallurgical solutions containing arsenic, including the industrial solution under investigation.

In the present work, three tests were carried out in order to verify the effect of the sulfate concentration. The industrial solution contained originally 3.5g/L of sulfate. An iron source should be added to the system in order to adjust the Fe/As molar ratio to approximately 1:1. In a first test, $FeSO_4$ was added as the iron source and H_2SO_4 was used to adjust pH - the final sulfate concentration was approximately 25g/L. In a second test, $FeCl_3$ was used as the iron source and HCl was used to acidify the system - the sulfate concentration was that of the original solution (3.5g/L). A third test was carried out using $FeSO_4$ and H_2SO_4, and an extra addition of $NaSO_4$ to create a condition of high sulfate concentration (100g/L). In these experiments the initial supersaturation was near to 10 and the equilibrium condition was reaching in values close to 1. A removal of 95.6% of arsenic from a solution containing 3.5g/L of sulfate was observed. In the tests with 25g/L and 100g/L of SO_4^{2-}, arsenic removal dropped to about 88%. The variation of arsenic concentration in solutions with different sulfate levels is shown in Figure 3.9. One may conclude that sulfate concentration above 25g/L has no further effect on scorodite precipitation. Similar results were reported by Singhania *et al.* (2006).

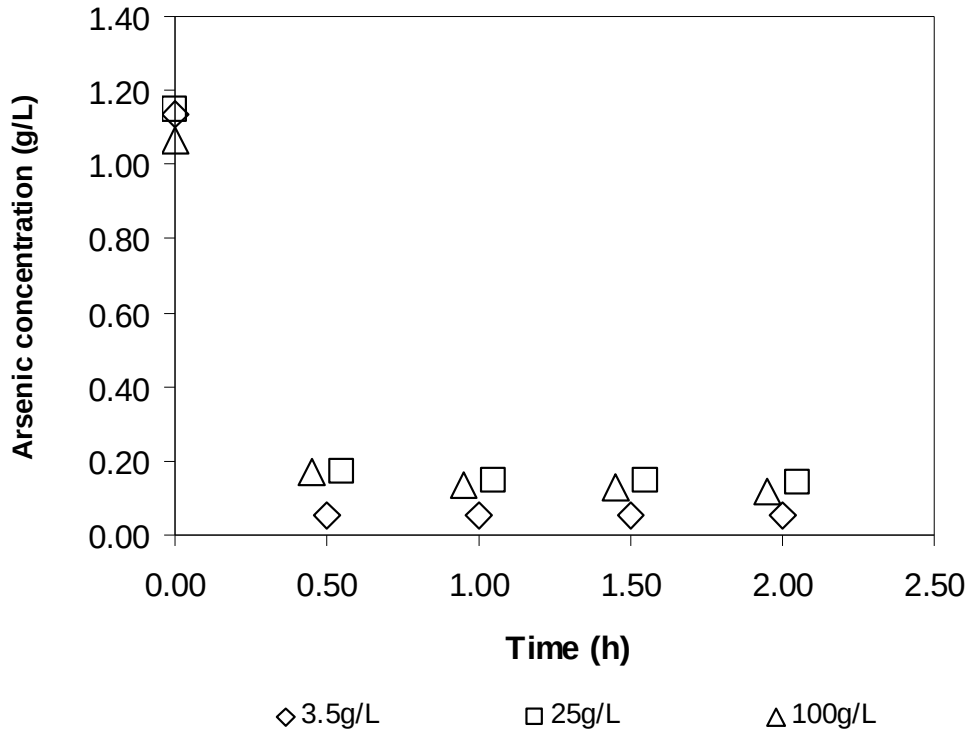

Figure 3.9 – Arsenic precipitation under different sulfate concentrations (T = 95ºC, scorodite seeds concentration = 40g/L, pH = 0.9).

3.3.5 Characterization of the Precipitates and Evaluation of TCLP - leachability

Scorodite system

Under conditions of high concentration of seeds, the amount of precipitate is very small if compared to amount of seeds added to the system. Therefore, it was difficult to discern fresh precipitates from the original scorodite seeds. The conclusions from bulk analyses become questionable. The solid production index (SPI) was created as an attempt to establish a criterion for the selection of samples. The SPI was defined as the mass ratio of the precipitates and the seeds added to the system. The SPI is inversely proportional to the seeds concentration in the system (Figure 3.10). The following analyses were carried out considering tests with SPI higher than 5%.

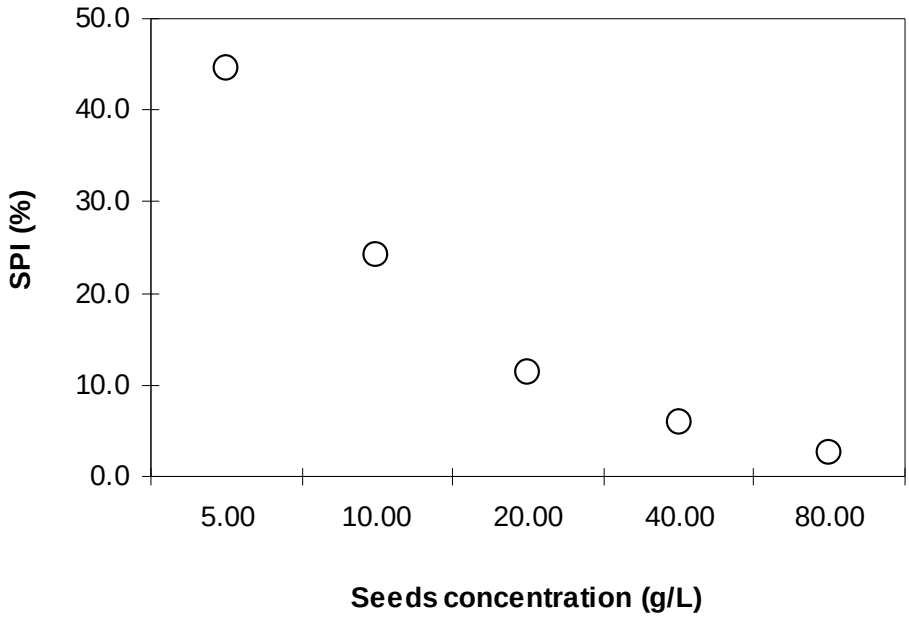

Figure 3.10 – Variation in the solid production index (SPI) as a function of seed concentration. Initial arsenic concentration of 1.1g/L, pH 0.9 and scorodite seeds produced in autoclave.

The micro-Raman spectra and the X-ray diffraction patterns of the precipitates are shown in Figures 3.11 and 3.12, respectively. The Raman spectra show the characteristic bands of scorodite (890, 840: As-O stretching; 472, 440: O-As-O bending), as reported by Farmer (1976). No other phase has been detected. Accordingly, the X-ray diffraction patterns do not show any indication of amorphous phases. Only scorodite was identified (ICDD 70-0825).

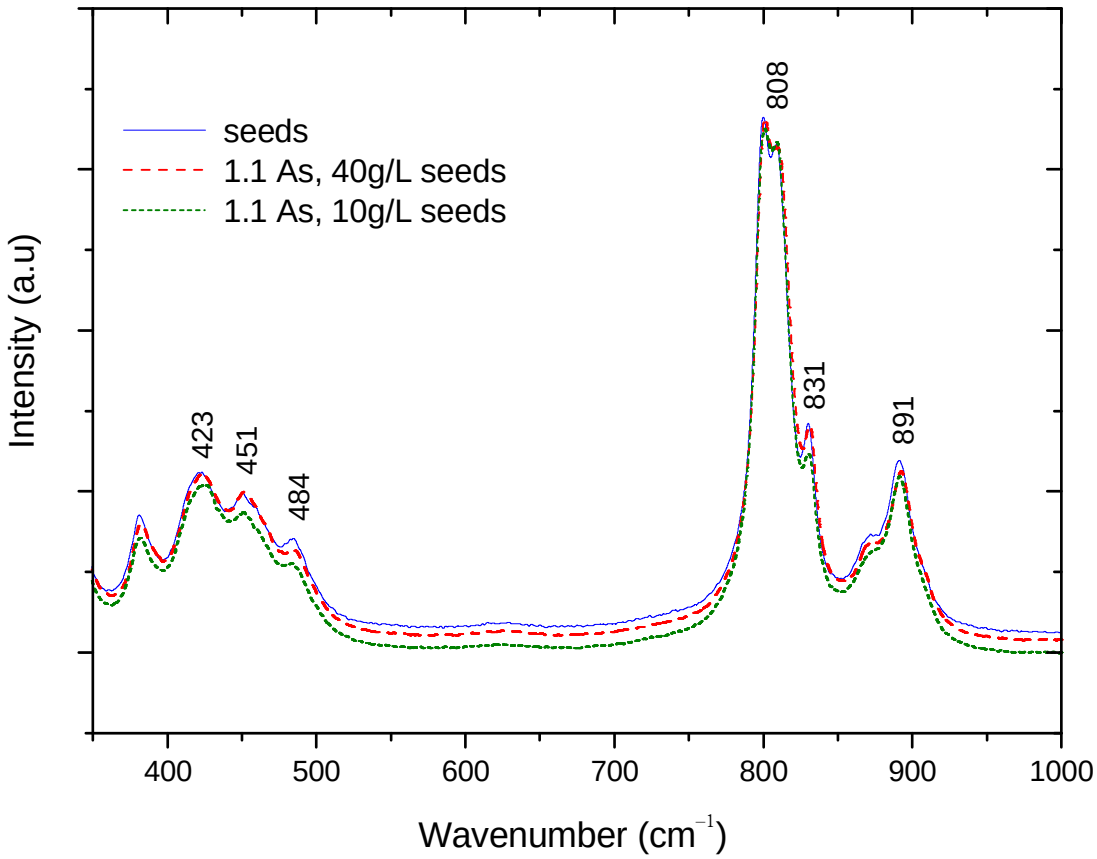

Figure 3.11 – Raman spectra in the range of 300-1000 cm^{-1} for the scorodite seeds produced in autoclave and precipitates from batch tests.

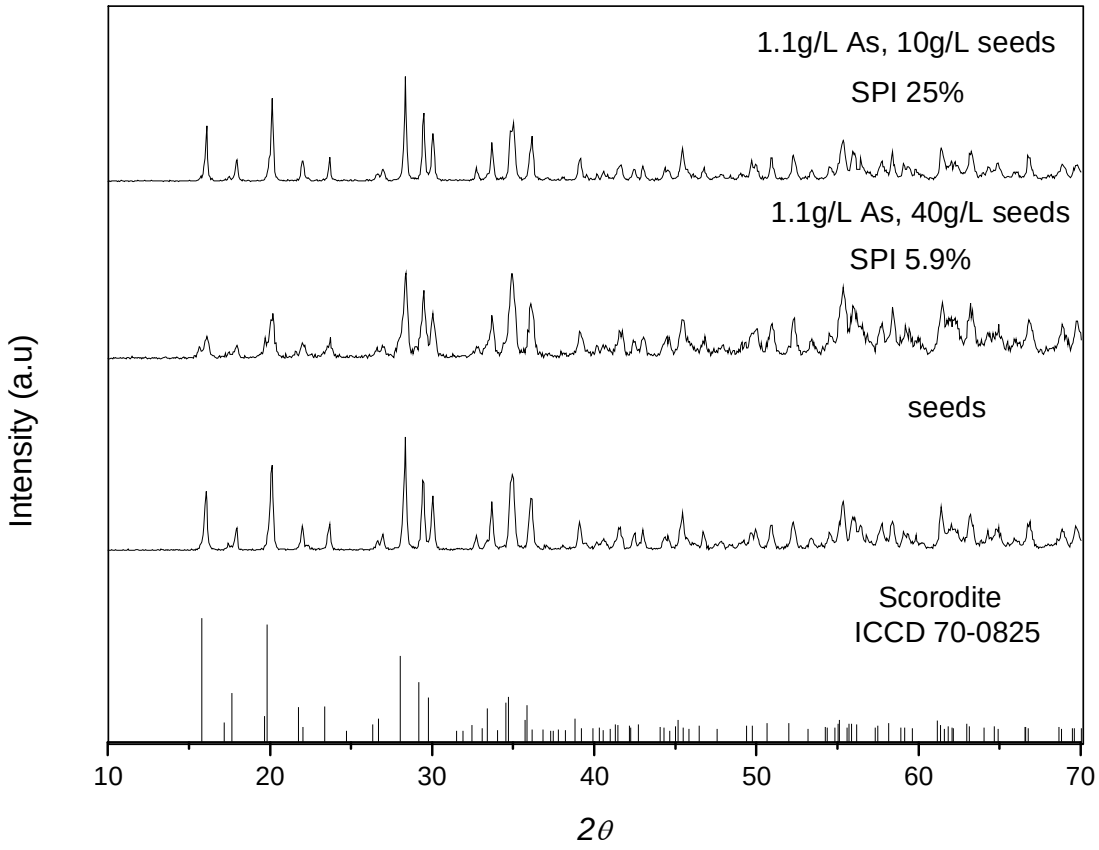

Figure 3.12 – X-ray diffraction patterns of solids precipitated in batch tests with different SPI (An amplified vision is presented in the Appendix A).

The SEM images indicate the formation of agglomerates with particles with round shape. It was not possible to verify a morphologic modification between the scorodite seeds produced in autoclave and the final mixture from the batch tests (Figures 3.13 and 3.14). The scorodite seeds, obtained under hydrothermal conditions present a specific surface area of 13.96m^2/g and an average diameter (D_{50}) of approximately 2.5μm. The growth of the scorodite crystals was verified with the consecutive use of these seeds in batch tests; the final average diameter was approximately 4.0 μm, after 8 hours of precipitation.

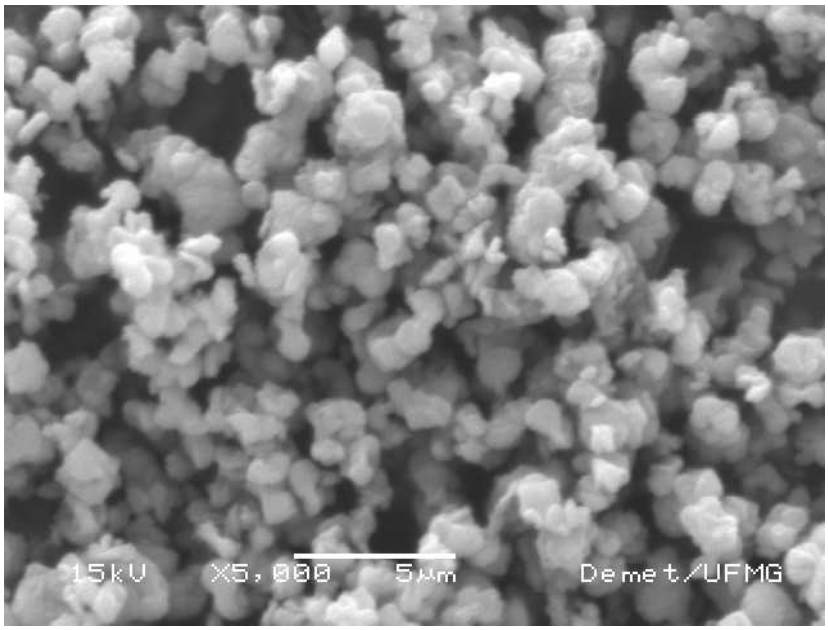

Figure 3.13 – SEM image of scorodite seeds produced by hydrothermal process (synthetic solutions of Fe(III) and As(V); 150ºC; 2 hours; pH = 1.5; Fe:As = 1:1).

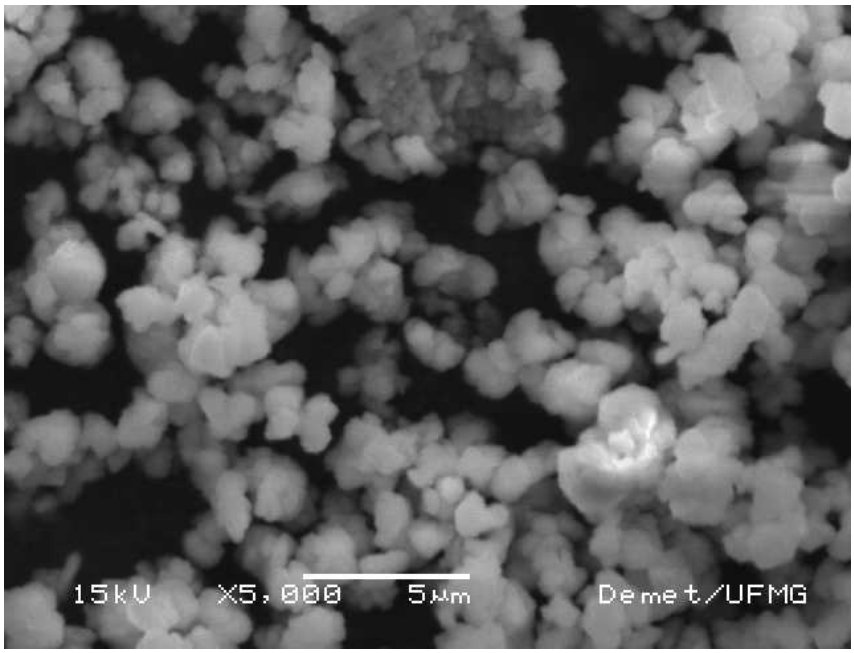

Figure 3.14 – SEM image of formed solids, after 8 hours of batch precipitation tests at ambient pressure conditions.

Gypsum system

The gypsum seeds presented a SSA of 3.8m^2/g, and an average diameter of approximately 2.4μm. The micro-Raman analyses indicated that the material used as seed consists in a mixture of gypsum ($CaSO_4$*$2H_2O$) with minor hemihydrate ($CaSO_4$*$0.5H_2O$) and anhydrite ($CaSO_4$) phases. The presence of these phases was evidenced by the presence of two bands in 1008 and 1014cm^{-1} (Figure 3.15), characteristics of the mixtures gypsum/anhydrite and hemihydrate/gypsum/anhydrite, respectively, that can be attributed of the $\nu_1(SO_4)$ vibration (Chio *et al.*, 2004). The presence of these phases can also be observed by XRD analyses (Figure 3.16).

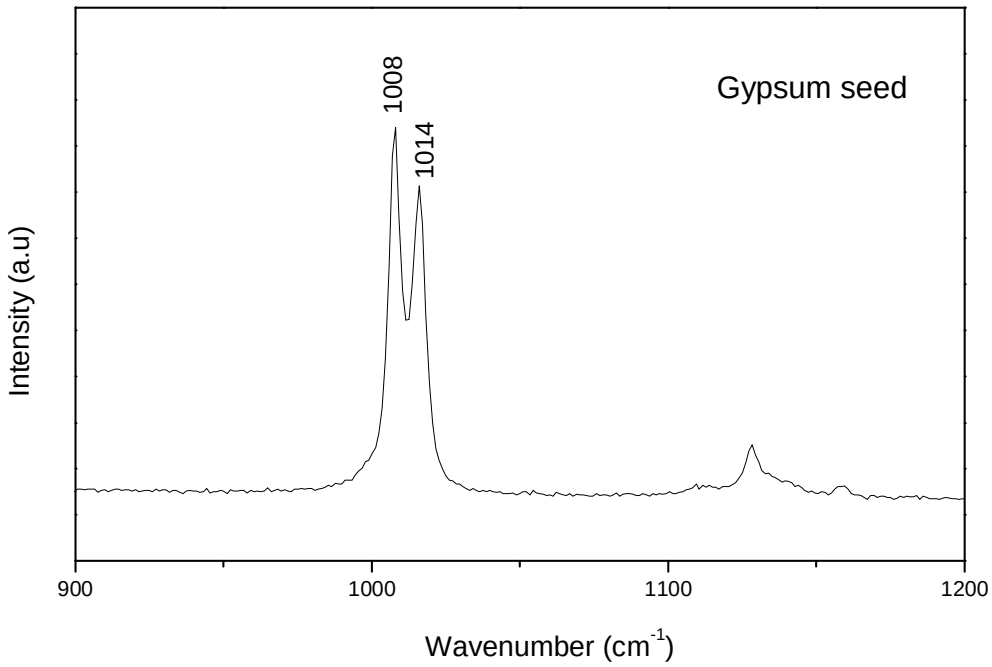

Figure 3.15 – Raman spectra in the range of 100-1200 cm^{-1} for the gypsum seeds.

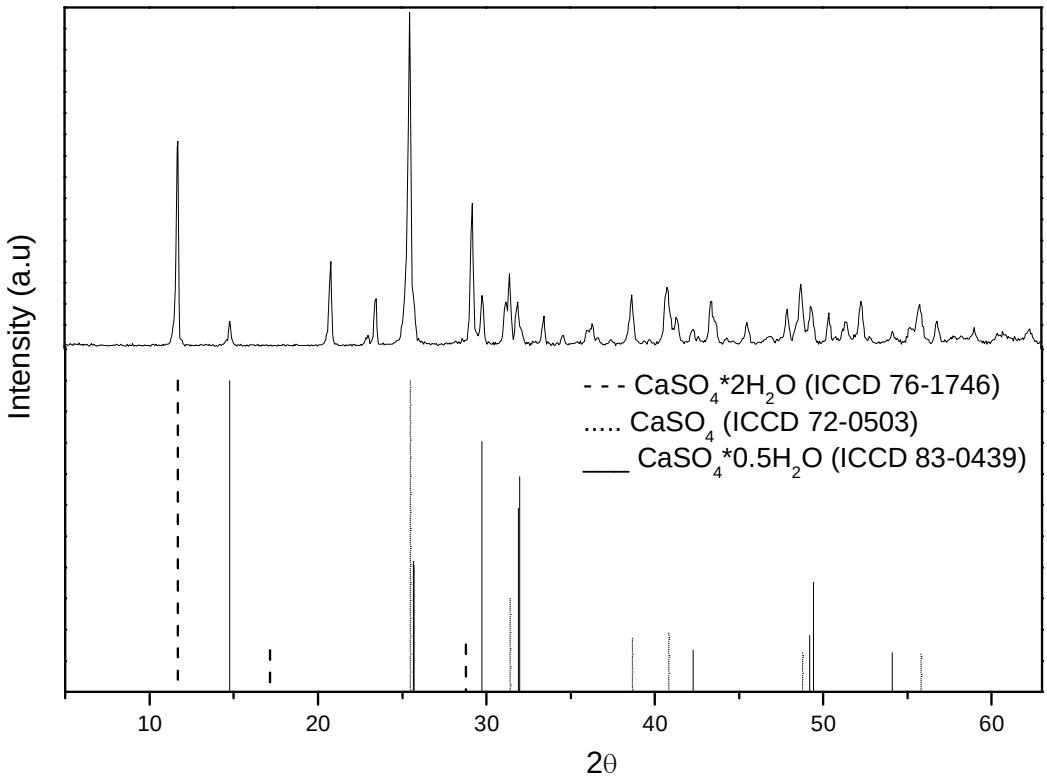

Figure 3.16 – X-ray diffraction patterns of the gypsum seeds.

The X-ray diffraction patterns of the solids precipitated in tests carried out with gypsum seeds showed the presence of only gypsum at low initial As concentrations (1.1 e 2.4g/L) and of both gypsum and scorodite phases at initial concentrations of 10g/L. There was no indication of formation of amorphous phases, as shown in Figure 3.17. The SEM images confirm the results obtained by X-ray diffraction. The formation of spherical scorodite particles is observed on the surface of the needles of gypsum crystals when a concentration of 10g/L As was used. No other phase was identified in the tests of initial arsenic concentration of 2.4g/L (Figure 3.18). According to the mass balance, under this conditions gypsum dissolution took place, and it's reprecipitated after the solution cooling.

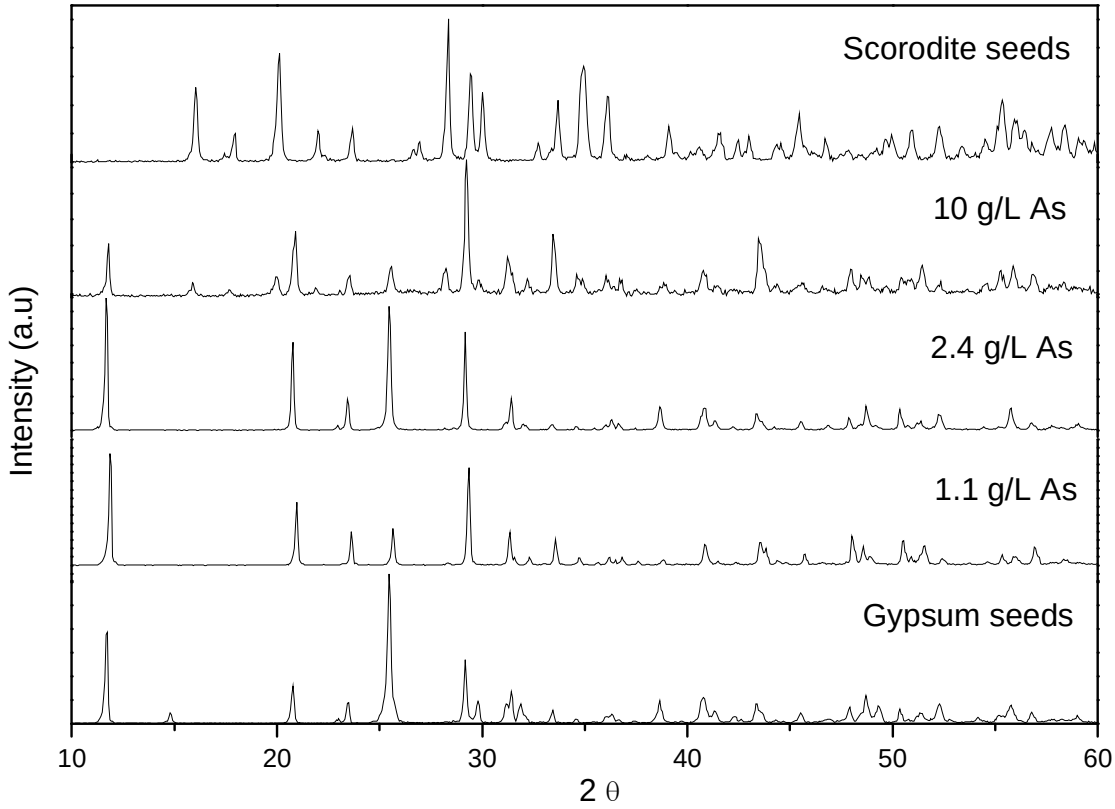

Figure 3.17 – X-ray diffraction patterns of the solids formed in batch tests with gypsum seed.

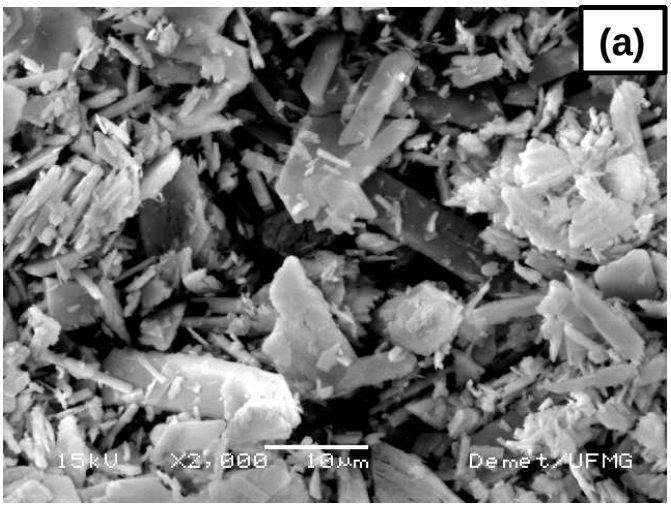
(a)
15kV X2,000 10µm Demet/UFMG

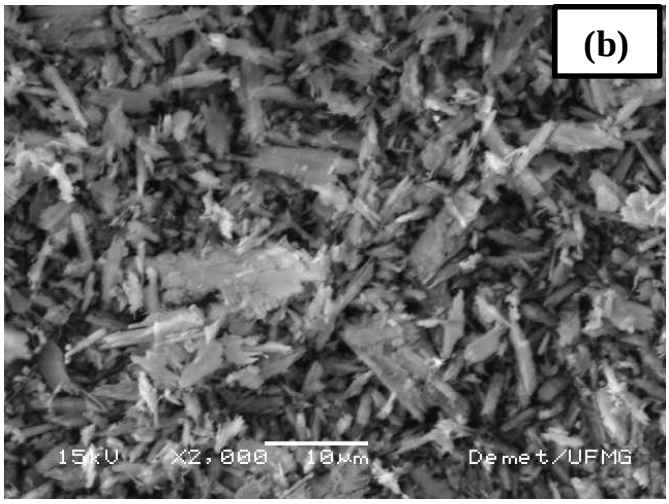
(b)
15kV X2,000 10µm Demet/UFMG

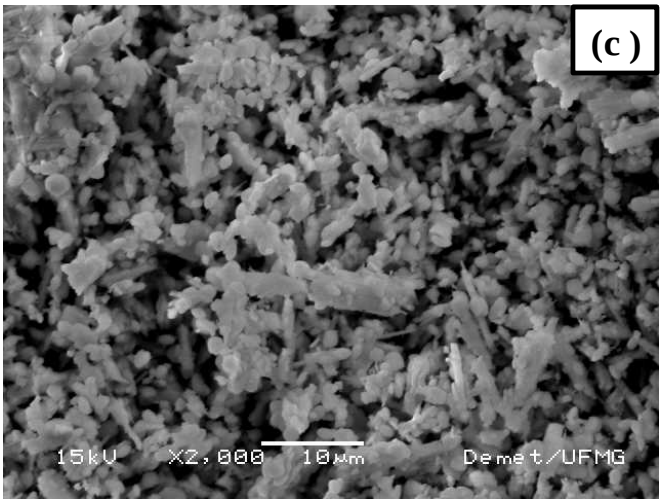
(c)
15kV X2,000 10µm Demet/UFMG

Figure 3.18 – SEM images (a) pure gypsum; (b) final product of the test with an initial arsenic concentration of 2.4g/L; (c) final products in tests with an initial arsenic concentration of 10g/L (95ºC; 4 hours; magnification of 2.000 times).

The products obtained in the tests with initial concentration of 10g/L As were submitted to analysis by energy dispersive spectrometry (EDS). The presence of As and Fe in the crust formed on gypsum surface is in agreement with the formation of scorodite (point (2) in Figure 3.19). On the other hand, on the flat surface only the elements of the typical gypsum composition were identified (point (1) in Figure 3.19). The micro-Raman spectra (Figure 3.20) confirmed the presence of the characteristics bands of crystalline scorodite (spectra (a), Figure 3.20) and the characteristic bands of gypsum (spectra (b) on the Figure 3.20) on the crust and flat surface, respectively.

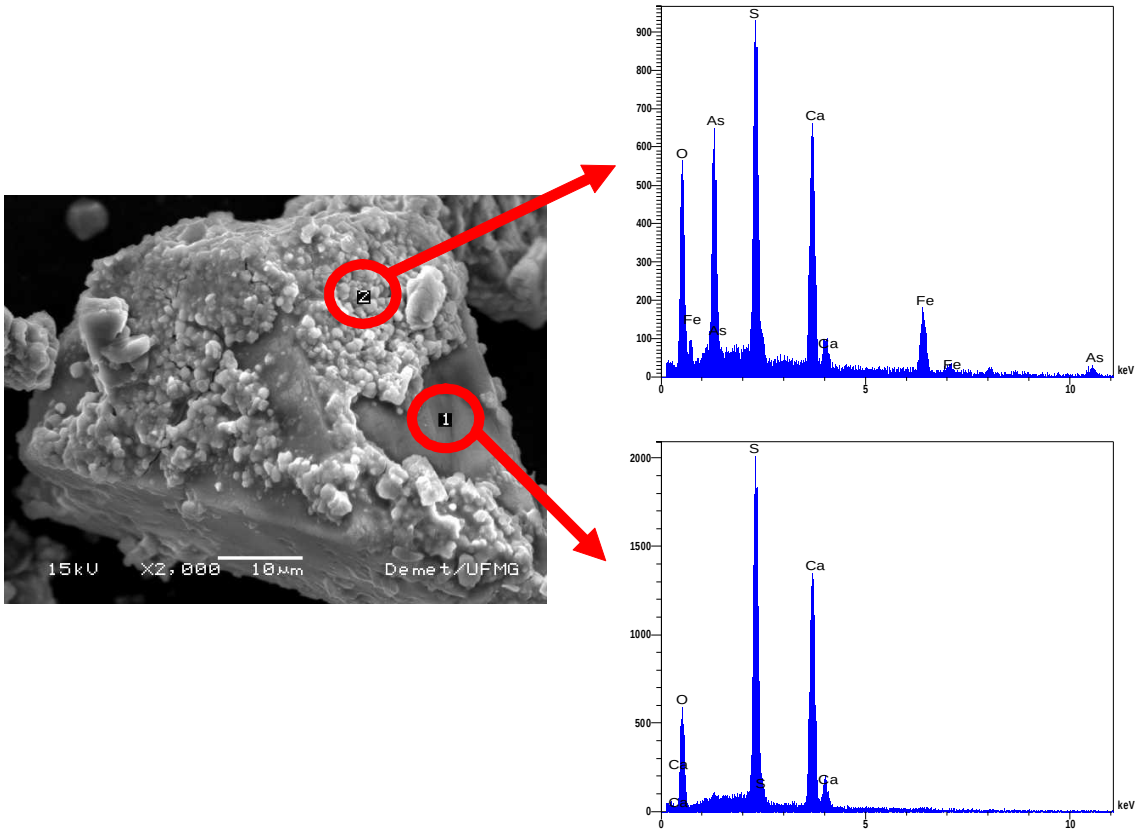

Figure 3.19 – Analysis by energy dispersive spectrometry (EDS) on the flat areas (1) and on the crust formed on gypsum surface (2).

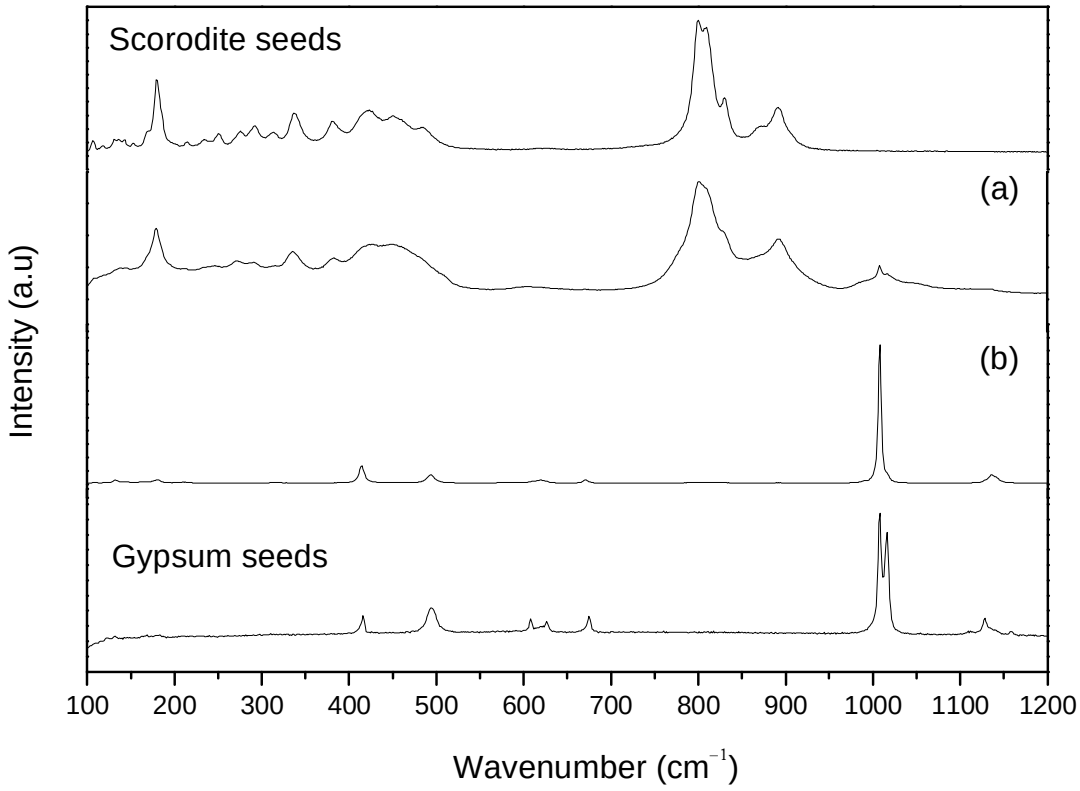

Figure 3.20 – Raman spectra in the range of 100-1200 cm^{-1} for the solids formed in the batch tests with gypsum seeds (arsenic concentration = 10g/L).

The scorodite seeds produced in autoclave and a solid sample from a batch tests, after 8 hours, were subjected to the toxicity characteristic leaching procedure (TCLP). The scorodite seeds produced in autoclave showed arsenic leachability of 13.6 mg/L that is higher than the limit allowed by American and Brazilian legislation (5 and 1mg/L, respectively). However, after 8 hours of reaction, the mixture seed/precipitates released only 0.1mg/L arsenic. This concentration level is below the current toxicity limits established by the TCLP test. The result indicates that ageing has an important effect on scorodite leachability. Crystal growth and consequently decrease in the surface area available to react with the extraction solution in the TCPL tests are possible reasons for this behavior.

The TCLP was performed on solids samples produced in the tests carried out with gypsum seeds and an initial arsenic concentration of 10g/L. The arsenic leachability was found to be 0.65mg/L that is also smaller than the limit allowed by the American

and Brazilian legislations. This result shows that the mixture gypsum/scorodite is stable for a final disposal in a landfill.

3.4 Conclusions

It was shown by the first time that industrial solutions with low arsenic concentrations (1.1 – 0.1g/L) can be treated in one stage of scorodite precipitation. Arsenic removal was in a range of 80.5 to 94.6%. The effect of seed concentration was evaluated. The results showed 73% of arsenic removal even for the lowest scorodite seed concentration (5g/L). The removal increases with the increase of seed concentration and become approximately constant (85-88%) in a range of 20 to 80g/L of seeds. Surface areas higher than 270m^2 are necessary to promote an arsenic removal of about 85%. The performance of gypsum seeds was compared with that of scorodite in experiments carried out with three levels of initial arsenic concentration (1.1, 2.4 and 10g/L). Gypsum promoted arsenic precipitation only from concentrated solutions (10g/L). However, even under this level of concentration, arsenic removal was smaller (61%) than that obtained with scorodite seeds (91%). The lower arsenic removal was attributed to gypsum's low surface area and a possible less favorable contact angle (θ) with the precipitates. Considering only the effect of the surface area, the results indicate that about 70g/L of gypsum would be required to achieve the same arsenic removal as about 20g/L of hydrothermal scorodite seeds. Scorodite precipitation was not significantly affected by up to 100 mg/L of sulfate concentration.

Scorodite was the only phase identified by micro-Raman and X-ray diffraction analyses of the precipitates. The SEM images indicate the formation of agglomerates with round-shape particles. The TCLP tests suggest that ageing play an important role on scorodite leachability, which decreased from 13.6 mg/L to 0.1mg/L after 8 hours of precipitation reaction. The mixture gypsum/scorodite also showed arsenic leachability of only 0.65mg/L, which is smaller than the limit allowed by the American and Brazilian legislation (5 and 1mg/L, respectively).

3.5 References

ABNT – ASSOCIAÇÃO BRASILEIRA DE NORMAS TÉCNICAS (2004). NBR 10005 – Procedimento para obtenção de extrato lixiviado de resíduos sólidos (*Procedure for obtention leaching extract of solid wastes*). Rio de Janeiro, p.16.

CALDEIRA, C.L., CIMINELLI, V.S.T., BATISTA, I.S. and MOURA, W. (2005). Precipitação de Escorodita a temperatura Controlada e Pressão Ambiente. Proceedings of XXI Encontro Nacional de Tratamento de Minérios e Metalurgia Extrativa – ENTMME, Natal, p.93-99.

CHIO, C.H., SHARMA, S.K. and MUENOW, D.W. (2004). Micro-Ramam Studies of Gypsum in the Temperature Range Between 9K and 373K. *American Mineralogist*, v. 89, p.390-395.

DEBEKAUSSEN, R., DROPPERT, D. and DEMOPOULOS, G. P. (2001). Ambient Pressure Hydrometallurgical Conversion of Arsenic Trioxide to Crystalline Scorodite. *CIM Bulletin*, v. 94, n. 1051, p.116-122.

DEMOPOULOS, G.P., DROPPERT, D. J. and VAN WEERT, G. (1995). Precipitation of Crystalline Scorodite ($FeAsO_4.2H_2O$) from Chloride Solutions. *Hydrometallurgy*, v. 38, p.245-261.

DEMOPOULOS, G.P. (2005). On the Preparation and Stability of Scorodite. In: Arsenic Metallurgy. R. G. Reddy and V. Ramachandran, eds, *TMS (The Minerals, Metals & Materials Society),* p.25-49.

DUTRIZAC, J.E. and JAMBOR, J.L. (1988). The Synthesis of Crystalline Scorodite, $FeAsO_4.2H_2O$, *Hydrometallurgy*, v. 19, n. 3, p.377-384.

EPA SW-846, (1992). Test Methods for Evaluating Solid Waste, Physical/Chemical Methods. Method 1311.

FARMER, V.C. (1976). The Infrared spectra of minerals. *Mineralogical Society*, London, 539p.

FILIPPOU, D. and DEMOPOULOS, G.P. (1997). Arsenic Imobilization by Controlled Scorodite Precipitation. *JOM*, v. 12, n. 14, p.52-55.

KRAUSE, E. and ETTEL, V.A. (1989). Solubilities and Stabilities of Ferric Arsenate Compounds. *Hydrometallurgy*, v.22, n. 3, p.311-337.

MERSMANN, A. (2001). Crystallization Technology Handbook. Second Edition – Revised and Expanded. Marcel Dekker, Inc. New York – Basel. 832p.

PAPANGELAKIS, V.G. and DEMOPOULOS, G.P. (1990). Acid Pressure Oxidation of Arsenopyrite: Part I, Reaction Chemistry. *Canadian Metallurgical Quarterly*, v. 29, n.1, p.1-12.

SINGHANIA, S., WANG, Q., FILIPPOU, D. and DEMOPOULOS, G.P. (2005). Temperature and Seeding Effects on the Precipitation of Scorodite from Sulfate Solutions under Atmospheric-Pressure Conditions. *Metalurgical and Materials Transactions B*, v. 36B, p.327-333.

SINGHANIA, S., WANG, Q., FILIPPOU, D. and DEMOPOULOS, G.P. (2006). Acidity, Valency and Third-Ion Effects on the Precipitation of Scorodite from Mixed sulfate Solutions under Atmospheric-Pressure Conditions. *Metalurgical and Materials Transactions B*, v. 37B, *in press*.

STANDARD METHODS FOR THE EXAMINATION OF WATER AND WASTEWATER (1998). Part 4000. 20th edition. Prepared and published by American Public Health Association, American Water Works Association and Water Environment Federation.

SWASH, P.M. and MONHEMIUS, A.J. (1994). Hydrothermal Precipitation from Aqueous Solutions Containing Iron(III), Arsenate and Sulphate. In: HIDROMETALLURGY ’94, 1. Cambridge, England. London: Chapman & Hall, [s.d.]. p.177-190.

SWASH, P.M. and MONHEMIUS, A.J. (1995). The Disposal of Arsenical Wastes: Technologies and Environmental Considerations. In: INTERNATIONAL MINERALS AND METALS TECHNOLOGY. Roberts, N.J.(ed.), Sabrecrown Publishing, London.

WANG, Q., DEMOPOULOS, G.P. and HARRIS, G.B. (2000). Arsenic Fixation in Metallurgical Plant Effluents in the Form of Crystalline Scorodite via a Non-autoclave Oxidation-Precipitation Process. In: Minor Elements, Young, C.A. (ed.), Soc. Min. Met. Expl., Littleton, CO, U.S.A., p.225-237.

4 SCORODITE PRECIPITATION IN A CONTINUOUS SYSTEM: EVALUATION OF ARSENIC REMOVAL AND PRODUCT STABILITY

4.1 Introduction

Scorodite ($FeAsO_4*2H_2O$) has been an option for arsenic disposal and immobilization in processes such as the pressure oxidation of auriferous sulfides, where the arsenate is a product of the treatment of refractory gold ores. However, the high investment and operation costs make the hydrothermal processes unlikely to be considered for the treatment of effluents. Demopoulos and co-workers (Demopoulos *et al*., 1995; Filippou and Demopoulos, 1997; Debekaussen *et al.*, 2001; Demopoulos, 2005; Singhania *et al.*, 2005) demonstrated the possibility to precipitate scorodite at ambient pressure. The option is cheaper than the hydrothermal process and can be operated despite an association with metal recovery (Singhania *et al.*, 2006). The ambient-pressure precipitation involves the supersaturation control and the addition of seeds in order to favor crystal growth against homogeneous nucleation.

An operational difficulty of the scorodite precipitation process under ambient pressure conditions is the pH control (i.e. supersaturation control) at 95ºC. Under batch conditions, pH is expected to decrease with time due to the production of sulfuric acid (Debekaussen *et al.*, 2001). Therefore, it is difficult to assure that the reaction is occurring within the working region defined by the equilibrium (C_{eq}) and the critical supersaturation (C_{cr}) lines. The critical supersaturation line is defined by the induction pH - the pH in which the homogeneous nucleation will occur, and must not be exceeded. Thus, the pH should be kept slightly below the induction pH. A fast increase in pH will result in creation of high supersaturation levels, which are unwanted. Figure 4.1 shows the dependence of the induction pH with arsenic concentration.

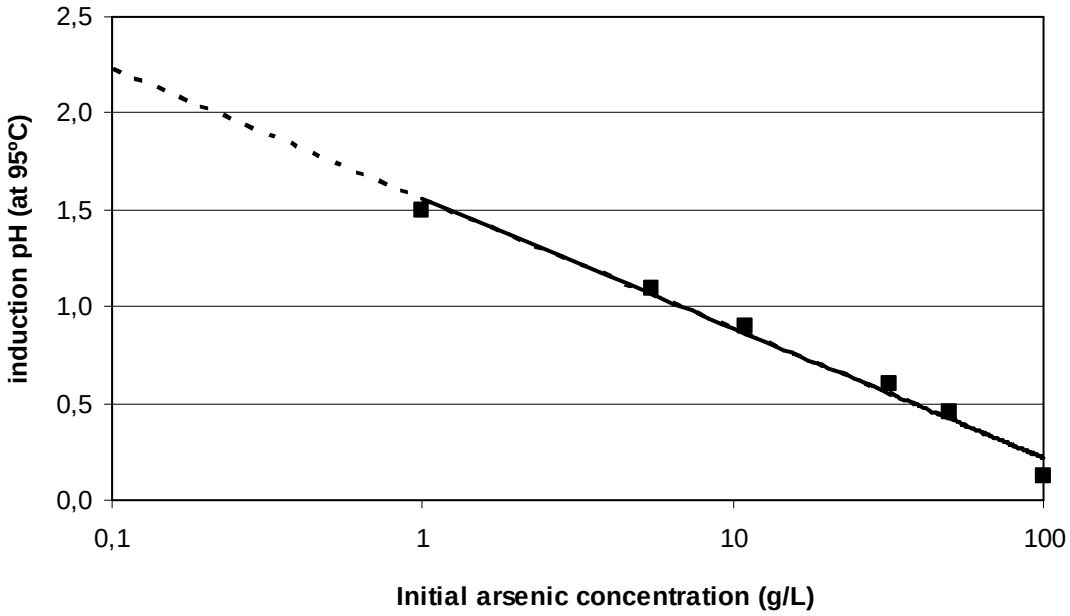

Figure 4.1 – Dependence of induction pH on arsenic concentration at 95ºC (adapted from Debekaussen *et al.*, 2001; by Caldeira *et al*., 2005).

In a continuous system, arsenic concentration can be maintained nearly constant, thus favoring the supersaturation control, which will favor scorodite precipitation. Nevertheless, the literature describes only results obtained under batch conditions.

The fine chemical industries often use batch crystallization reactors in view of the easiness and flexibility of the operation. Different phenomena, such as nucleation, crystal growth, and agglomeration will dominate at different times in an unsteady-state process. It is possible to vary the addition rate of reagents and some other variables; however, the degree of control is rather limited. Conversely, the precipitation in continuous systems results in a steady-state condition (i.e. constant with time), after an initial transient period. This allows the control of process variables, such as flow rates, residence time, and agitation rates and therefore, a much better control of supersaturation is achieved (Lawrence *et al.,* 1986).

This work aims the study of scorodite precipitation in a continuous system, under ambient pressure, and the determination of the product's solubility according to the Toxicity Leaching Procedure -TCLP (EPA, 1992). In addition to a better control of the

process variables, the continuous system represents better the operation conditions employed by the industry. This approach also helps the understanding of the reaction mechanism, through the determination of rates of nucleation and the rate of crystal growth.

4.2 Experimental Procedure

The tests were carried out in duplicate, with the industrial solution used in the batch tests (As_{total} = 1.1g/L, As(III) = 0.96g/L, Fe_{total} = 0.15g/L, Fe(II) = 0.13g/L, Fe/As = 0.2, pH = 2.3, SO_4^{2-} = 2.85g/L) and described in Chapter 3. Following the oxidation of iron and arsenic and the adjustment of the Fe/As molar ratio, the precipitation was carried out in a continuous system with recycle of solids. The system will be designated as *Mixed Suspension Mixed Product Removal with Recycle* - MSMPRR. The batch tests reported previously showed that 1 hour of reaction was sufficient to assure a high arsenic removal level, so this value was adopted as the residence time for the continuous experiments. In order to achieve steady state conditions, the experiments were carried out during at least eight residence times (8 hours). The temperature was kept constant at 95ºC by the hot oil circulation within the reactor jacket. Figure 4.2 shows the experimental set-up.

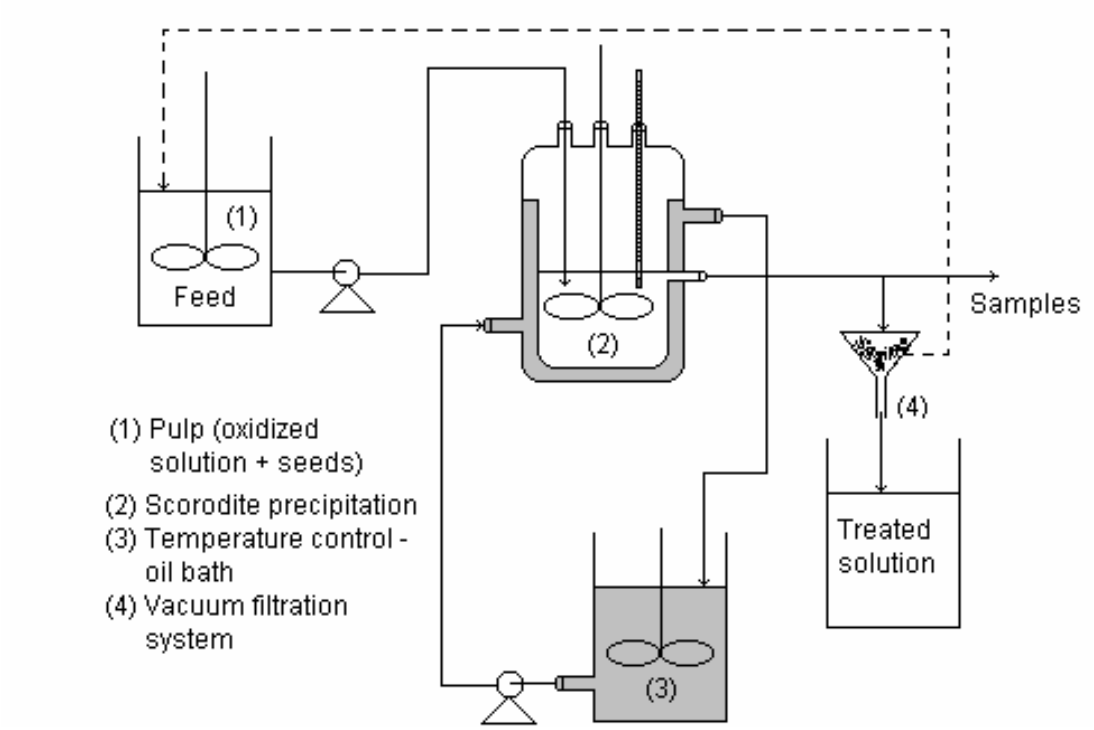

Figure 4.2 – Schematic representation of the continuous precipitation system with recycle of solids (MSMPRR).

The seeds were prepared by hydrothermal precipitation from concentrated $Fe_2(SO_4)_3.xH_2O$ and $Na_2HAsO_4.7H_2O$ synthetic solutions, with an Fe:As molar ratio of 1:1. The experimental conditions were selected as initial arsenic concentration of 33g/L, temperature of 150ºC, pH 1.3 and a reaction time of 2 hours. The industrial solution containing 40g/L of scorodite seeds was added to the reactor by a continuous controlled mass flow (approximately 1L/hour) using a peristaltic pump, previously calibrated. The heating and stirring systems were turned on, and when the temperature reached 95ºC was defined the time zero of the experiments. Every 15 minutes the pulp was collected and vacuum filtered. The solids were then mixed with industrial solution (1g/L As), maintaining the original solid/liquid ratio, and returned to the reactor. During the tests, samples were taken from the slurry leaving the reactor at regular periods of time (approximately 50mL/h). The pulp was vacuum filtered, and the solution was diluted using 50μL of concentrated nitric acid to prevent the formation of amorphous material and taken to chemical analyses. The solids were dried at 40ºC for 24 hours and characterized according to the procedures further

described. Figure 4.3 shows the schematic representation of the complete experimental procedure.

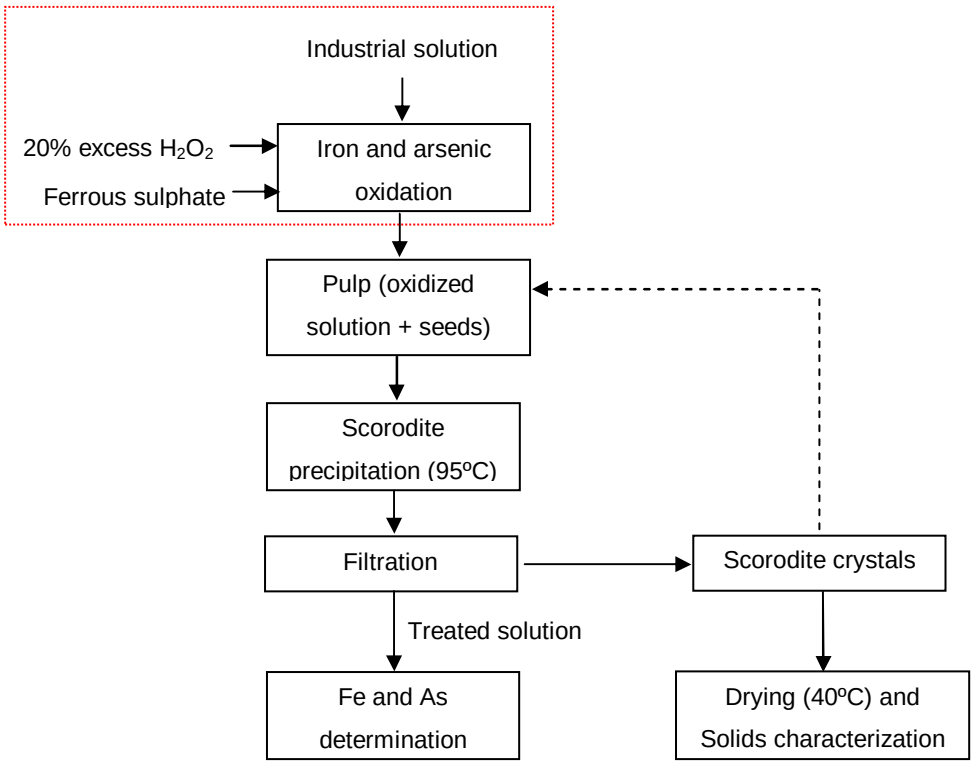

Figure 4.3 – Block diagram of the experimental procedure for continuous precipitation.

The As_{total} and Fe_{total} concentrations were determined by atomic absorption spectrometry (Perkin Elmer AAnalyst 300), with air/acetylene flame (wavelength of 328.1nm and 248.3nm for As_{total} and Fe_{total}, respectively). The scorodite seeds produced in autoclave as well as the products obtained in the precipitation tests were dried at 40ºC for 24 hours, and analyzed by X-ray diffraction analyses (Philips model PW1710), and scanning electron microscopy (MEV) (JEOL model JSM-6360L VI coupled to an energy dispersive spectrometer-EDS). In order to obtain the MEV images, the samples were covered with a carbon layer to assure electron conduction and heat dissipation. The particle size distribution and the specific surface area were determined by laser scattering (Cilas 1064) and nitrogen adsorption (Quantachrome, model Nova 1200), respectively. TCLP (Toxicity Characterization Leach Procedure) standard leaching tests (EPA, 1992) were carried out with the solids produced in each experiment in order to examine the solubility of the precipitates. Similar procedure has recently been adopted by Brazilian legislation (ABNT NBR-10005/2004). However, the

threshold for defining toxicity according to the Brazilian standards, 1.0mg/L (ABNT, 2004), is five times smaller than that adopted by the original TCLP test. The determination of arsenic and iron concentrations in the extract was carried out by an ELAN ® 9000 ICP-MS instrument (Perkins Elmer SCIEX, Concord, Ontario, Canada).

4.3 Results and Discussion

Figure 4.4 shows arsenic concentration in the exit solution of experiments carried out with and without the recycling of seeds. In the absence of recycling, arsenic concentration drops in the first hour and then further increases over time to reach the level of feed concentration after seven hours of reaction. Therefore, arsenic was not effectively removed in this system. With the recycling of seeds, arsenic concentration drops rapidly in the first hour, thus reaching a steady state condition, which corresponded to a residual arsenic concentration of 0.28g/L. In the absence of recycling, the concentration of solids within the reactor vessel decreases and approaches to zero after five hours of reaction. The difference in arsenic concentration after the first hour of reaction (0.32g/L without and 0.24g/L with recycle of seeds) can be attributed to the different pH values (0.9 and 1.1 respectively), which in turn affect the initial supersaturation level and establish the exit As concentration.

Figure 4.5 shows that the recycling keeps the solid concentration at a practically constant level (35-40%), which in turn provides enough surface area for crystal growth. For the treatment of dilute solutions (e.g. initial arsenic concentration of 1.0g/L) with a feed flow rate of approximately 1L/h, the recycling of solids is compulsory. The absence of recycling, would require a significant decrease in the feed flow rate in order to increase the residence time. However, very low flow rates usually imply in operational difficulties such as solid deposition on hoses causing flow blockage, which in turn increases the consumption of energy. These constraints are related to the rate of crystal growth.

Scorodite precipitation involves a very low rate of crystal growth that can be calculated according to the following equation:

$$G = \frac{V_{As(deposited)}}{t_R \times A_{seeeds}} \quad (4.1)$$

where G is the crystal growth rate (m/s), $V_{As\ deposited}$ is the volume of arsenic deposited during the test (calculated according to the mass balance and the scorodite true density), t_R is the residence time and A_{seeds} the BET specific surface area of the seeds. Another way to estimate this rate is by the difference between the final (df) and initial (di) particle diameter, as given by $G= (d_f - d_i)/ t_R$. The rate of crystal growth estimated by the two aforementioned approaches showed a difference of one order of magnitude. The difference was attributed to the uncertainty in the particle diameters determined by laser scattering due to the influence of shape factor and agglomeration. In this context, specific surface area was considered a more reliable parameter and the rate of crystal growth was estimated as 10^{-12}m/s.

Figure 4.4 indicates a removal of 70% of arsenic from an industrial solution containing 1.1g/L As at one stage of a MSMPRR reactor. The residual arsenic concentrations are also superior to the limits established by the local legislation for arsenic discharge (0.2mg/L). Thus, subsequent stages are required. After 4 hours at pH 1.4, the residual arsenic concentration reached 80mg/L (34% As removal or 92% As removal in the two combined cycles). The arsenic removal in this second continuous stage is higher than the values reported by Wang *et al*. (2000) and Demopoulos (2005) (11.4% and 7%, respectively) treating 0.5g As/L in a second batch precipitation. The value of 34% obtained in the second MSMPRR reactor is lower than the arsenic removed in our batch tests with an initial arsenic concentration of 0.5 and 0.1g/L (80.5% and 94.6%, respectively). If the option for the polishing step is the FH-As process, the amount of iron required in the co-precipitation with Fe(III)/As(V), pH 4, could be significantly reduced when compared with the amount of iron currently used in the FH-As process in the plant. Additionally, the fine amorphous ferryhydrite may be recycled as seeds to the scorodite reactor. Thus, an industrial waste with larger arsenic content than the one obtained with the ferrihydrite process alone will be obtained. This in turn will reduce the total waste volume generated and the cost associated with the final disposal.

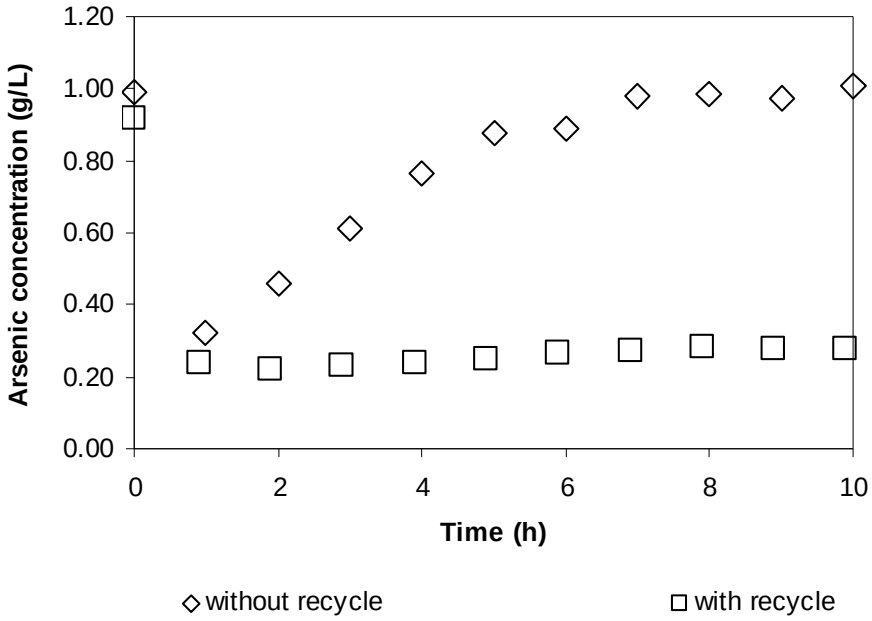

Figure 4.4 – Arsenic concentration in the solution leaving the reactor for tests carried out with (MSMPRR reactor) and without (MSMPR reactor) recycle of seeds (T = 95ºC, seeds concentration = 40g/L, Fe:As = 1.0).

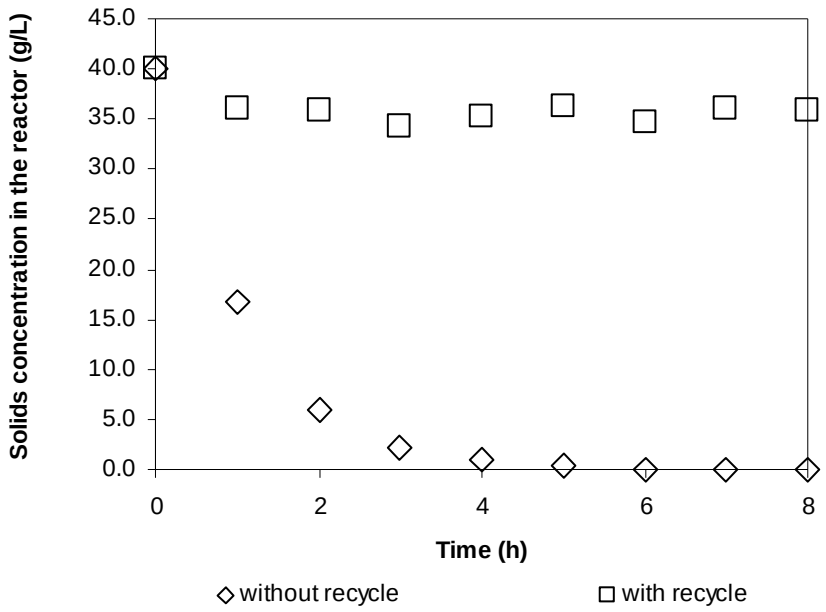

Figure 4.5 – Variation of the solids concentration for tests carried out in the MSMPRR and MSMPR reactors (T = 95ºC, initial seeds concentration = 40g/L, Fe:As = 1.0).

As mentioned previously, pH is the parameter that mostly affects supersaturation. Additionally, it is difficult to control the pH at high temperatures (95ºC) and a characteristic of the scorodite precipitation is the decrease of the pH as the reaction proceeds. Singhania *et al.* (2005) showed that the control of pH becomes unnecessary once the precipitation has been initiated, which was confirmed by our batch experiments. Thus, it is important to define an initial pH that guarantees that the reaction will occur within the region of crystal growth that favors scorodite precipitation. In this work, tests were carried out under two different pH values measured at ambient temperature (Figure 4.6), as an attempt to establish a more practical procedure than the methodology described in the literature (Singhania *et al.*, 2006). An arsenic removal of 52% was found at an initial pH of 0.9 (298K), against 70% in an initial pH of 1.1. The test carried out at an initial pH of 0.9 (final pH of 0.8) led to a decrease followed by an increase of arsenic concentration in the exit stream. In the test carried out at an initial pH of 1.1, pH decreases to a final value of 1.0, which was not low enough to cause redissolution of the solid phase. According to Eq. (3.3), the supersaturation level remained in a range of 3-5, after equilibrium condition was achieved. Another factor than can contribute to the different levels of arsenic removal is the decrease of the seed's specific surface area during consecutive runs in

the MSMPRR reactor. A decrease from approximately $4m^2/g$ to $1m^2/g$ (Figure 4.6) in the SSA of the seeds promoted a decrease of 86.4% to 72.6% in the arsenic removal.

Figure 4.6 also shows the effect of Fe/As ratio on arsenic removal. The results indicate 70% removal at a Fe/As molar ratio of 1:1 and 72.6% removal at a Fe/As molar ratio of 2:1, both tests carried out at pH 1.1. These results show that arsenic removal is not significantly affected by excess of iron in solution. This result does not agree with the findings of Singhania *et al.* (2006) and Demopoulos (2005) in batch systems, with an initial arsenic concentration of 10g/L. These authors found that arsenic precipitation decreases with the increase in the Fe(III)/As(V) molar ratio. Analyses of the residual concentrations of iron and arsenic are shown in Table IV.4.I. The results indicate that the excess of iron remained in solution and that a solid with a molar Fe/As 1:1, characteristic of scorodite, is produced, regardless the Fe/As molar ratio in the aqueous phase.

Table IV.1 – Variation of the iron and arsenic concentrations for a test carried out in a MSMPRR reactor (initial Fe:As = 2:1; T = 95ºC; seeds concentration = 40g/L) .

Time (h)	As (g/L)	Fe (g/L)	Fe/As molar ratio
0	0.92	1.40	2.04
1	0.50	1.03	2.76
2	0.48	1.05	2.92
3	0.13	0.75	7.89
4	0.13	0.74	7.83
5	0.13	0.74	7.53
6	0.14	0.74	7.17
7	0.14	0.74	6.84
8	0.15	0.75	6.65

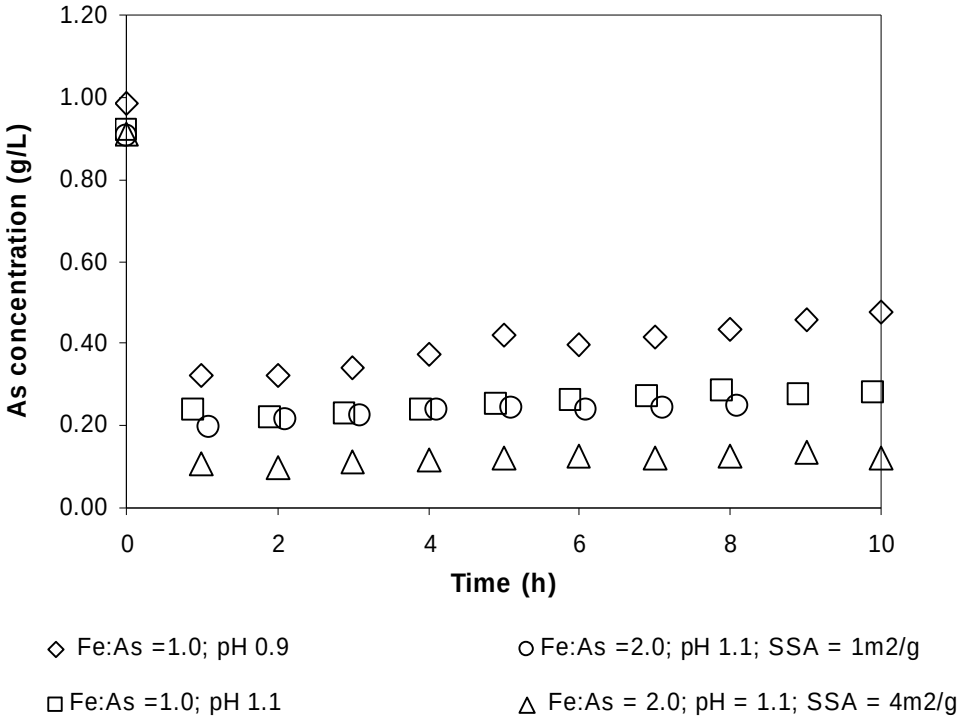

Figure 4.6 – Arsenic concentration in the exit solution for different Fe/As molar ratio, pH values and seeds with different specific surface area (T = 95ºC, seeds concentration = 40g/L).

4.3.1 Characterization of the Precipitates and Evaluation of TCLP - leachability

The seeds were produced in autoclave under different initial arsenic concentrations (25g/L and 33g/L) and pH values (1.5 and 1.3). Both parameters affect supersaturation, and consequently crystal growth. In the two cases, X-ray diffraction patterns indicated the formation of scorodite (showed in the Appendix B). According to the SEM images the scorodite seeds produced in the two tests present different morphologies. For an arsenic concentration of 25g/L and pH 1.5, agglomerates of particles with round shape, with a specific surface area of 13.96m^2/g and an average diameter of approximately 2.5 μm were formed (Figure 4.7 (a)). For an arsenic concentration of 33g/L and pH 1.3 particles with plate-like shape, with a specific surface area of 14.42m^2/g and an average diameter of approximately 1.6 μm were formed (Figure 4.7 (b)).

In a continuous system, the SPI ratio (the mass ratio of the produced solids and seeds added to the system) is higher than under batch conditions due to the treatment of high volumes of solutions and the recycle of solids. The SPI was always higher than 15%, and so it was not difficult to assure that the analyses were able to detect fresh precipitates. The X-ray diffraction patterns of the seeds as well as of the solids produced with Fe:As molar ratios of 1:1 and 2:1 (Figure 4.8) indicated the formation of scorodite; no other phase has been detected. The chemical analysis indicated a Fe:As molar ratio of 1:1 in the solids precipitated from the solution with a Fe:As molar ration of 1:1 and 2:1, in agreement with the formation of scorodite.

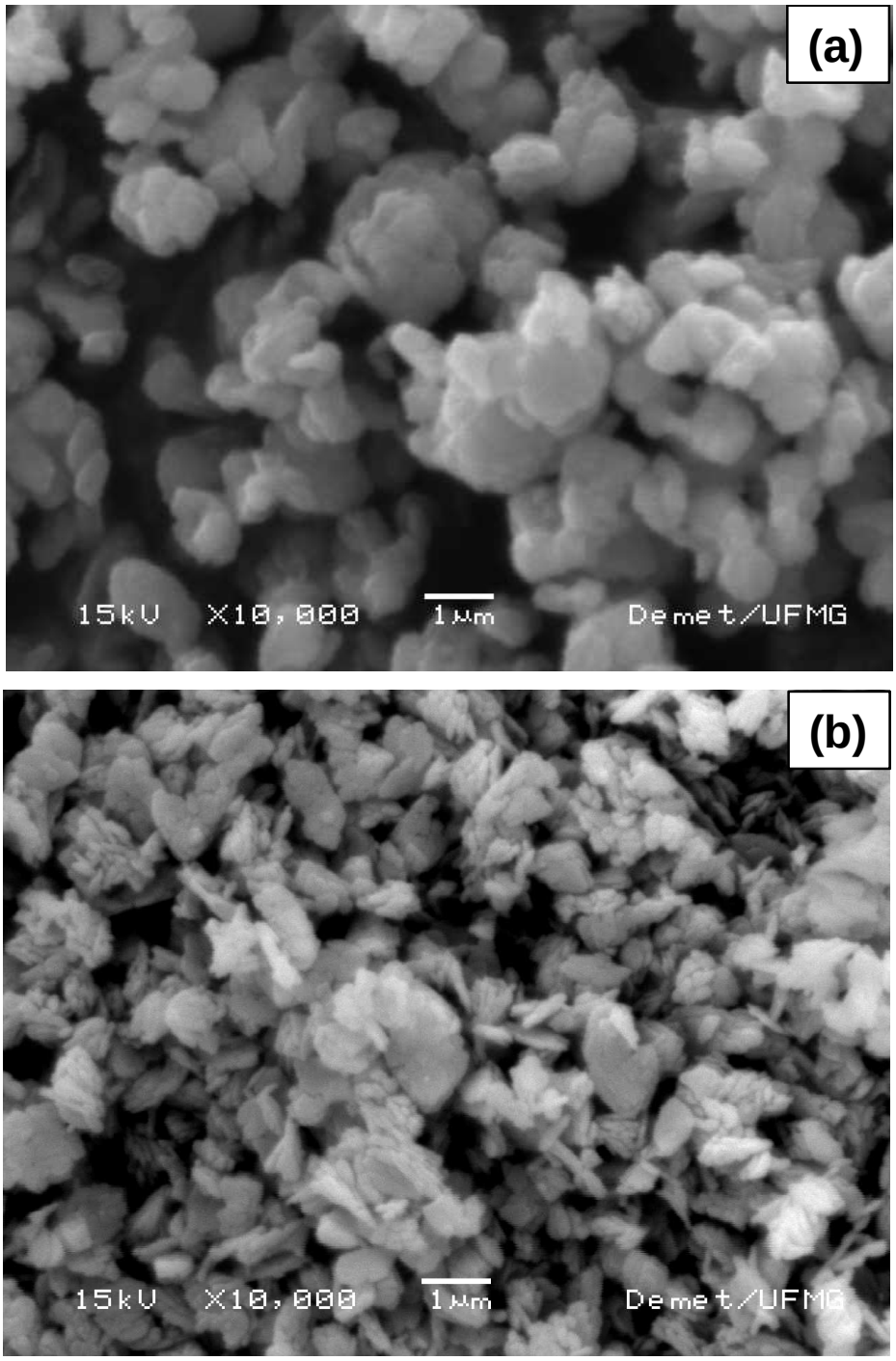

Figure 4.7 - SEM images obtained in the two syntheses in autoclave (a) arsenic concentration of 25g/L and pH 1.5; D_{50} = 2.5µm; SSA = 13.96m^2/g (b) arsenic concentration of 33g/L and pH 1.3; D_{50} = 1.6µm; SSA = 14.42m^2/g (magnification of 10.000 times).

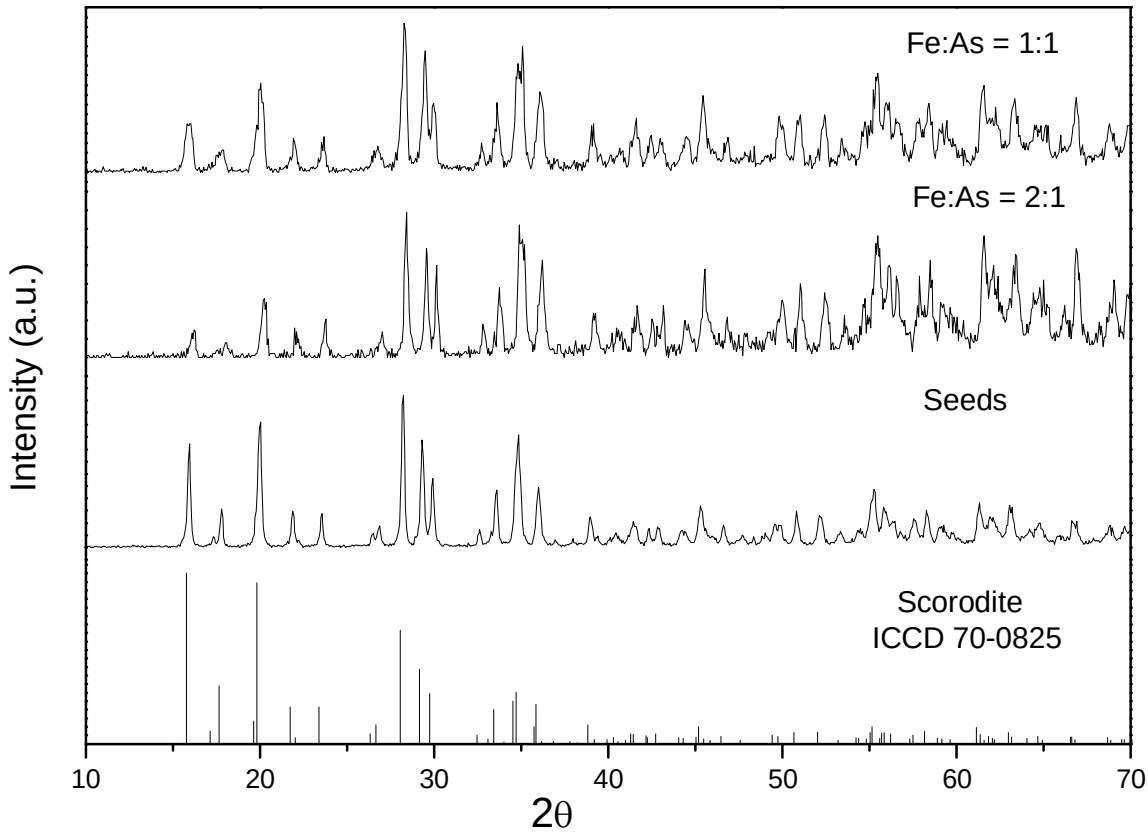

Figure 4.8 – X-ray diffraction patterns of solids obtained under different Fe:As molar ratios.

In the present work, the scorodite with plate-like shape, obtained under hydrothermal conditions was used as seeds. The growth of the fresh scorodite seeds was verified in consecutive runs in a MSMPRR reactor (Figure 4.9). The average diameter increases from 1.6μm to approximately 5.3μm in 62 hours of the precipitation process. A slight decrease of the particle size after 10 and 42 hours was explained by the solid dissolution due to a pH drop in this specific runs. The decrease of the specific surface area with the reaction time was expected as a result of crystal growth and mainly by the agglomeration process of the particles. The decrease was found to be significant (Figure 4.9) and associated with the densification process of the solids during the consecutive runs in a MSMPRR reactor. The initial specific surface area of 14.42m^2/g decreased to only 0.96m^2/g after 62 hours of reaction. The decrease in the specific surface area promotes a decrease in the available area for the crystal growth and consequently a decrease in the arsenic removal from the solution. Thus, a limited

number of recycles should be carried out, in order to assure better levels of arsenic removal.

Figure 4.10 shows the variation in the particle size in one precipitation test. The crystal growth was measured as 2.5μm in 10 hours of reaction. The crystal growth is also demonstrated by the SEM images (Figure 4.11). The SEM images also illustrate the morphologic modifications of the scorodite seeds as a function of reaction time (Figure 4.11). The initial agglomerates depicted a plate-like shape that is modified to agglomerates of round-shape particles after approximately 52 hours of reaction.

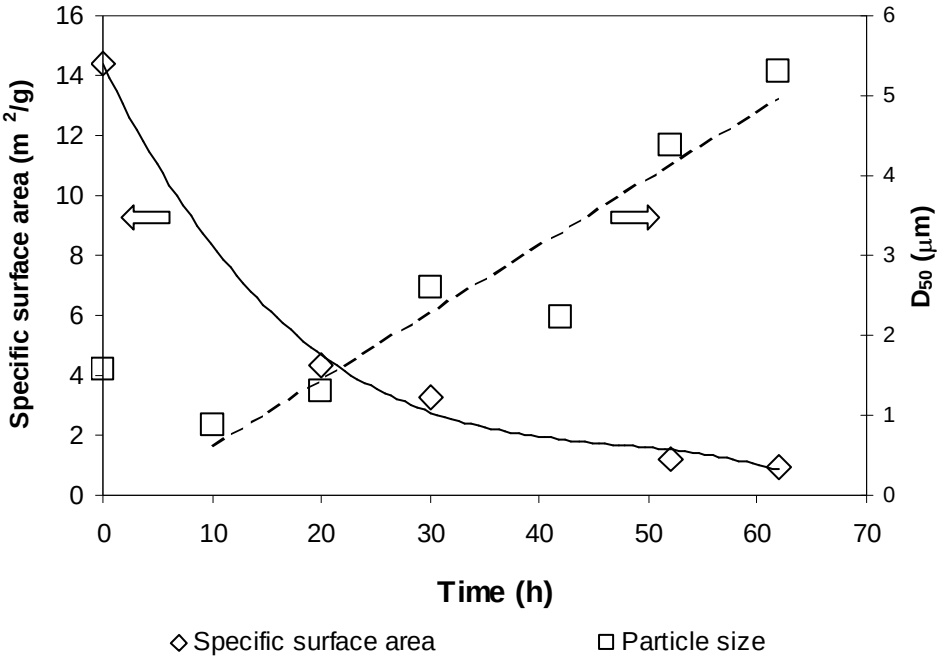

Figure 4.9 – Specific surface area and particle size of the solids (exit stream) as a function of time for consecutive runs in a MSMPRR reactor.

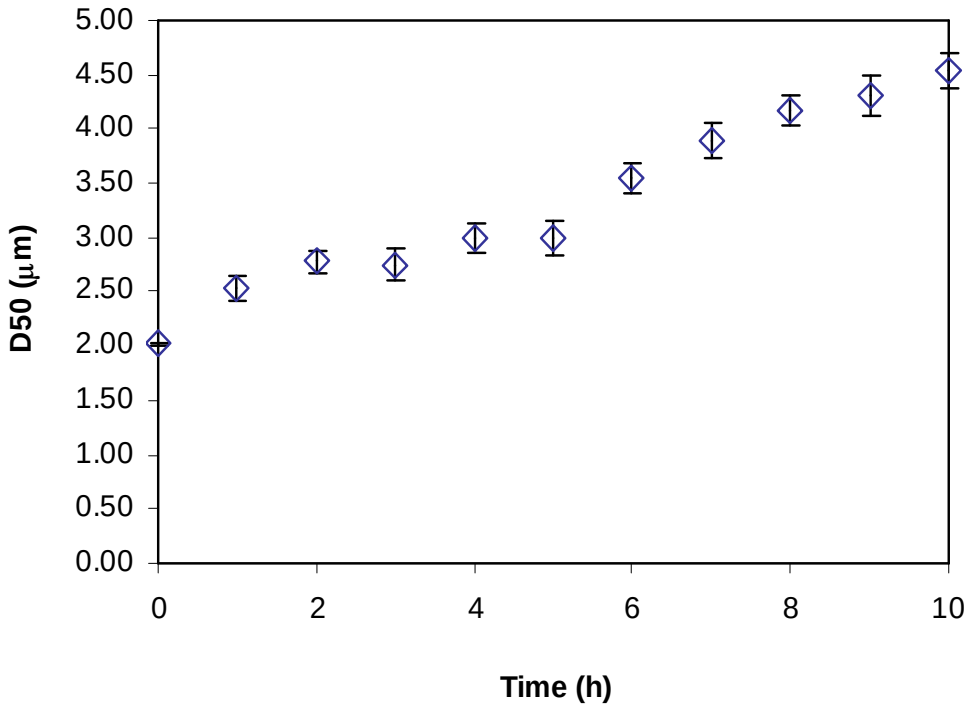

Figure 4.10 – Particle size as a function of time in a precipitation test of 10 hours (T = 95ºC, seeds concentration = 40g/L, Fe:As = 1.0).

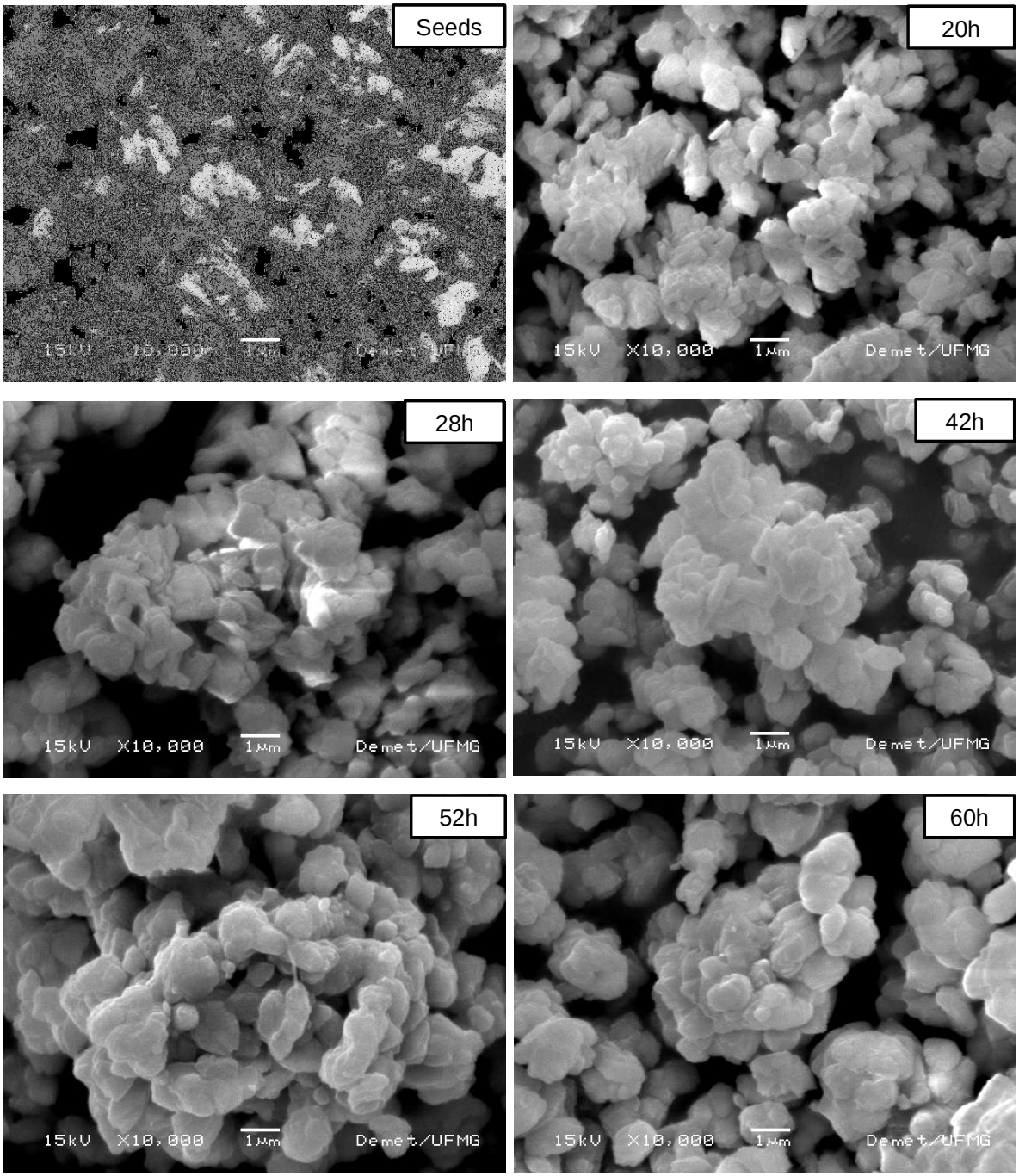

Figure 4.11 – SEM micrographs of scorodite seeds produced in autoclave and of precipitates after 20, 28, 42, 52 and 60 hours (magnification of 10.000 times).

Samples of the two seeds produced in autoclave were subjected to the toxicity characteristic leaching procedure (TCLP). The scorodite with round shape (Figure 4.7a) showed an arsenic leachability of 13.6 mg/L, against 5.0mg/L for the scorodite with plate-like shape (Figure 4.7b). This suggests that the morphology of the particles may influence the solid leachability, once the specific surface area of the two solids is practically the same (13.96 and 14.42m^2/g).

The solid samples produced in the continuous test were also submitted to the TCLP tests. According to Figure 4.12 the arsenic leachability dropped in the first 10 hours of reaction and was maintained in a low level (<1mg/L) until approximately 50 hours of reaction, reaching the limit allowed by Brazilian legislation (1mg/L) (ABNT, 2004). This result agrees with the findings of batch tests and indicates that the ageing plays an important role on scorodite leachability. The decrease of TCLP – solubility is attributed to the significant decrease in the SSA as a combination of crystal growth and densification, the latter even more evident in the work by Caldeira *et al.* (2005). However, a further increased was observed after 60 hours of reaction reaching approximately 2.0mg/L (the test was carried out in triplicate). This behavior may be associated with the increasing percentage of fresh precipitates within the reactor at longer reaction time.

According to the results of TCLP tests, it can be concluded that the morphology of the scorodite precipitated, influence in the solid solubility. Scorodite with round shape presents an arsenic leachability higher than the scorodite with plate-like shape, for the same specific surface area. Additionally, the ageing plays an important role on scorodite leachability; the solubility decrease due to the significant decrease in the SSA.

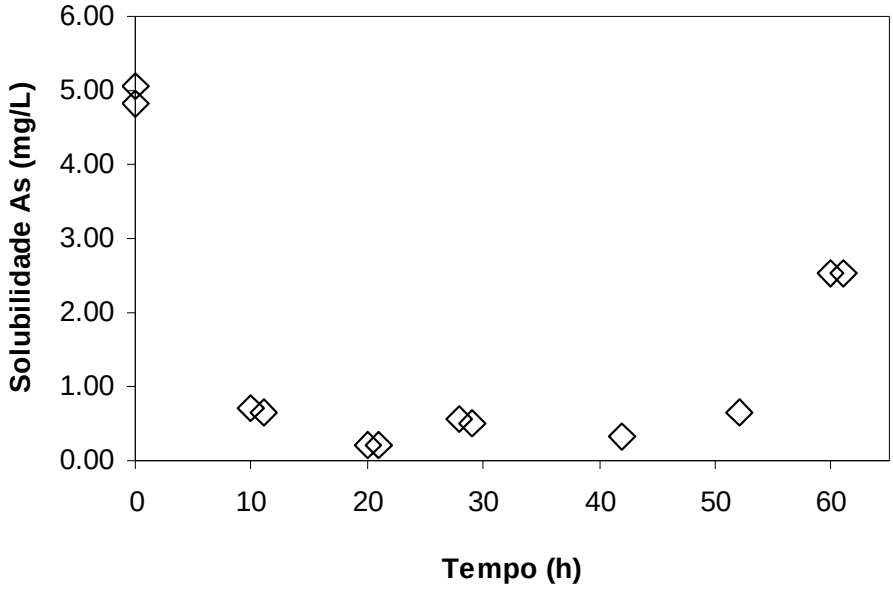

Figure 4.12 – Variation in the TCLP solubility with the time of recycle of solids (T = 95ºC; seeds concentration = 40g/L).

4.3.2 Application of the crystallizer model

The original project aimed the study of the mechanism of scorodite precipitation through the determination of the nucleation rate and the rate of crystal growth, using the reactor model MSMPR (*Mixed Suspension Mixed Product Removal*). This model assumes the absence of particles in the feed. However, as shown previously, it was not possible to carry out an efficient arsenic removal without the recycle of the solids (Figure 4.4). Thus, the MSMPR model could not be applied. The model that approaches better to the conditions of the present study is that of a crystallizer with classified product removal. However, this model includes a classification apparatus and the recycle of the treated solution, which does not correspond to the operational conditions used in the work.

In a MSMPR crystallizer, the nucleation rate and the growth rate is calculated by plotting ln(*n)* versus crystal size (*L*), where ln*(n)* is the population density of nucleus (in number of particles/volume(V)*range of size (ΔL)). This model was discussed in Chapter 2. The nucleation rate and the growth rate are determined by the intercept on the Y-axis and the slope ($-1/G\tau$), respectively of the straight line ln(*n)* vs. (*L*). In the

present work, the experimental data was plotted (Figure 4.13) in order to compare the variation of the population density with crystal size in the MSMPRR reactor. In order to obtain the population density, firstly the crystal size distribution was carried out in a sample taken from the reactor after the steady state has been reached. Figure 4.14 shows the crystal size distribution of the solids obtained in 9 hours of reaction with recycle of seeds. After 9 hours, steady state has been reached, as shown by the constant arsenic concentration in the exit stream (Figure 4.4). A bimodal distribution was observed: the fine particles with an average diameter of approximately 0.3μm (region (a) in Figure 4.14), and the large particles with an average diameter of approximately 6 μm (region (b) in Figure 4.14). The plot of population density was plotted as a function of crystal size showed two different slopes (Figure 4.14), thus confirming the deviation from the MSMPR model. The slope (a) in Figure 4.13 corresponds to the region (a) in Figure 4.14. Attrition or other breakage process may have produced the fines particles. The slope (b) in Figure 4.13 corresponds to the region (b) in Figure 4.14 and indicates very low growth rates.

Thus, an additional investigation is required in order to identify and to extend the existing models to the present study. A broader discussion of the mechanism of scorodite precipitation based on parameters such as nucleation rate and the growth rate is not possible yet.

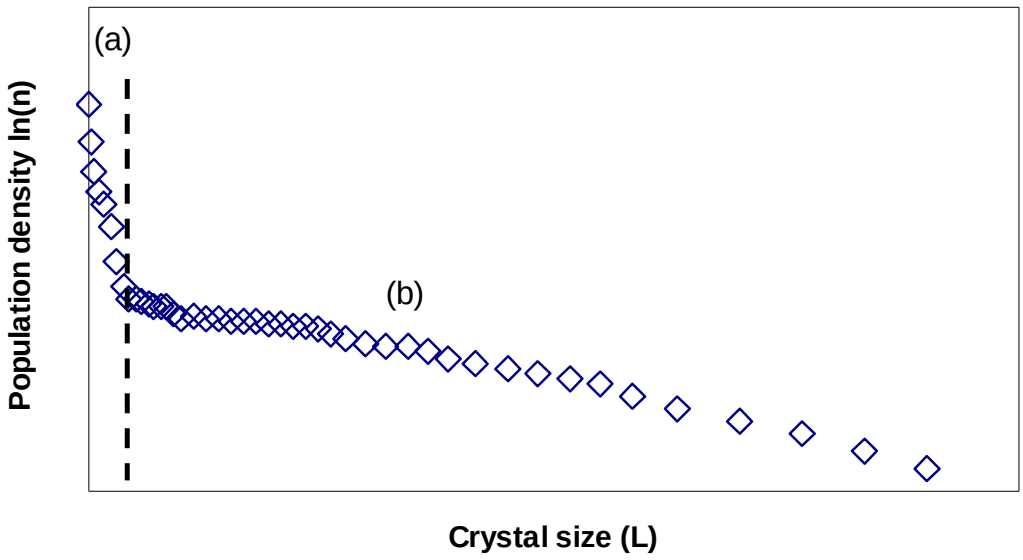

Figure 4.13 – Population density versus crystal size for a sample taken from the slurry after 9 hours of reaction (with recycle of seeds).

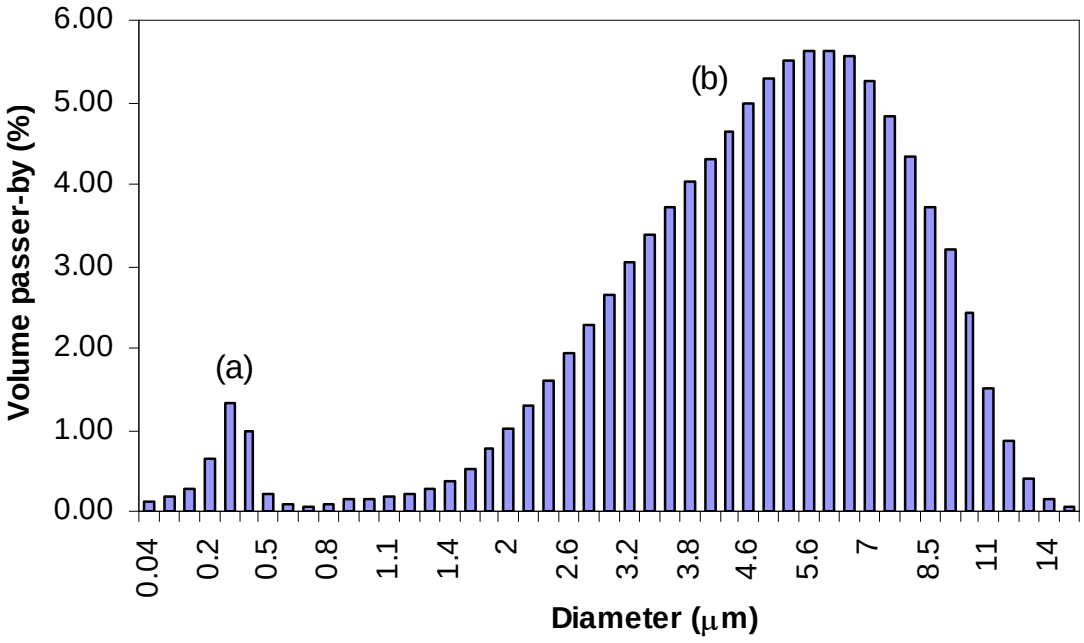

Figure 4.14 – Crystals size distribution in a sample taken from the slurry after 9 hours of reaction (with recycle of seeds).

4.4 Conclusions

A methodology to achieve high yields of arsenic removal by precipitation of scorodite in continuous system was established. It was demonstrated that due to the low rate of crystal growth, the full recycle of seeds becomes always necessary (considering a residence time of 1 hour). For a Fe:As molar ratio of 1:1, 70% of the arsenic was removed from the solution. For the Fe:As molar ratio of 2:1, the arsenic removal increased to 72.6%. This result shows that the arsenic removal is not significativelly affected by the iron excess. Another factor than can contribute to the different levels of arsenic removal is the decrease in the specific surface area of the seeds used in the consecutive runs in a MSMPRR reactor. A decrease from approximately $4m^2/g$ to $1m^2/g$ in the SSA of the seeds promoted an decrease of 86.4% to 72.6% in the arsenic removal.

The arsenic leachability (TCLP) dropped in the first 10 hours of reaction down to a level of <1mg/L (the limit allowed by Brazilian legislation; ABNT NBR 10005/2004), then remaining approximately constant up to 50 hours of reaction. This finding confirms the results obtained in batch reactor, which showed that aging plays an important role on scorodite leachability, by favoring crystal growth and the decrease of surface area. For the same specific surface area, the TCLP tests show that particles with round shape showed an arsenic leachability higher than the particles with plate-like shape.

4.5 References

ABNT – ASSOCIAÇÃO BRASILEIRA DE NORMAS TÉCNICAS (2004). NBR 10005 – Procedimento para obtenção de extrato lixiviado de resíduos sólidos (*Procedure for obtention leaching extract of solid wastes*). Rio de Janeiro, p.16.

CALDEIRA, C.L., CIMINELLI, V.S.T., BATISTA, I.S. and MOURA, W. (2005). Precipitação de Escorodita a temperatura Controlada e Pressão Ambiente. Proceedings of XXI Encontro Nacional de Tratamento de Minérios e Metalurgia Extrativa – ENTMME, Natal, p.93-99.

DEBEKAUSSEN, R., DROPPERT, D. and DEMOPOULOS, G. P. (2001). Ambient pressure hydrometallurgical conversion of arsenic trioxide to crystalline scorodite. *CIM Bulletin*, v. 94, n. 1051, p.116-122.

DELIBERAÇÃO NORMATIVA COPAM Nº10, de 16 de dezembro de 1986. Publicação Diário do Executivo – Minas Gerais, 10-1-1987. Estabelece normas e padrões para qualidade das águas, lançamento de efluentes nas coleções de águas, e dá outras providências.

DEMOPOULOS, G.P., DROPPERT, D. J. and VAN WEERT, G. (1995). Precipitation of Crystalline Scorodite ($FeAsO_4.2H_2O$) from Chloride Solutions. *Hydrometallurgy*, v. 38, p.245-261.

DEMOPOULOS, G.P. (2005). On the Preparation and Stability of Scorodite. In: Arsenic Metallurgy. R. G. Reddy and V. Ramachandran, eds, *TMS (The Minerals, Metals & Materials Society),* p.25-49.

EPA SW-846, (1992). Test Methods for Evaluating Solid Waste, Physical/Chemical Methods. Method 1311.

FILIPPOU, D. and DEMOPOULOS, G.P. (1997). Arsenic Imobilization by Controlled Scorodite Precipitation. *JOM*, v. 12, n. 14, p.52-55.

LAWRENCE, B. and VOIGT, J. (1986). Aqueous precipitation in hydrometallurgy. In: Metallurgical Society Annual Meeting, March 2-6, New Orleans, Lousiania. Hydrometallurgical Reactor design and kinetics. Edited by BAUTISTA, R.G., WESELY, R.J. and WARREN, G.W. p.441-456.

SINGHANIA, S., WANG, Q., FILIPPOU, D. and DEMOPOULOS, G.P. (2005). Temperature and Seeding Effects on the Precipitation of Scorodite from Sulfate Solutions under Atmospheric-Pressure Conditions. *Metalurgical and Materials Transactions B*, v. 36B, p.327-333.

SINGHANIA, S., WANG, Q., FILIPPOU, D. and DEMOPOULOS, G.P. (2006). Acidity, Valency and Third-Ion Effects on the Precipitation of Scorodite from Mixed sulfate Solutions under Atmospheric-Pressure Conditions. *Metalurgical and Materials Transactions B*, v. 37B, *in press*.

WANG Q., DEMOPOULOS G.P. and HARRIS G.B. (2000). Arsenic Fixation in Metallurgical Plant Effluents in the Form of Crystalline Scorodite via a Non-autoclave Oxidation-Precipitation Process. *Minor Elements*, C.A. Young (editor), Soc. Min. Met. Expl., Littleton, CO, U.S.A., p.225-237.

5 REFERENCES

CALDEIRA, C.L., CIMINELLI, V.S.T., BATISTA, I.S. and MOURA, W. (2005). Precipitação de Escorodita a temperatura Controlada e Pressão Ambiente. Proceedings of XXI Encontro Nacional de Tratamento de Minérios e Metalurgia Extrativa – ENTMME, Natal, p.93-99.

CHENG, R.C., LIANG, S., WANG, H. and BEUHLER, M.D. (1994). Enhanced coagulation for arsenic removal. *Jounal AWWA*, v. 86, n. 9, p. 79-90.

DEBEKAUSSEN, R., DROPPERT, D. and DEMOPOULOS, G. P. (2001). Ambient pressure hydrometallurgical conversion of arsenic trioxide to crystalline scorodite. *CIM Bulletin*, v. 94, n. 1051, p.116-122.

DESCHAMPS, E., CIMINELLI, V.S.T., and HOLL, W.H. (2005). Removal of As(III) and As(V) from water using a natural Fe and Mn enriched sample. *Water Research*, v.39, p.5212–5220.

DELIBERAÇÃO NORMATIVA COPAM Nº10, de 16 de dezembro de 1986. Publicação Diário do Executivo – Minas Gerais, 10-1-1987. Estabelece normas e padrões para qualidade das águas, lançamento de efluentes nas coleções de águas, e dá outras providências.

DEMOPOULOS, G.P., DROPPERT, D. J. and VAN WEERT, G. (1995). Precipitation of Crystalline Scorodite ($FeAsO_4.2H_2O$) from Chloride Solutions. *Hydrometallurgy*, v. 38, p. 245-261.

DEMOPOULOS, G.P. (2005). On the Preparation and Stability of Scorodite. In: Arsenic Metallurgy. R. G. Reddy and V. Ramachandran, eds, *TMS (The Minerals, Metals & Materials Society),* p.25-49.

DUTRÉ, V. and VANDECASTEELE, C. (1998). Immobilization Mechanism of Arsenic in Waste Solidified Using Cement and Lime. *Environmental Science & Technology*, v. 32, n. 18, p.2782-2787.

DUTRIZAC, J.E. and JAMBOR, J.L. (1998). The occurence and constitution of natural and synthetic ferrihydrites, a widespread ion oxyhydroxide. *Chemical Reviews* v.7, p. 2549. Apud HARRIS, B. (2003). The removal of arsenic from process solutions: theory and industrial practice. Hydrometallurgy 2003 – Fifth International Conference in Honor of Professor Ian Ritchie, v.2: Electrometallurgy and Environmental hydrometallurgy. Edited by Harris, B., Young, C.A., Alfantazi, A.M., Anderson, C.G., Dreisinger, D.B., and James, A. TMS (The Minerals, Metals & Materials Society).

EMETT, M., ZAM, M. and LOWSON, R. (2001). Ensuring the long term stability of arsenic bearing wastes. 26th Annual Minerals Council of Australia Environmental Workshop.

FILIPPOU, D. and DEMOPOULOS, G.P. (1997). Arsenic Imobilization by controlled Scorodite Precipitation. *JOM*, v. 12, n. 14, p.52-55.

HARRIS, G.B. and KRAUSE, E. (1993). The disposal of arsenic from metallurgical process: Its status regarding ferric arsenate. In The Paul E. Queneau International Symposium – Extrative Metalurgy of Copper, Nickel and Cobalt, Volume 1, Fundamental Aspects. Edited by R.G. Reddy and R.N. Weizenback. The Minerals, Metals and Materials Society, Warrendale, p.1221-1237. Apud DEBEKAUSSEN, R., DROPPERT, D. and DEMOPOULOS, G. P. (2001). Ambient pressure hydrometallurgical conversion of arsenic trioxide to crystalline scorodite. *CIM Bulletin*, v. 94, n. 1051, p.116-122.

HARRIS, B. (2003). The removal of arsenic from process solutions: theory and industrial practice. Hydrometallurgy 2003 – Fifth International Conference in Honor of Professor Ian Ritchie, v.2: Electrometallurgy and Environmental hydrometallurgy. Edited by Harris, B., Young, C.A., Alfantazi, A.M., Anderson, C.G., Dreisinger, D.B., and James, A. TMS (The Minerals, Metals & Materials Society).

HSC Chemistry. (1999). Chemical Reaction and Equilibrium Software with Extensive Thermochemical database. Ver. 4.1, Outokumpu Research Oy, Pori, finland.

IPT – INSTITUTO DE PESQUISAS TECNOLÓGICAS. (1997). TU Delft. Industrial Crystallisation and Precipitation. São Paulo. 19-21 November.

IPT – INSTITUTO DE PESQUISAS TECNOLÓGICAS. (2004). TU Delft. Lectures on Industrial Crystallization and Precipitation. São Paulo. 24-26 November.

KRAUSE, E. and ETTEL, V.A. (1989). Solubilities and Stabilities of Ferric Arsenate Compounds. *Hydrometallurgy*, v.22, n. 3, p.311-337.

KUMARESAN, M. and RIYAZUDDIN, P. (2001). Overview of speciation chemistry of arsenic. *Current Science*, v. 80, n. 7, p.837-846.

LADEIRA, A. C. Q. and CIMINELLI, V, S, T. (2004). Adsorption and desorption of arsenic on an oxisol and its constituents. *Water Research*, vol. 38, p.2087-2094.

LAWRENCE, B. and VOIGT, J. (1986). Aqueous precipitation in hydrometallurgy. In: Metallurgical Society Annual Meeting, March 2-6, New Orleans, Lousiania. Hydrometallurgical Reactor design and kinetics. Edited by BAUTISTA, R.G., WESELY, R.J. and WARREN, G.W. p.441-456.

LEIST, M., CASEY, R.J. and CARIDI, D. (2000). The management of arsenic wastes: problems and prospects. *Jounal of Hazardous Materials*, v.76, n. 1, p.125-138.

MAMBOTE, R.C.M., REUTER, M.A., SANDWIJK., A. and KRIJGSMAN, P. (2001). Immobilization of arsenic in crystalline form from aqueous solution by hydrothermal processing above 483,15K. *Minerals Engineering*, v. 14, n. 4, p.391-403.

MERSMANN, A. (2001). Crystallization Technology Handbook. Second Edition – Revised and Expanded. Marcel Dekker, Inc. New York – Basel. 832p.

PAPASSIOPI, N., VIRCÍKOVÁ, E., NENOV, V., KONTOPOULOS, A., MOLNÁR, L.. (1996). Removal and fixation of arsenic in the form of ferric arsenates. Three parallel experimental studies. *Hydrometallurgy*, v.41, n. 2-3, p.234-253.

PORTARIA 1469/2000 do Ministério da Saúde, de 29 de dezembro de 2000. Estabelece os procedimentos e responsabilidades relativos ao controle e vigilância da qualidade da água para consumo humano e seu padrão de potabilidade, e dá outras providências. Brazil. p. 25.

RANDOLPH, A.D. and LARSON, M.A. (1998). Theory of Particulate Process. Analysis and Techniques of continuous crystallization. Second edition. Chapter 4, p.80-86.

SINGHANIA, S., WANG, Q., FILIPPOU, D. and DEMOPOULOS, G.P. (2005). Temperature and Seeding Effects on the Precipitation of Scorodite from Sulfate Solutions under Atmospheric-Pressure Conditions. *Metalurgical and Materials Transactions B*, v. 36B, p.327-333.

SINGHANIA, S., WANG, Q., FILIPPOU, D. and DEMOPOULOS, G.P. (2006). Acidity, Valency and Third-Ion Effects on the Precipitation of Scorodite from Mixed sulfate Solutions under Atmospheric-Pressure Conditions. *Metalurgical and Materials Transactions B*, v. 37B, *in press*.

SMEDLEY, P.L. and KINNIBURGH, D.G. (2002). A review of the source, behavior and distribution of arsenic in natural waters. *Applied Geochemistry*, v.17, n.5, p.517–568.

SÖHNEL, O. and GARSIDE, J.. (1992). Precipitation; Basic principles and industrial applications. First published. London: Butterworth Heinemann, p.391.

SWASH, P.M. and MONHEMIUS, A.J. (1994). Hydrothermal precipitation from aqueous solutions containing iron(III), arsenate and sulphate. In: HIDROMETALLURGY ’94, 1. Cambridge, England. London: Chapman & Hall, [s.d.]. p.177-190.

SWASH, P.M. and MONHEMIUS, A.J. (1995). The disposal of arsenical wastes: technologies and environmental considerations. In: N.J. Roberts, Editor, INTERNATIONAL MINERALS AND METALS TECHNOLOGY, Sabrecrown Publishing, London.

WELHAM, N.J., MALATT, K.A. and VUKCEVIC, S. (2000). The stability of iron phases presently used for disposal from metallurgical systems – A review. *Minerals Engineering*, v. 13, n. 8-9, p.911-931.

WHO – WORLD HEALTH ORGANIZATION. (1993). Guidelines for drinking water quality. Geneva, Switzerland.

6 APPENDICES

6.1 Appendix A: X-ray diffraction patterns of solids precipitated in batch tests with different SPI.

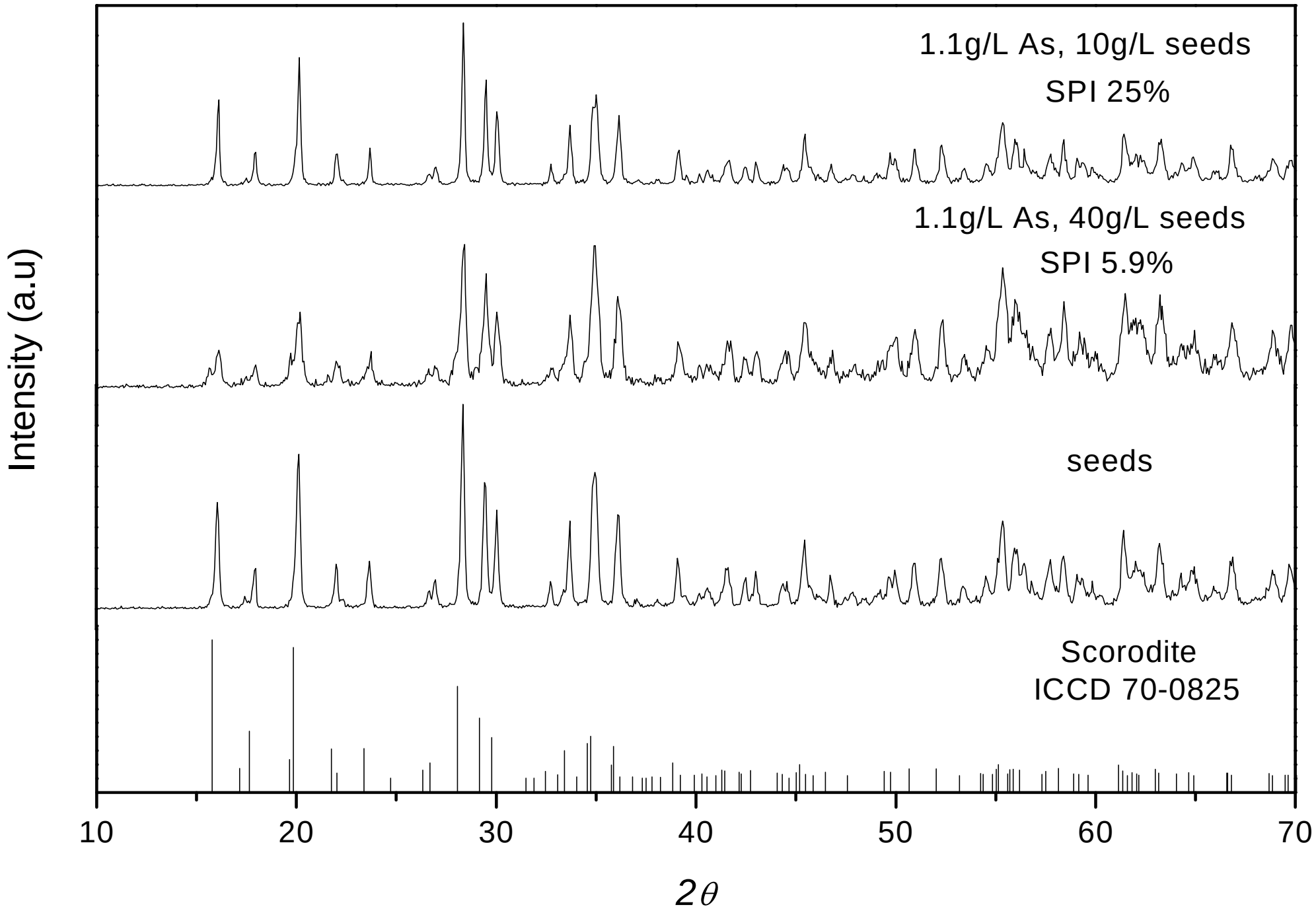
1.1g/L As, 10g/L seeds
SPI 25%
1.1g/L As, 40g/L seeds
SPI 5.9%
seeds
Scorodite
ICCD 70-0825
Intensity (a.u)
10
20
30
40
50
60
70
2θ

6.2 Appendix B: X-ray diffraction patterns of the two syntheses of scorodite seeds in autoclave.

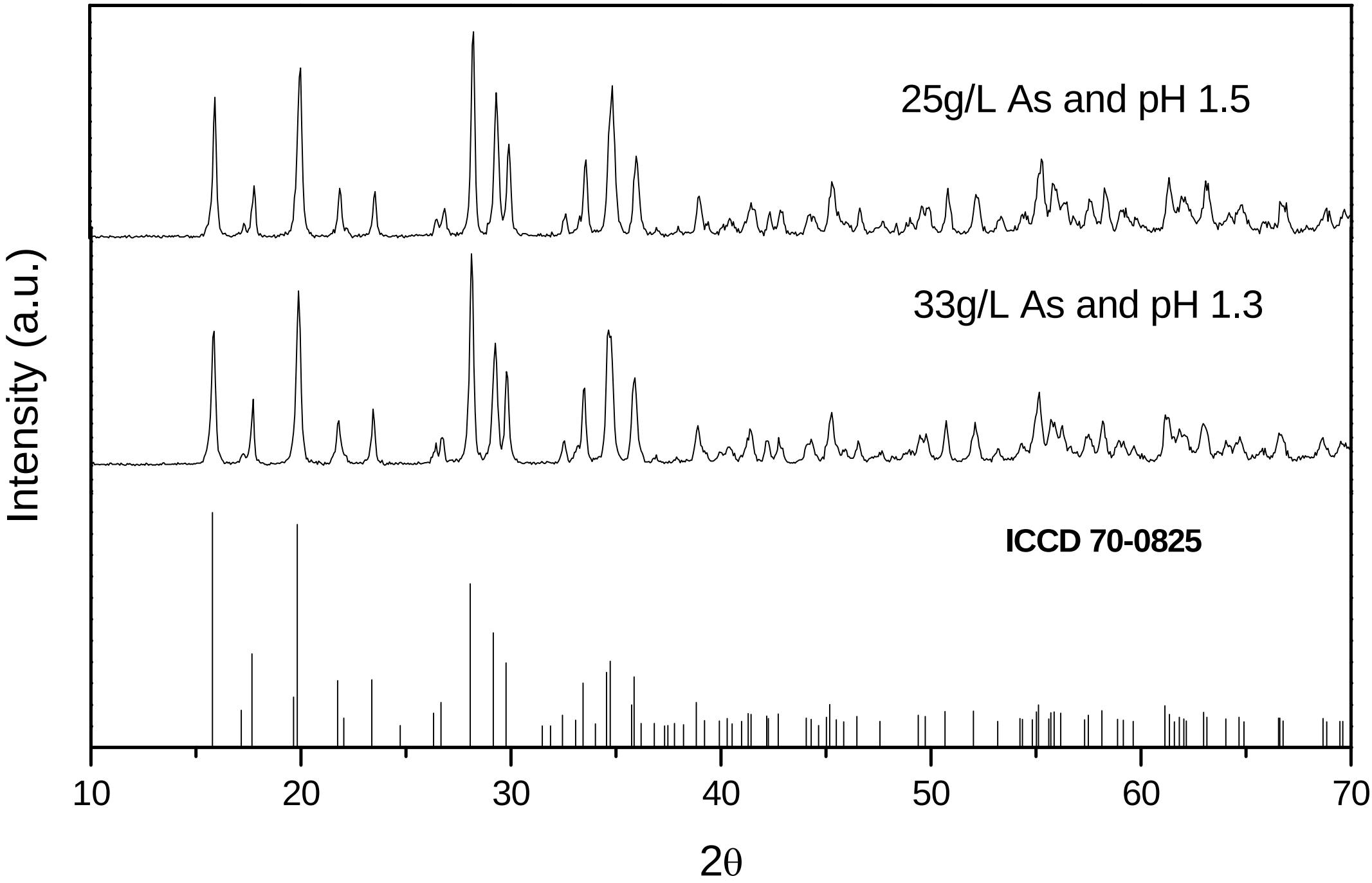
25g/L As and pH 1.5
33g/L As and pH 1.3
ICCD 70-0825
Intensity (a.u.)
10
20
30
40
50
60
70
2θ

6.3 Appendix C: Results of the chemical analyses – Batch Tests

Avaliação da concentração inicial de As

EB26 — 0,10g As/L

Amostra	tempo (h)	As total (g/L)	Fe total (g/L)	Δ [As]	M esc.teórica (g)	IPS (%)
EB26T0	0	0.10	0.08	0.09	0.29	
EB26T1	0.5	0.01	0.03		M esc. obtida (g)	
EB26T2	1	0.01	0.03	Efic. Remoção	0	0.0
EB26T3	1.5	0.01	0.03	94.6	Rend. (%)	
EB26T4	2	0.01	0.03		0.00	

EB27 — 0,5g As/L

Amostra	tempo (h)	As total (g/L)	Fe total (g/L)	Δ [As]	M esc.teórica (g)	IPS (%)
EB27T0	0	0.47	0.36	0.38	1.16	
EB27T1	0.5	0.12	0.09		M esc. obtida (g)	
EB27T2	1	0.10	0.08	Efic. Remoção	0	0.00
EB27T3	1.5	0.09	0.07	80.5	Rend. (%)	
EB27T4	2	0.09	0.07		0.00	

EB16 — 1,1g As/L

Amostra	tempo (h)	As total (g/L)	Fe total (g/L)	Δ [As]	M esc.teórica (g)	IPS (%)
EB16T0	0	1.15	0.76	1.08	3.32	
EB16T1	0.5	0.10	0.10		M esc. obtida (g)	
EB16T2	1	0.09	0.09	Efic. Remoção	2.79	6.98
EB16T3	1.5	0.08	0.09	93.8	Rend. (%)	
EB16T4	2	0.08	0.09		84.0	
EB16T5	2.5	0.07	0.08			
EB16T6	3	0.07	0.08			
EB16T7	3.5	0.07	0.08			
EB16T8	4	0.07	0.08			

EB1 — 2,4g As/L

Amostra	tempo (h)	As total (g/L)	Fe total (g/L)	Δ [As]	M esc.teórica (g)	IPS (%)
EB1T0	0	2.42	2.25	2.09	6.44	
EB1T1	0.5	0.52	0.87		M esc. obtida (g)	
EB1T2	1	0.38	0.41	Efic. Remoção	5.46	13.65
EB1T3	1.5	0.35	0.42	86.3	Rend. (%)	
EB1T4	2	0.33	0.40		84.8	

EB25	9.6g As/L

Amostra	tempo (h)	As total (g/L)	Fe total (g/L)	Δ [As]	M esc.teórica (g)	IPS (%)
EB25T0	0	9.60	6.53	8.76	26.99	
EB25T1	0.5	1.94	1.59		M esc. obtida (g)	
EB25T2	1	1.44	1.18	Efic. Remoção	32.76	81.90
EB25T3	1.5	1.17	0.90	91.3	Rend. (%)	
EB25T4	2	1.05	0.88		121.4	
EB25T5	2.5	1.00	0.76			
EB25T6	3	0.92	0.75			
EB25T7	3.5	0.88	0.69			
EB25T8	4	0.84	0.68			
EB25TF	*	0.88	0.71			

Comparação entre sementes de gesso e de escorodita

EB4	40g/L escorodita	1g As/L

Amostra	tempo (h)	As total (g/L)	Fe total (g/L)	Δ [As]	M esc.teórica (g)	IPS (%)
EB4T0	0	1.15	0.85	1.01	3.10	
EB4T1	0.5	0.17	0.15		M esc. obtida (g)	
EB4T2	1	0.15	0.14	Efic. Remoção	2.36	5.91
EB4T3	1.5	0.14	0.13	87.6	Rend. (%)	
EB4T4	2	0.14	0.13		76.2	

EB6	40g/L gesso	1g As/L

Amostra	tempo (h)	As total (g/L)	Fe total (g/L)	Δ [As]	M esc.teórica (g)	IPS (%)
EB6T0	0	1.19	0.87	0.00	0.00	
EB6T1	0.5	1.18	0.84		M esc. obtida (g)	
EB6T2	1	1.21	0.83	Efic. Remoção		0.00
EB6T3	1.5	1.15	0.82	0.0	Rend. (%)	
EB6T4	2	1.20	0.83			

EB1	40g/L escorodita	2,4g As/L

Amostra	tempo (h)	As total (g/L)	Fe total (g/L)	Δ [As]	M esc.teórica (g)	IPS (%)
EB1T0	0	2.42	2.25	2.09	6.44	
EB1T1	0.5	0.52	0.87		M esc. obtida (g)	
EB1T2	1	0.38	0.41	Efic. Remoção	5.46	13.65
EB1T3	1.5	0.35	0.42	86.3	Rend. (%)	
EB1T4	2	0.33	0.40		84.8	

EB2	40g/L gesso	2,4g As/L

Amostra	tempo (h)	As total (g/L)	Fe total (g/L)	Δ [As]	M esc.teórica (g)	IPS (%)
EB2T0	0	2.33	1.91	0.30	0.92	
EB2T1	0.5	2.23	1.79		M esc. obtida (g)	
EB2T2	1	2.17	1.63	Efic. Remoção		0.00
EB2T3	1.5	2.10	1.92	12.9	Rend. (%)	
EB2T4	2	2.03	1.60		0.00	

EB25	40g/L escorodita	9.6g As/L

Amostra	tempo (h)	As total (g/L)	Fe total (g/L)	Δ [As]	M esc.teórica (g)	IPS (%)
EB25T0	0	9.60	6.53	8.76	26.99	
EB25T1	0.5	1.94	1.59		M esc. obtida (g)	
EB25T2	1	1.44	1.18	Efic. Remoção	32.76	81.90
EB25T3	1.5	1.17	0.90	91.3	Rend. (%)	
EB25T4	2	1.05	0.88		121.40	
EB25T5	2.5	1.00	0.76			
EB25T6	3	0.92	0.75			
EB25T7	3.5	0.88	0.69			
EB25T8	4	0.84	0.68			
EB25TF	*	0.88	0.71			

EB28	40g/L gesso	9.9g As/L

Amostra	tempo (h)	As total (g/L)	Fe total (g/L)	Δ [As]	M esc.teórica (g)	IPS (%)
EB28T0	0	9.88	6.94	6.015	18.53	
EB28T1	0.5	8.90	7.03		M esc. obtida (g)	
EB28T2	1	8.57	6.38	Efic. Remoção	5.54	13.85
EB28T3	1.5	7.80	5.81	60.91	Rend. (%)	
EB28T4	2	7.03	5.27		29.90	
EB28T5	2.5	6.26	4.61			
EB28T6	3	5.10	3.88			
EB28T7	3.5	4.61	3.31			
EB28T8	4	3.86	3.05			
EB28TF	*	3.97	3.06			

Avaliação da concentração de sementes de escorodita

EB24 5g sementes/L

Amostra	tempo (h)	As total (g/L)	Fe total (g/L)	Δ [As]	M esc.teórica (g)	IPS (%)
EB24T0	0	1.00	0.55	0.74	2.27	
EB24T1	0.5	0.38	0.31		M esc. obtida (g)	
EB24T2	1	0.31	0.26	Efic. Remoção	2.23	44.60
EB24T3	1.5	0.29	0.24	73.5	Rend. (%)	
EB24T4	2	0.27	0.23		98.1	

EB20 10g sementes/L

Amostra	tempo (h)	As total (g/L)	Fe total (g/L)	Δ [As]	M esc.teórica (g)	IPS (%)
EB20T0	0	1.10	0.72	0.88	2.71	
EB20T1	0.5	0.29	0.23		M esc. obtida (g)	
EB20T2	1	0.24	0.19	Efic. Remoção	2.41	24.10
EB20T3	1.5	0.23	0.18	80.5	Rend. (%)	
EB20T4	2	0.21	0.18		88.8	

EB8 20g sementes/L

Amostra	tempo (h)	As total (g/L)	Fe total (g/L)	Δ [As]	M esc.teórica (g)	IPS (%)
EB8T0	0	1.16	0.87	1.00	3.08	
EB8T1	0.5	0.25	0.20		M esc. obtida (g)	
EB8T2	1	0.19	0.16	Efic. Remoção	2.30	11.49
EB8T3	1.5	0.17	0.14	86.2	Rend. (%)	
EB8T4	2	0.16	0.13		74.6	

EB4 40g sementes/L

Amostra	tempo (h)	As total (g/L)	Fe total (g/L)	Δ [As]	M esc.teórica (g)	IPS (%)
EB4T0	0	1.15	0.85	1.01	3.10	
EB4T1	0.5	0.17	0.15		M esc. obtida (g)	
EB4T2	1	0.15	0.14	Efic. Remoção	2.36	5.91
EB4T3	1.5	0.14	0.13	87.6	Rend. (%)	
EB4T4	2	0.14	0.13		76.2	

EB12 80g sementes/L

Amostra	tempo (h)	As total (g/L)	Fe total (g/L)	Δ [As]	M esc.teórica (g)	IPS (%)
EB12T0	0	1.20	0.76	1.03	3.16	
EB12T1	0.5	0.19	0.12		M esc. obtida (g)	
EB12T2	1	0.18	0.12	Efic. Remoção	2.1	2.63
EB12T3	1.5	0.17	0.12	85.6	Rend. (%)	
EB12T4	2	0.17	0.12		66.4	

Avaliação do efeito da concentração de sulfato

EB5 $[SO_4^{2-}]$ = 3,5g/L

Amostra	tempo (h)	As total (g/L)	Fe total (g/L)	Δ [As]	M esc.teórica (g)	IPS (%)
EB5T0	0	1.14	0.84	1.08	3.34	
EB5T1	0.5	0.05	0.09		M esc. obtida (g)	
EB5T2	1	0.05	0.09	Efic. Remoção	2.07	5.17
EB5T3	1.5	0.05	0.09	95.6	Rend. (%)	
EB5T4	2	0.05	0.09		61.9	

EB4 $[SO_4^{2-}]$ = 25g/L

Amostra	tempo (h)	As total (g/L)	Fe total (g/L)	Δ [As]	M esc.teórica (g)	IPS (%)
EB4T0	0	1.15	0.85	1.01	3.10	
EB4T1	0.5	0.17	0.15		M esc. obtida (g)	
EB4T2	1	0.15	0.14	Efic. Remoção	2.36	5.91
EB4T3	1.5	0.14	0.13	87.6	Rend. (%)	
EB4T4	2	0.14	0.13		76.2	

EB11 $[SO_4^{2-}]$ = 100g/L

Amostra	tempo (h)	As total (g/L)	Fe total (g/L)	Δ [As]	M esc.teórica (g)	IPS (%)
EB11T0	0	1.07	0.77	0.95	2.91	
EB11T1	0.5	0.17	0.12		M esc. obtida (g)	
EB11T2	1	0.14	0.11	Efic. Remoção	3.88	9.70
EB11T3	1.5	0.13	0.10	88.7	Rend. (%)	
EB11T4	2	0.12	0.10		133.3	

6.4 Appendix D: Results of the chemical analyses – Determination of the Experimental Error

1g/L As e 40g/L sementes

EB15 pH = 1.0

Amostra	tempo (min)	As total (g/L)	Fe total (g/L)	Δ [As]
EB15T0	0	0.997	0.775	0.921
EB15T1	30	0.084	0.082	
EB15T2	60	0.088	0.090	Efic. Remoção
EB15T3	90	0.083	0.089	92.38
EB15T4	120	0.080	0.084	
EB15T5	150	0.075	0.087	
EB15T6	180	0.078	0.084	
EB15T7	210	0.073	0.084	
EB15T8	240	0.076	0.083	
EB15TF	*	0.069	0.093	

EB16 pH = 1.0

Amostra	tempo (min)	As total (g/L)	Fe total (g/L)	Δ [As]
EB16T0	0	1.150	0.761	1.079
EB16T1	30	0.103	0.100	
EB16T2	60	0.088	0.091	Efic. Remoção
EB16T3	90	0.082	0.086	93.81
EB16T4	120	0.079	0.087	
EB16T5	150	0.074	0.084	
EB16T6	180	0.065	0.080	
EB16T7	210	0.070	0.085	
EB16T8	240	0.071	0.083	
EB16TF	*	0.069	0.085	

EB18 pH = 0,9

Amostra	tempo (min)	As total (g/L)	Fe total (g/L)	Δ [As]
EB18T0	0	1.045	0.682	0.953
EB18T1	30	0.113	0.121	
EB18T2	60	0.107	0.110	Efic. Remoção
EB18T3	90	0.100	0.107	91.15
EB18T4	120	0.092	0.103	
EB18TF	*	0.104	0.117	

EB	Ef remoção	Desv Pad
15	92.4	1.3
16	93.8	Média
18	91.2	92.4

1g/L As e 10g/L sementes

EB9 pH = 0,9

Amostra	tempo (min)	As total (g/L)	Fe total (g/L)	Δ [As]
EB9T0	0	0.926	0.731	0.747
EB9T1	30	0.291	0.244	
EB9T2	60	0.235	0.199	Efic. Remoção
EB9T3	90	0.201	0.177	80.69
EB9T4	120	0.179	0.161	
EB9TF	*	0.195	0.173	

EB13 pH = 1.0

Amostra	tempo (min)	As total (g/L)	Fe total (g/L)	Δ [As]
EB13T0	0	1.040	0.824	0.936
EB13T1	30	0.214	0.183	
EB13T2	60	0.166	0.153	Efic. Remoção
EB13T3	90	0.140	0.136	90.00
EB13T4	120	0.124	0.123	
EB13T5	150	0.117	0.119	
EB13T6	180	0.110	0.114	
EB13T7	210	0.120	0.112	
EB13T8	240	0.104	0.107	
EB13TF	*	0.120	0.121	

EB14 pH = 1.1

Amostra	tempo (min)	As total (g/L)	Fe total (g/L)	Δ [As]
EB14T0	0	1.020	0.828	0.947
EB14T1	30	0.133	0.128	
EB14T2	60	0.096	0.102	Efic. Remoção
EB14T3	90	0.088	0.095	92.79
EB14T4	120	0.080	0.093	
EB14T5	150	0.080	0.092	
EB14T6	180	0.076	0.088	
EB14T7	210	0.074	0.086	
EB14T8	240	0.074	0.089	
EB14TF	*	0.081	0.094	

EB	Ef remoção	Desv Pad
9	80.7	6.3
13	90.0	Média
14	92.8	87.8

0.1g/L As e 40g/L sementes

EB26

Amostra	tempo (h)	As total (g/L)	Fe total (g/L)	Δ [As]
EB26T0	0	0.10	0.08	0.09
EB26T1	0.5	0.01	0.03	
EB26T2	1	0.01	0.03	Efic. Remoção
EB26T3	1.5	0.01	0.03	94.6
EB26T4	2	0.01	0.03	

EB29

Amostra	tempo (h)	As total (g/L)	Fe total (g/L)	Δ [As]
EB29T0	0	0.10	0.07	0.09
EB29T1	0.5	x	x	
EB29T2	1	x	x	Efic. Remoção
EB29T3	1.5	x	x	89.0
EB29T4	2	0.01	0.01	

EB30

Amostra	tempo (h)	As total (g/L)	Fe total (g/L)	Δ [As]
EB30T0	0	0.10	0.07	0.08
EB30T1	0.5	x	x	
EB30T2	1	x	x	Efic. Remoção
EB30T3	1.5	x	x	80.2
EB30T4	2	0.02	0.01	

EB	Ef remoção	Desv. Pad
26	94.6	7.3
29	89	Média
30	80.2	87.9

6.5 Appendix E: Results of the chemical analyses – Continuous Tests

Tratamento dos dados - EC3 → Sem reciclo de sólidos

Amostra	tempo (h)	As total (g/L)	Fe total (g/L)	∆ [As]	M esc.teórica (g)	IPS (%)
EC3T0	0	0.99	0.75			
EC3T1	1	0.32	0.25		M esc. obtida (g)	
EC3T2	2	0.46	0.35	Efic. Remoção (%)		
EC3T3	3	0.61	0.47		Rend. (%)	
EC3T4	4	0.77	0.59			
EC3T5	5	0.88	0.68			
EC3T6	6	0.89	0.68			
EC3T7	7	0.98	0.75	p Hi = 0.9		
EC3T8	8	0.98	0.75	pHf = 0.9		
EC3T9	9	0.97	0.74			
EC3T10	10	1.01	0.77			

Tratamento dos dados - EC4

Amostra	tempo (h)	As total (g/L)	Fe total (g/L)	∆ [As]	M esc.teórica (g)	IPS (%)
EC4T0	0	0.99	0.74	0.508	20.35	
EC4T1	1	0.32	0.24		M esc. obtida (g)	
EC4T2	2	0.32	0.25	Efic. Remoção (%)	19.7	49.2
EC4T3	3	0.34	0.27	51.58	Rend. (%)	
EC4T4	4	0.37	0.28		96.8	
EC4T5	5	0.42	0.32			
EC4T6	6	0.40	0.30			
EC4T7	7	0.41	0.31	p Hi = 0.9		
EC4T8	8	0.43	0.32	pHf = 0.8		
EC4T9	9	0.46	0.33			
EC4T10	10	0.48	0.34			

Tratamento dos dados - EC5

Amostra	tempo (h)	As total (g/L)	Fe total (g/L)	∆ [As]	M esc.teórica (g)	IPS (%)
EC5T0	0	0.91	1.22	0.785	27.81	
EC5T1	1	0.11	0.59		M esc. obtida (g)	
EC5T2	2	0.10	0.56	Efic. Remoção (%)	25.4	31.75
EC5T3	3	0.11	0.59	86.44	Rend. (%)	
EC5T4	4	0.12	0.59		91.3	
EC5T5	5	0.12	0.60			
EC5T6	6	0.13	0.60	p Hi = 1.1		
EC5T7	7	0.12	0.58	pHf = 1.0		
EC5T8	8	0.13	0.58			
EC5T9	9	0.14	0.59			
EC5T10	10	0.12	0.57			

Tratamento dos dados - EC6

Amostra	tempo (h)	As total (g/L)	Fe total (g/L)	∆ [As]	M esc.teórica (g)	IPS (%)
EC6T0	0	0.92	1.40	0.768	26.01	18.75
EC6T1	1	0.50	1.03		M esc. obtida (g)	
EC6T2	2	0.48	1.05	Efic. Remoção (%)	15	
EC6T3	3	0.13	0.75	83.46	Rend. (%)	
EC6T4	4	0.13	0.74		57.66	
EC6T5	5	0.13	0.74			
EC6T6	6	0.14	0.74			
EC6T7	7	0.14	0.74	p Hi = 1.2		
EC6T8	8	0.15	0.75	pHf = 1.1		

Tratamento dos dados - EC7

Amostra	tempo(h)	As total(g/L)	Fe total (g/L)	∆ [As]	M esc.teórica (g)	IPS (%)
EC7T0	0	0.28	0.84	0.09		
EC7T1	1	0.18	0.79		M esc. obtida (g)	
EC7T2	2	0.18	0.76	Efic. Remoção (%)		
EC7T3	3	0.18	0.77	33.78	Rend. (%)	
EC7T4	4	0.18	0.78			
H0	0	0.27	0.85			
H1	1	0.17	0.78			
H2	2	0.17	0.76	p Hi = 1.4		
H3	3	0.18	0.78	pHf = 1.4		
H4	4	0.18	0.78			

Tratamento dos dados - EC8

Amostra	tempo (h)	As total (g/L)	Fe total (g/L)	∆ [As]	M esc.teórica (g)	IPS (%)
EC8T0	0	0.93	0.78	0.42	15.68	18.4
EC8T1	1	0.40	0.40		M esc. obtida (g)	
EC8T2	2	0.40	0.38	Efic. Remoção (%)	14.74	
EC8T3	3	0.41	0.38	45.5	Rend. (%)	
EC8T4	4	0.42	0.38		94	
EC8T5	5	0.44	0.39			
EC8T6	6	0.45	0.39			
EC8T7	7	0.43	0.38	p Hi = 0.9		
EC8T8	8	0.43	0.38	pHf = 0.8		
EC8T9	9	0.44	0.38			
EC8T10	10	0.51	0.40			

Tratamento dos dados - EC9

Amostra	tempo (h)	As total (g/L)	Fe total (g/L)	∆ [As]	M esc.teórica (g)	IPS (%)
EC9T0	0	0.92	0.87	0.638	23.6	
EC9T1	1	0.24	0.29		M esc. obtida (g)	
EC9T2	2	0.22	0.27	Efic. Remoção (%)		
EC9T3	3	0.23	0.29	69.56	Rend. (%)	
EC9T4	4	0.24	0.29			
EC9T5	5	0.25	0.31			
EC9T6	6	0.26	0.31			
EC9T7	7	0.27	0.32	p Hi = 1.1		
EC9T8	8	0.28	0.33	pHf = 1.0		
EC9T9	9	0.28	0.32			
EC9T10	10	0.28	0.33			

Tratamento dos dados - EC10

Amostra	tempo (h)	As total (g/L)	Fe total (g/L)	∆ [As]	M esc.teórica (g)	IPS (%)
EC10T0	0	1.09	0.54	0.70	20.44	
EC10T1	1	0.35	0.28		M esc. obtida (g)	
EC10T2	2	0.33	0.27	Efic. Remoção (%)	14.22	17.78
EC10T3	3	0.34	0.28	64.3	Rend. (%)	
EC10T4	4	0.34	0.29		69.31	
EC10T5	5	0.35	0.29			
EC10T6	6	0.36	0.30			
EC10T7	7	0.36	0.14	p Hi = 1.1		
EC10T8	8	0.39	0.15	pHf = 1.0		